THE UNIVERSITY
OF MICHIGAN

SEP 14 1962

ENGINEERING
LIBRARY

АВТОМАТИКА
и
ТЕЛЕМЕХАНИКА

Vol. 22, No. 5, May, 1961

Translation Published November, 1961

SOVIET INSTRUMENTATION AND
CONTROL TRANSLATION SERIES

Automation and Remote Control

(The Soviet Journal *Avtomatika i Telemekhanika* in English Translation)

■ This translation of a Soviet journal on automatic control is published as a service to American science and industry. It is sponsored by the Instrument Society of America under a grant in aid from the National Science Foundation, continuing a program initiated by the Massachusetts Institute of Technology.

SOVIET INSTRUMENTATION AND CONTROL TRANSLATION SERIES

Instrument Society of America

Philip A. Sprague
President
Dr. Ralph H. Tripp
Past President
Nathan Cohn
President-elect-Secretary
Henry J. Noebels
Dept. Vice President
Dr. Benjamin W. Thomas
Dept. Vice President-elect
E. A. Adler
Dept. Vice President
Francis S. Hoag
Dept. Vice President
John J. McDonald
Dept. Vice President
John R. Mahoney
Dept. Vice President-elect
John C. Koch
Treasurer
Alonzo B. Parsons
Dist. I Vice President
H. Kirk Fallin
Dist. II Vice President
Harold J. Bowman
Dist. III Vice President
Fred R. Gilmer
Dist. IV Vice President
Charles H. Callier
Dist. V Vice President
Otto J. Lessa
Dist. VI Vice President
J. Howard Park, III
Dist. VII Vice President
C. Roy Horton
Dist. VIII Vice President
Max Curtis
Dist. IX Vice President
Kenneth S. Vriesen
Dist. X Vice President
Allan E. Lee
Dist. XI Vice President

International Headquarters

William H. Kushnick
Executive Director
Charles W. Covey
Editor, ISA Journal
Herbert S. Kindler
Director, Tech. & Educ. Services

ISA Publications Committee

Charles O. Badgett, *Chairman*

Jere E. Brophy	George A. Larsen	Joshua Stern
Dr. Enoch J. Durbin	Thomas G. MacAnespie	Frank S. Swaney
Prof. Richard W. Jones	John E. Read	Richard A. Terry

Translations Advisory Board of the Publications Committee

Jere E. Brophy, *Chairman*

T. J. Higgins	S. G. Eskin	G. Werbizky

■ This translation of the Soviet Journal *Avtomatika i Telemekhanika* is published and distributed at nominal subscription rates under a grant in aid to the Instrument Society of America from the National Science Foundation. This translated journal, and others in the Series (see back cover), will enable American scientists and engineers to be informed of work in the fields of instrumentation, measurement techniques, and automatic control reported in the Soviet Union.

The original Russian articles are translated by competent technical personnel. The translations are on a cover-to-cover basis and the Instrument Society of America and its translators propose to translate faithfully all of the scientific material in *Avtomatika i Telemekhanika*, permitting readers to appraise for themselves the scope, status, and importance of the Soviet work. All views expressed in the translated material are intended to be those of the original authors and not those of the translators nor the Instrument Society of America.

Publication of *Avtomatika i Telemekhanika* in English translation started under the present auspices in April, 1958, with Russian Vol. 18, No. 1 of January, 1957. The program has been continued with the translation and printing of the 1958-1961 issues.

Transliteration of the names of Russian authors follows the system known as the British Standard. This system has recently achieved wide adoption in the United Kingdom, and is currently being adopted by a large number of scientific journals in the United States.

Readers are invited to submit to the Instrument Society of America comments on the quality of the translations and the content of the articles. Pertinent correspondence will be published in the Society's monthly publication, the ISA JOURNAL. Space will also be made available in the ISA JOURNAL for such replies as may be received from Russian authors to comments or questions by the readers.

1961 Volume 22 Subscription Prices:

Per year (12 issues), starting with Vol. 22, No. 1

General:	*United States and Canada*	$35.00
	Elsewhere	38.00
Libraries of nonprofit academic institutions:		
	United States and Canada	$17.50
	Elsewhere	20.50
Single issues to everyone, each		$ 6.00

1957 Volume 18, 1958 Volume 19, 1959 Volume 20, and 1960 Volume 21 issues also available. Prices upon request.

See back cover for combined subscription to entire Series.

Subscriptions and requests for information on back issues should be addressed to the:

Instrument Society of America
530 William Penn Place, Pittsburgh 19, Penna.

Translated and printed by Consultants Bureau Enterprises, Inc.

Copyright © 1961 by the Instrument Society of America

Automation and Remote Control

A translation of Avtomatika i Telemekhanika, a publication of the Academy of Sciences of the USSR

EDITORIAL BOARD OF AVTOMATIKA I TELEMEKHANIKA

D. I. Ageikin
M. A. Aizerman
A. B. Chelyustkin *(Assoc. Editor)*
E. G. Dudnikov
N. Ya. Festa
V. A. Ilin
A. G. Iosuf'yan
V. V. Karibskii
A. V. Khramoi
B. Ya. Kogan
V. S. Kulebakin
S. A. Lebedev
A. Ya. Lerner
A. M. Letov *(Assoc. Editor)*
V. S. Malov
B. N. Petrov
Yu. P. Portnov-Sokolov
B. S. Sotskov
A. A. Tal' *(Corresp. Secretary)*
V. A. Trapeznikov *(Editor in Chief)*
Ya. Z. Tsypkin
G. M. Ulanov
A. A. Voronov
S. V. Yablonskii

Vol. 22, No. 5 Russian Original Dated May, 1961 November, 1961

CONTENTS

	PAGE	RUSS. PAGE
A Practical Method for Calculating the Coupling Operator in Linear Approximation. L. N. Lipatov and Yu. P. Leonov	483	561
Determination of Correlation Functions of Outputs from Linear Dynamic Systems by Means of Two-Dimensional Laplace Transforms. A. N. Skl'yarevich	491	571
Structure Transformation of Linear Varying-Parameter Systems. A. V. Solodov	497	577
The Analysis of Nonlinear and Extremal Pulse Systems by Applying the Incremental Phase Plane Method. V. M. Kuntsevich	509	589
Relay System with Self-Oscillating Mode of Operation Disturbed by Randon Signals. V. Ya. Katkovnik and A. A. Pervozvanskii	517	599
Compensation of Delay in a Relay System. N. A. Korolev	523	605
Influence of Hysteresis on the Mode of Periodic Processes in Pulsed Relay Systems. V. P. Kazakov	530	613
On One Method of Automatic Search for the Extremum of a Function of Many Variables. K. B. Norkin	534	618
A Servomechanism with a Two-Phase Asynchronous Motor Whose Control Winding is Powered by a Current Generator. N. P. Vlasov	539	624
Investigating a Thyratron Pulse Converter with a Step Motor. V. M. Kolesnikov	544	630
The Calculation of Thermal Conditions in Transistors. A. N. Afanas'ev	554	641
A Magnetic-Thermistor Time Relay. O. P. D'yakov, N. M. Tishchenko, and N. P. Udalov	560	648
An Automatic Pneumatic Optimizer. N. V. Grishko	565	654
Noise Stability of Frequency Remote Control Systems in the Case of Fluctuating Noise. Yu. I. Chugin	573	664

SOVIET INSTRUMENTATION AND
CONTROL TRANSLATION SERIES

Automation and Remote Control

Vol. 22, No. 5 November, 1961

CONTENTS

A PRACTICAL METHOD FOR CALCULATING THE COUPLING OPERATOR IN LINEAR APPROXIMATION

L. N. Lipatov and Yu. P. Leonov

(Moscow)

Translated from Avtomatika i Telemekhanika, Vol. 22, No. 5,
pp. 561-570, May, 1961
Original article submitted August 1, 1960

The problem is considered of obtaining a simple numerical method for determining the weight function of a linear object. As an example, the weight function for the coupling between the parameters of a continuously operating coil boiler is calculated.

The problem of the statistical analysis of the relation between random functions has recently become of great importance. This is due to the fact that at a certain level in the precision of describing a complex system, it ceases to be clear how to write the differential equations of the system. In the operation of such a system, too many different factors affect the operation of the system (sometimes factors that are unknown to us), and it becomes difficult to take them all into account. This situation arises, in particular, in the solution of certain problems of automatic control, when precision control of a certain object requires that it be described accurately. A statistical description of the coupling in this case can lead to the design of a more accurate control system.

We will consider a simple method of obtaining a linear model of a coupling, which will be suitable for practical calculations. We will use as an example the determination of the coupling between the parameters of a continuously operating coil boiler.

1. The Problem

Let there be an object relative to which two signals $X_1(t)$ and $Y(t)$ are recorded by some device. The signal $X_1(t)$ can be assumed to be the input and the signal $Y(t)$ the output of the system. It is desired to determine the coupling operator between $X_1(t)$ and $Y(t)$ under the assumption that the problem is linear. In other words, we wish to construct a mathematical model of the object.

2. Solution of the Problem

To solve this problem, we can use the general method of finding the coupling operator described in [1]. In order to do this, we must seek the operator yielding the best approximation in the sense of that operator that gives the minimum of the mean square difference between the function $Y(t)$ and the transform $A_\tau^t X(\tau)$ of $X(\tau)$, i.e., the minimum of

$$\varepsilon_1^2 = M\{Y(t) - A_\tau^t X(\tau)\}^2. \tag{1}$$

In agreement with the conditions of the problem, we consider operators A_τ^t from the class of linear operators. Then $A_\tau^t X(\tau)$ can be written in the form

$$A_\tau^t X(\tau) = \int_{-\infty}^{+\infty} w(t, \tau) X_1(\tau)\, d\tau. \tag{2}$$

From (1) we therefore have

$$\varepsilon_1^2 = M\left\{Y(t) - \int_{-\infty}^{+\infty} w(t, \tau) X_1(\tau)\, d\tau\right\}^2. \tag{3}$$

The usual procedure for minimizing this squared functional leads to the integral function

$$\int_{-\infty}^{+\infty} w(t,\tau)\,\Gamma_{X_1X_1}(\tau,\tau_1)\,d\tau = \Gamma_{YX_1}(t,\tau_1) \quad (-\infty<\tau_1<+\infty). \tag{4}$$

for the weight function, where $\Gamma x_1\ x_1(t_1, t_2)$ and $\Gamma yx_1(t_1, t_2)$ are the first moment of the function $X_1(t)$ and the mixed first moment of the functions $Y(t)$ and $X_1(t)$ respectively. In particular, if $X_1(t)$ and $Y(t)$ are stationary random functions and have a stationary relation between them, and have zero mathematical expectation, then

$$\int_{-\infty}^{+\infty} w(\tau)\,k_{X_1X_1}(t-\tau)\,d\tau = k_{YX_1}(t) \quad (-\infty<t<+\infty). \tag{5}$$

where $k_{x_1x_1}(\tau)$ and $K_{yx_1}(\tau)$ are respectively the correlation of $x_1(t)$ and the mutual correlation of the functions $Y(t)$ and $X_1(t)$.

The weight function corresponds in this case to a linear operator with constant parameters. The solution of the equation (5) is trivial if we calculate the two-sided Laplace transform of the left and the right hand sides. However, if it is required that $w(t)$ satisfy the condition $w(t) = 0$ for $t \leq 0$, then we obtain a Wiener-Hopf equation, the solution of which is known from the theory of optimal systems [1]. If it is desired that a model of the object be realized by a physical device, then the condition $w(t) \equiv 0$ for $t \leq 0$ must of necessity be satisfied.

The problem of constructing a linear model of the coupling thus reduces to the solution of the integral equation (4) for the weight function of the linear operator, or, in the particular case, to the solution of (5). The first moments $\Gamma x_1x_1(t_1, t_2)$ and $\Gamma yx_1(t_1, t_2)$ are determined from a record of the random functions $X_1(t)$ and $Y(t)$ obtained in practice.

Two cases can occur in the construction of a linear model of the coupling. In the first case, the linear model is approximate. This means that the operator A_τ^{*1} the first approximation in (1) is nonlinear, but the best approximation is sought in the class of linear operators. The second case arises when the operator A_τ^{*1}, for which the lower bound of ϵ^2 is attained, is linear. The linear model of the object is then exact.

As has already been shown, the equation (5) can be solved in closed form, at least for certain classes of correlation functions. In what follows, however, we will use the approximate solution. This is due to two circumstances. Firstly, the functions $k_{x_1x_1}(t)$ and $K_{yx_1}(t)$ are usually approximated by certain analytic expressions, and only after this approximation can the equation (5) be solved. The solution is then obtained by approximate methods. In addition to the approximate solution of the equation, the question arises of the choice of the functions to use in approximating the above functions. Secondly, the solution obtained by this procedure sometimes does not correspond to the problem. It is well known, in particular, that the solution of the Wiener-Hopf equation for the weight function to be used in a physically realizable system can contain delta-functions and their derivatives [2]. But a real object can not involve such functions. This difficulty is evidently connected with the fact that the functions $k_{x_1x_1}(t)$ and $k_{yx_1}(t)$, for which the equation is solved, must have Laplace transforms that are rational fractions, while the real correlation and mutual correlations functions do not necessarily possess this property in the general case.

We finally mention the numerical solution of the equation (5) that does not require any approximation to the functions $k_{x_1x_1}(t)$ and $k_{yx_1}(t)$. In this case the integral equation (5) is reduced to a system of linear algebraic equations. The number of these equations is usually rather large (equal to the number of values of the weighting function), and so a digital computer is required for the calculation.

We consider below a simple graphical-analysis method for obtaining an approximate solution for the equation (5), suitable for practical calculations. It does not require the use of a digital computer. For the calculation, we must have a sufficient number of characteristics (moments) of the random processes at the output and input of the object. These moments are obtained either directly from the random processes themselves [3], or from the corresponding correlation functions. The proposed graphical-analysis method for obtaining the solution is naturally not the only one, but in the authors' opinion it is suitable for practical calculations.

We introduce the normed moments $\bar{\alpha}_n$ of the function $w(t)$:

$$\bar{\alpha}_n = \frac{\alpha_n}{\alpha_0} \tag{6}$$

where

$$\alpha_n = \int_{-\infty}^{+\infty} w(t)\, t^n\, dt. \tag{6a}$$

We also introduce the central normed moments

$$\bar{\alpha}_{n0} = \frac{1}{\alpha_0} \int_{-\infty}^{+\infty} (t - \bar{\alpha}_1)^n\, w(t)\, dt. \tag{7}$$

Between the normed moments and the central normed moments there exist the following obvious relations:

$$\begin{aligned} &\bar{\alpha}_{10} = 0,\ \bar{\alpha}_{20} = \bar{\alpha}_2 - (\bar{\alpha}_1)^2. \\ &\bar{\alpha}_{30} = \bar{\alpha}_3 - 3\bar{\alpha}_2\bar{\alpha}_1 + 2(\bar{\alpha}_1)^3. \\ &\bar{\alpha}_{40} = \bar{\alpha}_4 - 4\bar{\alpha}_3\bar{\alpha}_1 + 6\bar{\alpha}_2(\bar{\alpha}_1)^2 - 3(\bar{\alpha}_1)^4. \\ &\cdots\cdots\cdots\cdots\cdots\cdots \\ &\cdots\cdots\cdots\cdots\cdots\cdots \\ &\cdots\cdots\cdots\cdots\cdots\cdots \end{aligned} \tag{8}$$

We will denote the normed moments for the functions $k_{x_1x_1}(t)$ and $k_{yx_1}(t)$ by $\overline{\gamma_{n0}}$ and $\overline{\beta_{n0}}$ respectively.

It can easily be shown [3] that between $\overline{\alpha_{n0}}$ for a function w(t) satisfying the equation (5), $\overline{\gamma_{n0}}$ and $\overline{\beta_{n0}}$, the relations

$$\begin{aligned} &\alpha_0 = \frac{\beta_0}{\gamma_0}. \\ &\bar{\alpha}_1 = \bar{\beta}_1 - \bar{\gamma}_1. \\ &\vdots\quad\quad\vdots \\ &\bar{\alpha}_{n0} = \bar{\beta}_{n0} - \bar{\gamma}_{n0} \end{aligned} \tag{9}$$

hold.

In order to obtain an approximate solution of (5), it is convenient to have the form of the transfer function w(p), which depends on certain arbitrary parameters. After this, we can choose the m arbitrary parameters so that the m equations in (9) are satisfied. The moments $\overline{\beta_{n0}}$ and $\overline{\gamma_{n0}}$ are also assumed to be known. We note that the moments can often be calculated from the Laplace transforms of the corresponding functions. Thus, if w(p) is the two-sided Laplace transform of the function w(t), then from (6a) we easily obtain the relation

$$\alpha_k = (-1)^k w^{(k)}(p)\big|_{p=0}. \tag{10}$$

It was shown in [3] how to determine directly values for the moments $\overline{\beta_{n0}}$ and $\overline{\gamma_{n0}}$ from the realizations $x_i(t)$ and $y(t)$ of the random functions $X_i(t)$ and $Y(t)$.

We can, in particular, take w(p) to be of the form

$$w(p) = k\, \frac{\prod_{p=1}^{m_1} (T_{1p}p^2 + T_{2p}p + 1) \prod_{q=1}^{m_2} (T_q p + 1)\, e^{-\tau p}}{\prod_{i=1}^{m_3} (T'_{1i}p^2 + T'_{2i}p + 1) \prod_{j=1}^{m_4} (T'_j p + 1)}. \tag{11}$$

Then, using the formula (10), we can easily express the moments of the weight function w(t) in terms of the parameters of the transfer function w(p). For the first four moments we have

$$\begin{aligned} &\alpha_0 = k. \\ &\bar{\alpha}_1 = \sum_{i=1}^{m_3} T'_{2i} + \sum_{j=1}^{m_4} T'_j - \sum_{p=1}^{m_1} T_{2p} - \sum_{q=1}^{m_2} T_q + \tau. \end{aligned} \tag{12}$$

$$\bar{\alpha}_{20} = \sum_{i=1}^{m_3} (T_{2i}'^2 - 2T_{1i}') + \sum_{j=1}^{m_4} T_j'^2 - \sum_{p=1}^{m_1} (T_{2p}^2 - 2T_{1p}) - \sum_{q=1}^{m_2} T_q^2.$$

$$\bar{\alpha}_{30} = \sum_{i=1}^{m_3} (T_{2i}'^3 - 3T_{1i}'T_{2i}') + \sum_{j=1}^{m_4} T_j'^3 - \sum_{p=1}^{m_1} (T_{2p}^3 - 3T_{1p}T_{2p}) - \sum_{q=1}^{m_2} T_q^3. \tag{12}$$

$$\bar{\alpha}_{40} = \sum_{i=1}^{m_3} (T_{2i}'^4 - 4T_{1i}'T_{2i}'^2 + 2T_{1i}'^2) + \sum_{j=1}^{m_4} T_j'^4 -$$

$$- \sum_{p=1}^{m_1} (T_{2p}^4 - 4T_{1p}T_{2p}^2 + 2T_{1p}^2) - \sum_{q=1}^{m_2} T_q^4.$$

It is somewhat arduous to solve the system of equations (12). It is therefore expedient to use an expression for the transfer function w(p) that may possibly be simpler. Here we will consider the graphical analytic solution for a function w(p) having the forms

$$w(p) = k \frac{T_3 p + 1}{T^2 p^2 + 2T\xi p + 1} e^{-\tau p} \tag{13}$$

and

$$w(p) = k \frac{e^{-\tau p}}{(T^2 p^2 + 2T\xi p + 1)(T_3 p + 1)} \tag{13a}$$

depending on the five parameters k, T, ξ, T_3 and τ.

The transfer functions in a large number of industrial cases can be written with sufficient accuracy in either the form (13) or the form (13a). In these cases, the relations between the moments and parameters are

$$\begin{aligned} \bar{\alpha}_1 &= 2\xi T + \tau \pm T_3, \\ \bar{\alpha}_{20} &= [(2\xi)^2 - 2]\, T^2 \pm T_3^2, \\ \bar{\alpha}_{30} &= [(2\xi)^3 - 6\xi]\, T^3 \pm T_3^3, \\ \bar{\alpha}_{40} &= [(2\xi)^4 - 16\xi^2 + 2]\, T^4 \pm T_3^4. \end{aligned} \tag{14}$$

The plus sign for T_3 corresponds to the expression (13a), and the minus sign to (13).

For the solution of the system of equations (14) it is convenient to write these relations in the form

$$\begin{aligned} \alpha_0 &= k, \\ \bar{\alpha}_1 &= 2\xi T + \tau \pm T_3, \\ T &= \frac{\bar{\alpha}_{30} \mp T_3^3}{\alpha_{20} \mp T_3^2} \psi_1(\xi) = \frac{\alpha_{40} \mp_* T_3^4}{\alpha_{30} \mp_* T_3^3} \psi_2(\xi), \\ T_3 &= \sqrt{|[(2\xi)^2 - 2]\, T^2 - \bar{\alpha}_{20}|}. \end{aligned} \tag{15}$$

In the equations (15) the minus sign corresponds to the expression (13a). The functions $\psi_1(\xi)$ and $\psi_2(\xi)$ are given by

$$\psi_1(\xi) = \frac{(2\xi)^2 - 2}{(2\xi)^3 - 6\xi}, \quad \psi_2(\xi) = \frac{(2\xi)^3 - 6\xi}{(2\xi)^4 - 16\xi^2 + 2}. \tag{16}$$

These functions are shown graphically in Fig. 1. For more accurate calculations, the values of $\psi_1(\xi)$ and $\psi_2(\xi)$ and of the ratio ψ_1/ψ_2 can be obtained from the table (see the appendix).

The equations (15) can be solved by the method of successive approximations (either by iteration or by Newton's method [4]). By using the graphs of $\psi_1(\xi)$ and $\psi_2(\xi)$ (or the tables of their values), we can solve the third equation of the system (15) and determine the values of T and ξ by successive approximations. In order to facilitate the use of the graph in Fig. 1, we can use the supplementary graph in Fig. 2. In the latter, we show the regions, relative to the quantities R_1 and R_2, corresponding to various ranges of ξ. Here

$$R_1 = \frac{\alpha_{30} + T_3^3}{\alpha_{20} + T_2^2}, \quad R_2 = \frac{\alpha_{40} + T_3^4}{\alpha_{20} + T_3^3}. \tag{17}$$

From (17), the third equation of the system (15) can be written in the form

$$R_2 = R_1 \frac{\psi_1(\xi)}{\psi_2(\xi)}. \tag{18}$$

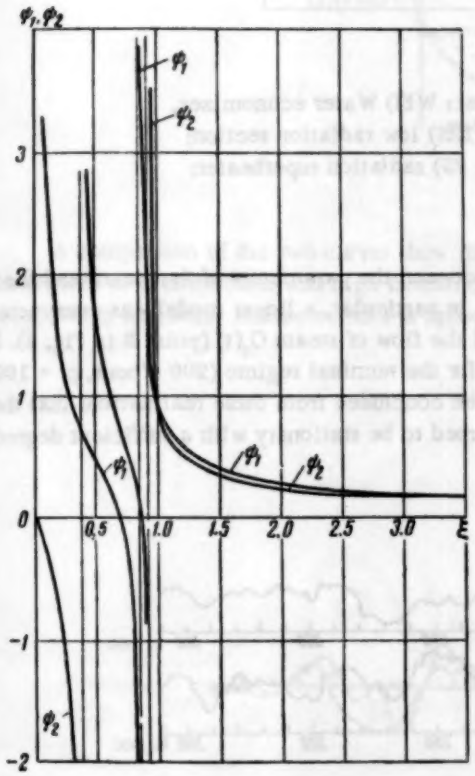

Fig. 1

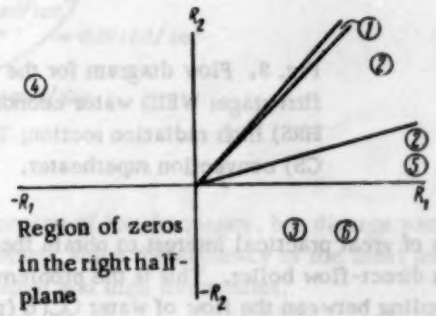

Fig. 2

It follows from (18), that for different ranges of the variable ξ, the regions of variation of R_1 and R_2 are sectors. These regions are numbered in Fig. 2 (the numbers in the circles) for the following ranges of variation of ξ:

$$\begin{array}{lll}
\xi = 1 - \infty & \text{for} & \alpha_1.\ \alpha_2.\ \alpha_3.\ \alpha_4 > 0: \\
\xi = 0.92 - 1 & \text{for} & \alpha_1.\ \alpha_2.\ \alpha_3.\ \alpha_4 > 0: \\
\xi = 0.86 - 0.92 & \text{for} & \alpha_1.\ \alpha_2.\ \alpha_3 > 0.\ \alpha_4 < 0: \\
\xi = 0.7 - 0.86 & \text{for} & \alpha_2 > 0.\ \alpha_3.\ \alpha_4 < 0: \\
\xi = 0.38 - 0.7 & \text{for} & \alpha_2.\ \alpha_3.\ \alpha_4 < 0: \\
\xi = 0 - 0.38 & \text{for} & \alpha_2.\ \alpha_3 < 0.\ \alpha_4 > 0.
\end{array} \tag{19}$$

(The signs of the moments are given to facilitate finding the interval of ξ.)

If the graph in Fig. 2 is used, then for each approximate solution the values of R_1 and R_2 determine a rough value of ξ. From this rough value, a more accurate value can be obtained from the graph in Fig. 1 or from the table. If we now use the conditions (19) or Fig. 2, we can see that the solution of the system (15) we have obtained is unique.

3. The Coupling Between the Parameters of a Continuously Operating Coil Boiler

The method we have described for determining coupling operators (the operators of the object) was applied to the calculation of the coupling between the parameters of a continuously operating 67-2SP 230/100 boiler. This boiler was chosen for the object, since its characteristics are difficult to determine accurately by the usual methods (for example, by artificial perturbation methods). The nominal output of the experimental boiler was 230 t/hour of steam at a pressure of 100 atms. In its operation under a normal regime with a turbine, it was therefore highly undesirable to introduce any perturbations into the system. Such perturbations could upset the whole normal regime of the boiler-turbine system.

The nominal flow diagram of the boiler is shown in Fig. 3. One of the main elements of the boiler is a system of tubes into which water is directly injected. The tubes are heated by burning gases, and the water is heated and converted into steam. In spite of the apparent simplicity of this continuous flow boiler, heat engineers have not yet

obtained a satisfactory analytic relation between its parameters because of the complexity of the relation, which is described generally in terms of partial derivatives. In particular, no such quantitative relation has been obtained between the input parameters of the water and the output parameters of the steam. The aim of the present study was to find certain dynamic characteristics of the boiler. These characteristics were determined by two methods: 1) by the usual method of determining the frequency characteristics* [5]; and 2) by the statistical method.

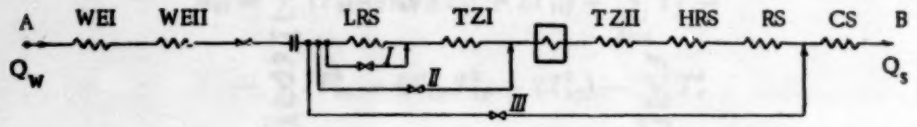

Fig. 3. Flow diagram for the 67-2SP 230/100 boiler: WEI) Water economizer, first stage; WEII) water economizer, second stage; LRS) low radiation section; HRS) high radiation section; TZ) transitional zone; RS) radiation superheater; CS) convection superheater.

It is of great practical interest to obtain the coupling operators between the parameters of the steam and the water in a direct-flow boiler. This is the problem we consider below. In particular, a linear model was constructed of the coupling between the flow of water $Q_w(t)$ (point A in Fig. 3) and the flow of steam $Q_s(t)$ (point B in Fig. 3). In order to do this, a realization of the random functions $Q_w(t)$ and $Q_s(t)$ for the nominal regime (200 t/hour, p = 100 atms) was recorded, and part of this record is shown in Fig. 4. It can be concluded from these realizations that the mathematical expectation is constant, and that the process can be assumed to be stationary with a sufficient degree of accuracy.

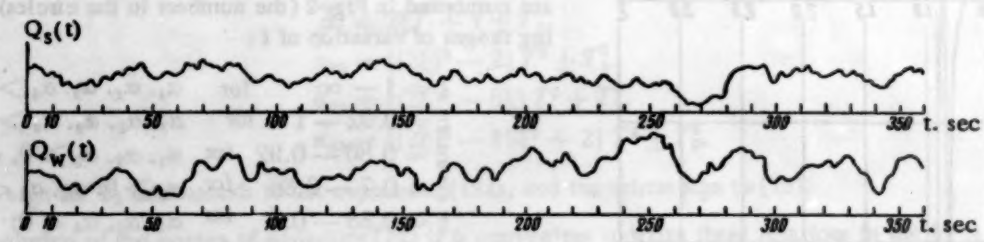

Fig. 4

In this case, the problem of obtaining a linear model of the coupling reduces to the determination of the weighting function w(t) from Eq. (5). For the approximate determination of w(p), the methods described in the previous paragraph were used. It was assumed that w(p) had the form (13), and so the problem was reduced to that of finding the parameters of the function w(p). First of all, by using experimental results, the moments of the correlation and the mixed correlation functions were obtained from the realizations of $q_w(t)$ and $q_s(t)$. For this calculation, the calculating device described in [3] was used. By an application of (9), the following values for the moments of the weighting function were obtained

$$\alpha_0 = 1{,}08;\ \bar{\alpha}_1 = 365;\ \bar{\alpha}_{20} = 98800;\ \bar{\alpha}_{30} = 274 \cdot 10^5;\ \bar{\alpha}_{40} = 8 \cdot 10^9.$$

The parameters of the function w(p) were then obtained by successive approximation.

The final values of the parameters were thus taken to be

$$k = 1{,}08;$$
$$\tau = 32;\quad T = 205;\quad \xi = 1{,}08;\quad T_3 = 110.$$

* The experimental frequency characteristics of the boiler were determined by V. Dement'ev (TsNIIKA).

For these values of the parameters, the frequency characteristic w(jω) of the object was constructed. It is shown as a continuous curve in Fig. 5. In this diagram we also show the frequency characteristic of the coupling (the dotted curve), determined experimentally by the usual methods of artificial perturbation.

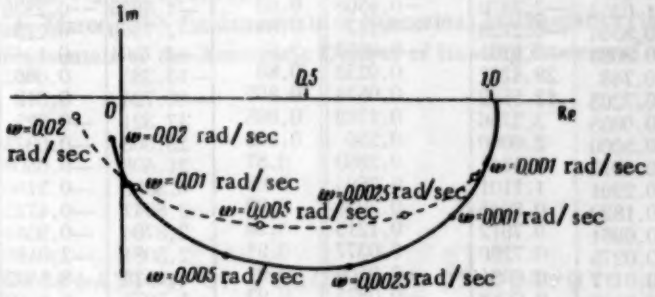

Fig. 5

A comparison of the two curves show that they agree in the region of low frequency, but diverge somewhat in the regions of intermediate and high frequency. This is to be expected, since the accuracy of the usual methods for determining frequency characteristics is appreciably lower for medium and high frequencies.

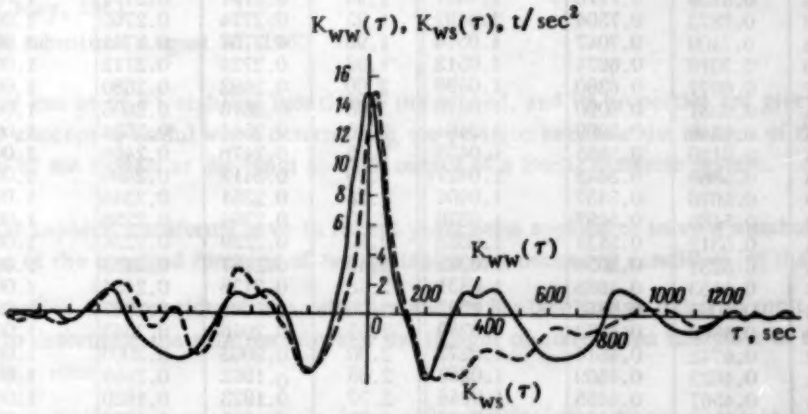

Fig. 6

Fig. 6 shows the correlation (the continuous line) and the mutual correlation (the dotted line) functions for $Q_w(t)$ and $Q_s(t)$. In particular, Fig. 6 shows that the delay occurring in the system is 30 sec, and this agrees well with the value τ = 32 sec that was obtained.

The authors wish to thank Ya. I. Khurgin for several useful comments he made in reviewing the manuscript of the present article.

APPENDIX

Table of Functions

ξ	Φ_1	Φ_2	Φ_1/Φ_2	ξ	Φ_1	Φ_2	Φ_1/Φ_2
0.00	$+\infty$	0	∞	0.74	—0.1589	0.6101	—0.2604
0.05	6.6555	—0.1525	—43.643	0.75	—0.2222	0.5806	—0.3827
0.10	3.3108	—0.3215	—10.298	0.77	—0.3840	0.5197	—0.7389
0.15	2.1879	—0.5314	—4.1172	0.80	—0.7954	0.4150	—1.9166

APPENDIX (continued)

ξ	ψ_1	ψ_2	ψ_1/ψ_2	ξ	ψ_1	ψ_2	ψ_1/ψ_2
0.20	1.6197	−0.8199	−1.9755	0.81	−1.0260	0.3779	−2.7150
0.25	1.2727	−1.2941	−0.9845	0.82	−1.3545	0.3339	−4.0566
0.30	1.0354	−2.2970	−0.4508	0.83	−1.8625	0.2839	−6.5604
0.35	0.8594	−6.2728	−0.137	0.84	−2.7560	0.2254	−12.227
0.37	0.8003	−16.5735	−0.0483	0.85	−4.7594	0.1548	−30.745
0.39	0.746	29.4227	0.0253	0.86	−13.385	0.0662	−202.19
0.40	0.7203	12.5532	0.0574	0.865	−80.724	0.012	−6727.0
0.45	0.6038	3.3756	0.1789	0.868	47.321	−0.025	−1892.84
0.50	0.5000	2.0000	0.250	0.869	28.508	−0.0373	−764.29
0.55	0.4012	1.4311	0.2803	0.87	21.408	−0.0508	−421.417
0.60	0.2991	1.1101	0.2694	0.88	6.3888	−0.2160	−49.5778
0.65	0.1820	0.8945	0.2035	0.89	3.8947	−0.4723	−8.2462
0.68	0.0961	0.7912	0.1215	0.90	2.8704	−0.9349	−3.0703
0.70	0.0275	0.7286	0.0377	0.91	2.3081	−2.0486	−1.1267
0.71	−0.0117	0.6984	−0.0168	0.92	1.9529	−8.8577	−0.2205
0.72	−0.0552	0.6688	−0.0825	0.93	1.7073	6.5560	0.2604
0.73	−0.1038	0.6395	−0.1623	0.94	1.5272	2.8349	0.5387
0.95	1.3891	1.9574	0.7097	1.80	0.3057	0.3036	1.0069
0.96	1.2796	1.5617	0.8194	1.82	0.3015	0.2995	1.0067
0.97	1.1905	1.3342	0.8923	1.84	0.2975	0.2956	1.0064
0.98	1.1164	1.1854	0.9418	1.85	0.2956	0.2937	1.0065
0.99	1.0538	1.0797	0.9760	1.86	0.2936	0.2918	1.0062
1.00	1.0000	1.0000	1.0000	1.88	0.2898	0.2882	1.0056
1.02	0.9122	0.8867	1.0288	1.90	0.2862	0.2846	1.0055
1.04	0.8432	0.8086	1.0428	1.92	0.2826	0.2811	1.0053
1.05	0.8139	0.7776	1.0467	1.94	0.2791	0.2777	1.0051
1.06	0.7873	0.7504	1.0492	1.95	0.2774	0.2760	1.0050
1.08	0.7409	0.7047	1.0514	1.96	0.2757	0.2744	1.0047
1.10	0.7016	0.6674	1.0512	1.98	0.2724	0.2712	1.0044
1.12	0.6677	0.6360	1.0498	2.00	0.2692	0.2680	1.0044
1.14	0.6381	0.6090	1.0478	2.05	0.2616	0.2605	1.0042
1.15	0.6246	0.5969	1.0464	2.10	0.2544	0.2534	1.0039
1.16	0.6120	0.5855	1.0453	2.15	0.2476	0.2468	1.0032
1.18	0.5886	0.5645	1.0427	2.20	0.2412	0.2405	1.0029
1.20	0.5676	0.5457	1.0401	2.25	0.2351	0.2345	1.0026
1.22	0.5486	0.5287	1.0376	2.30	0.2294	0.2288	1.0026
1.24	0.5312	0.5131	1.0353	2.35	0.2239	0.2234	1.0022
1.25	0.5231	0.5058	1.0342	2.40	0.2187	0.2183	1.0018
1.26	0.5153	0.4988	1.0331	2.45	0.2138	0.2134	1.0018
1.28	0.5005	0.4856	1.0307	2.50	0.2091	0.2087	1.0019
1.30	0.4869	0.4732	1.0289	2.55	0.2046	0.2043	1.0015
1.32	0.4742	0.4616	1.0273	2.60	0.2003	0.2000	1.0015
1.34	0.4623	0.4509	1.0253	2.65	0.1962	0.2959	1.0015
1.35	0.4567	0.4458	1.0244	2.70	0.1923	0.1920	1.0015
1.36	0.4512	0.4408	1.0236	2.75	0.1885	0.1883	1.0011
1.38	0.4408	0.4312	1.0223	2.80	0.1849	0.1847	1.0011
1.40	0.4309	0.4221	1.0208	2.85	0.1814	0.1812	1.0011
1.42	0.4216	0.4135	1.0196	2.90	0.1780	0.1779	1.0007
1.44	0.4128	0.4053	1.0185	2.95	0.1748	0.1747	1.0006
1.45	0.4086	0.4014	1.0179	3.00	0.1717	0.1716	1.0005
1.46	0.4044	0.3975	1.0173	3.05	0.1687	0.1687	1.0
1.48	0.3965	0.3901	1.0164	3.10	0.1658	0.1657	1.0
1.50	0.3889	0.3830	1.0154	3.15	0.1631	0.1629	1.0
1.52	0.3816	0.3762	1.0143	3.20	0.1604	0.1603	1.0
1.54	0.3747	0.3696	1.0138	3.25	0.1578	0.1577	1.0
1.55	0.3714	0.3665	1.0134	3.30	0.1552	0.1552	1.0
1.56	0.3681	0.3634	1.0129	3.35	0.1528	0.1527	1.0
1.58	0.3617	0.3574	1.0120	3.40	0.1505	0.1504	1.0
1.60	0.3557	0.3516	1.0117	3.45	0.1482	0.1481	1.0
1.62	0.3498	0.3460	1.0110	3.50	0.1640	0.1459	1.0
1.64	0.3442	0.3406	1.0106	3.55	0.1438	0.1438	1.0
1.65	0.3414	0.3380	1.0101	3.60	9.1417	0.1417	1.0
1.66	0.3387	0.3354	1.0098	3.65	0.1397	0.1397	1.0
1.68	0.3335	0.3304	1.0094	3.70	0.1377	0.1377	1.0
1.70	0.3285	0.3256	1.0089	3.75	0.1358	0.1358	1.0
1.72	0.3236	0.3209	1.0084	3.80	0.1340	0.1339	1.0
1.74	0.3189	0.3163	1.0082	3.85	0.1322	0.1321	1.0
1.75	0.3166	0.3141	1.008	3.90	0.1304	0.1304	1.0
1.76	0.3143	0.3119	1.0077	3.95	0.1287	0.1287	1.0
1.78	0.3099	0.3077	1.0071	4.00	0.1270	0.1270	1.0

LITERATURE CITED

1. Yu. P. Leonov, in the Discussion of the report of D. Westcott at the First IFAK Congress in(Moscow, 1960).
2. D. Kh. Lening and R. G. Bettin, Random Processes in Problems of Automatic Control [Russian translation] (Izd-vo inostr. lit-ry, 1958).
3. Yu. P. Leonov and L. N. Lipatov, "Statistical methods of determining the dynamic characteristics of objects," Avtomatika i Telemekhanika 21, No. 2(1960).*
4. B. P. Demidovich and I. A. Maron, The Fundamentals of Numerical Mathematics [in Russian](Fizmatgiz, 1960).
5. E. G. Dudinkov, The Fundamentals of the Automatic Control of Heating Processes [in Russian](Gosenergoizdat, 1956).

DETERMINATION OF CORRELATION OF FUNCTIONS OF OUTPUTS FROM LINEAR DYNAMIC SYSTEMS BY MEANS OF TWO-DIMENSIONAL LAPLACE TRANSFORMS

A. N. Skl'yarevich
(Riga)

Translated from Avtomatika i Telemekhanika, Vol. 22, No. 5,
pp. 571-576, May, 1961
Original article submitted August 30, 1960

The incomplete image of a weighting function is introduced, and its properties are given; it is shown that the concept is useful when determining the relation between the images of the correlation function of the signals at the input and the output of a linear dynamic system.

Two-dimensional Laplace transforms have in recent years been applied to solve a number of problems. The existence of the image of the required function of two variables is a necessary condition for their use.

A correlation function is a function of two variables and its Laplace image exists in most cases. It would, therefore, seem important to determine the relation between the images of correlation functions at the input and the output of a given dynamic system.

For the sake of simplicity we assume a single input and a single output in our dynamic system. The correlation functions of the signals at the input and at the output are denoted by $K_x(t, t_1)$, $K_y(t, t_1)$ respectively. When $g(t, s)$ denotes the system's weighting function then [1]

$$K_y(t.\ t_1) = \int_0^t \int_0^{t_1} g(t.\ s)\, g(t_1.\ s_1)\, K_x(s.\ s_1)\, ds\, ds_1. \tag{1}$$

We multiply both sides of the formula (1) by e^{-pt-qt_1}, and integrating with respect to t and t_1 from 0 to ∞

$$\int_0^\infty \int_0^\infty K_y(t.\ t_1)\, e^{-pt-qt_1}\, dt\, dt_1 = \tag{2}$$

$$= \int_0^\infty \int_0^\infty e^{-pt-qt_1} \left[\int_0^t \int_0^{t_1} g(t.\ s)\, g(t_1.\ s_1)\, K_x(s.\ s_1)\, ds\, ds_1 \right] dt\, dt_1.$$

The left-hand side of (2) represents the two-dimensional Laplace transform of the correlation function $K_y(t,t_1)$ [2]. Denoting by $\Phi_{ky}(p, q)$ the image of the correlation function $K_y(t, t_1)$, and inverting the order of integration in the right-hand side of (2), we find that

$$\Phi_{ky}(p.\ q) = \int_0^\infty \int_0^\infty K_x(s.\ s_1) \left[\int_s^\infty g(t.\ s)\, e^{-pt}\, dt \int_{s_1}^\infty g(t_1.\ s_1)\, e^{-qt_1}\, dt_1 \right] ds\, ds_1. \tag{3}$$

*See English translation.

We introduce the function

$$G(p.\ s) = \int_{s}^{\infty} g(t.\ s)\, e^{-pt}\, dt, \tag{4}$$

and shall call it the incomplete image of the weighting function, incomplete in view of its lower integration limit. The incomplete image of a weighting function is the outcome of an incomplete one-sided Laplace transformation of the original.

One should bear in mind that for physically realizable linear dynamic systems the incomplete image of its weighting function coincides with its one-sided image, as in this case we have $g(t,s) = 0$ when $t < s$, and therefore

$$\int g(t.\ s)\, e^{-pt}\, dt = \int_{0}^{\infty} g(t.\ s)\, e^{-pt}\, dt.$$

By making use of the incomplete image of a weighting function together with its one-sided image it is possible to simplify the proofs of certain statements, as the region in which the function under the integral sign is not vanishing identically stands out more distinctly.

The more important properties of the incomplete Laplace transform are similar in the general case (that is, when not only the weighting functions can be the originals) to the corresponding properties of the ordinary (complete) one-sided transforms [3, 4]. We cite the following:

1. The limiting value theorem for the incomplete transform: if $s \neq 0$, then

$$\lim_{p\to\infty} G(p.\ s) = 0. \tag{5}$$

2. The theorem with regard to the product of an incomplete and a complete image: if $G(p,s)$ is an incomplete image of the function $g(t,s)$, and $F(p)$ is the one-sided image of the function $f(t)$, then the imcomplete image of the function

$$g_1(t.\ s) = \int_{s}^{t} g(\tau.\ s)\, f(t-\tau)\, d\tau \tag{6}$$

is the product $G(p,s)F(p)$.

3. The theorem on the incomplete image of a product of functions: $G(p,s)$ is the incomplete image of $g(t,s)$ and $\varphi(t)$ a function which admits a Laurent expansion, then the incomplete image of the product $g_1(t,s) = \varphi(t)\, g(t,s)$ is given by the formula

$$G_1(p.\ s) = \varphi(-r)\, G(p.\ s) \tag{7}$$

where $r \equiv \frac{\partial}{\partial p}$, $\varphi(-r)$ represents an operator acting on the function $G(p,s)$. In order to find the value of the expression $\varphi(-r)G(p,s)$ it is necessary to expand the operator $\varphi(-r)$ into a Laurent series; subsequently we operate with every term of this series on the function $G(p,s)$.

Using (4) we bring the relation (3) into the form

$$\Phi_{xy}(p.\ q) = \int_{0}^{\infty}\int_{0}^{\infty} G(p.\ s)\, G(q.\ s_1)\, K_x(s,\ s_1)\, ds\, ds_1. \tag{8}$$

The formula (8) shows that the image of the correlation function of a signal at the output of a dynamic system is given in terms of the signal's correlation function at its input and of the incomplete image of its weighting function.

We shall find the incomplete image of a weighting function in three cases which are of practical interest. It shall be assumed when determining the image that the initial values of the weighting function vanish together with the initial values of its relevant derivatives or integrals. Initial values of a weighting function or its derivatives and integrals are understood to be its values corresponding to the time moment t = s.

1. The behavior of a dynamic system is described by the equation

$$Q(p)\,x = f(t) \tag{9}$$

where x(t) is the required response to the excitation f(t). Its weighting function is given by the equation

$$Q(p)\,g(t.\ s) = \delta(t - s). \tag{10}$$

We multiply both sides of the equation (10) by e^{-pt} and integrate with respect to t from s to ∞. In view of the rules governing the incomplete image of a weighting function, and those of the δ-function, we obtain

$$G(p.\ s) = \frac{e^{-ps}}{Q(p)} \tag{11}$$

where p is complex. It is obvious that $\frac{1}{Q(p)}$ is the transfer function of our system.

Substituting (11) into the formula (8) we get

$$\Phi_{ky}(p, q) = \frac{\Phi_{kx}(p, q)}{Q(p)\,Q(q)} \tag{12}$$

where $\Phi_{kx}(p, q)$ is the image of the signal correlation function at the input. Thus, in the case when the linear dynamic system is stationary, the image of the correlation function of the output signal can be found by multiplying the image of the correlation function of the input signal first by the system transfer function with argument p, subsequently by the same transfer function but with argument q. The formula (12) has previously been obtained by V. L. Lebedev [5] and also independently by N. P. Sevost'yanov.

The formula (12) serves as a basis for compiling the tables which simplify the determination of the correlation function of the output signal of a stationary dynamic system when its operation time is finite. The tables enable one to estimate the effect of separate elements on the accurate working of the whole system; they also enable one to detect the elements which matter most as well as those whose effect is slight, and thus reduce the analysis of the operation of a given system to a more simple one. The tables, their derivation and also examples showing their application are the subject of a separate paper.

2. Let the behavior of a dynamic system be described by the formula

$$Q(p)\,[\varphi(t)\,x] = f(t) \tag{13}$$

where $\varphi(t)$ is a known function, x(t) is the required response to the excitation f(t). The weighting function g(t, s) is given by the equation

$$Q(p)\,[\varphi(t)\,g(t.\ s)] = \delta(t - s). \tag{14}$$

We introduce the notation

$$g_1(t.\ s) = \varphi(t)\,g(t.\ s). \tag{15}$$

Then, as in the formulas (10) and (11), the incomplete image of the function $g_1(t, s)$ is given by the formula

$$G_1(p.\ s) = \frac{e^{-ps}}{Q(p)}. \tag{16}$$

But in accordance with the formulas (7) and (15), the incomplete images of the function $g_1(t,s)$ and $g(t,s)$ are related by the formula

$$G(p.\ s) = \frac{1}{\varphi(-r)} G_1(p.\ s)$$

and therefore

$$G(p.\ s) = \frac{1}{\varphi(-r)}\left[\frac{e^{-ps}}{Q(p)}\right]. \qquad G(q.\ s_1) = \frac{1}{\varphi(-r_1)}\left[\frac{e^{-qs_1}}{Q(q)}\right] \tag{17}$$

where $r \equiv \frac{\partial}{\partial p}$, $r_1 \equiv \frac{\partial}{\partial q}$. Substituting the expressions (17) into the formula (8) we obtain

$$\Phi_{kv}(p.\ q) = \frac{1}{\varphi(-r)\,\varphi(-r_1)}\left[\frac{\Phi_{kx}(p.\ q)}{Q(p)\,Q(q)}\right]. \tag{18}$$

The square brackets in the formulas (17) and (18) are here to indicate that the operators $\frac{1}{\varphi(-r)}$ and $\frac{1}{\varphi(-r_1)}$ operate on the expressions within these brackets.

In the particular case of $\varphi(t)=t$ we have

$$\Phi_{kv}(p.\ q) = \int_p^\infty \int_q^\infty \frac{\Phi_{kx}(u.\ u_1)}{Q(u)\,Q(u_1)}\,du\,du_1. \tag{19}$$

3. Let the behavior of the system be described by the equation

$$Q_1(p)\,[\varphi_1(t)\,x] + Q_2(p)\,[\varphi_2(t)\,x] = f(t) \tag{20}$$

where $\varphi_1(t)$ and $\varphi_2(t)$ are known functions, $x(t)$ the required response to the excitation $f(t)$. The weighting function is given by the equation

$$Q_1(p)\,[\varphi_1(t)\,g(t.\ s)] + Q_2(p)\,[\varphi_2(t)\ g(t.\ s)] = \delta(t-s). \tag{21}$$

We multiply both sides of the equation (21) by e^{-pt} and integrate with respect to t from s to ∞. We thus obtain the equation

$$Q_1(p)\,\varphi_1(-r)\,G(p.\ s) + Q_2(p)\,\varphi_2(-r)\,G(p.\ s) = e^{-ps} \tag{22}$$

which determines the incomplete image $G(p,s)$ of the weighting function.

The equation (22) is essentially different from (21). In the equation (21) $Q_1(p)$ and $Q_2(p)$ are operators and $\varphi_1(t)$ and $\varphi_2(t)$ are known functions of the independent variable t, but in the equation (22) $Q_1(p)$ and $Q_2(p)$ are known functions of a new independent variable p with $\varphi_1(-r)$ and $\varphi_2(-r)$ as operators. This signifies that for comparitively simple $\varphi_1(t)$ and $\varphi_2(t)$ functions, the equation (22) can be of a lower order than (21), and so the derivation of the equation (22) seems useful.

However, if even one of the functions $\varphi_1(t)$ or $\varphi_2(t)$ is more complicated than $\phi_1(p)$ or $\phi_2(p)$, or if the weighting function has already been found, then using the equation (22) instead of the equation (21) is not justified.

In particular, when $\varphi_1(t) = t$, $\varphi_2(t) = 1$, the incomplete image of the weighting function can be determined from a linear differential equation of the first order

$$-Q_1(p)\frac{dG(p,s)}{dp} + Q_2(p)\,G(p.\ s) = e^{-ps}. \tag{23}$$

The solution of the above equation which satisfies the theorem on the limiting value of the incomplete image, can be expressed by the formula

$$G(p.\ s) = \frac{1}{T(p)} \int_p^\infty e^{-us} \frac{T(u)}{Q_1(u)}\, du \tag{24}$$

where the function T(u) is given by the relation

$$\ln T(u) = -\int_a^u \frac{Q_2(v)}{Q_1(v)}\, dv \tag{25}$$

(a is fixed and can be selected in any suitable way).

Similarly,

$$G(q.\ s_1) = \frac{1}{T(q)} \int_q^\infty e^{-u_1 s_1} \frac{T(u_1)}{Q_1(u_1)}\, du_1. \tag{26}$$

Substituting the formulas (24) and (26) into the relation (8) and inverting the order of integration we obtain

$$\Phi_{ky}(p.\ q) = \frac{1}{T(p)\,T(q)} \int_p^\infty \int_q^\infty \frac{T(u)}{Q_1(u)} \frac{T(u_1)}{Q_1(u_1)} \Phi_{kx}(u.\ u_1)\, du\, du_1. \tag{27}$$

Having compared the formula (27) with formulas (19) and (12) we conclude that the correlation function of the output signal of a dynamic system described by the equation

$$Q_1(p)(tx) + Q_2(p)\,x = f(t) \tag{28}$$

is the same as the correlation function of an output signal of an open system consisting of three units in series: a unit with the transfer function $T(p)/Q_1(p)$, a multiplier unit by 1/t, and a unit with transfer function $1/T(p)$.

The above can be of use when determining the correlation function of the signal at the output of a nonstationary dynamic system.

Example. White noise is fed to the input of a system described by the equation

$$tx + (ct + 2)\,x = f(t). \tag{29}$$

We shall determine the correlation function of its output signal.

Using the procedure worked out in [5], the equation (29) takes the form

$$(p + c)(tx) + x = f(t).$$

In the case under consideration we have

$$Q_1(p) = p + c. \quad \varphi_1(t) = t. \quad Q_2(p) = 1. \quad \varphi_2(t) = 1.$$

In order to simplify, we take a = c - 1, and therefore

$$T(u) = \frac{1}{u + c}.$$

$$\Phi_{kx}(u.\ u_1) = \int_0^\infty \int_0^\infty \delta(t - t_1)\, e^{-ut - u_1 t_1}\, dt\, dt_1 = \frac{1}{u + u_1}. \tag{30}$$

$$\Phi_{ky}(p.\ q) = (p + c)(q + c) \int_p^\infty \int_q^\infty \frac{du\, du_1}{(u + c)^2 (u_1 + c)^2 (u + u_1)}$$

As far as the performance of the system is concerned, it is equivalent to one containing three units in series.

1. A unit with its transfer function equal to $\frac{1}{(p+c)^2}$. The image of the correlation function of the signal at the output of such a unit is given by the expression

$$\Phi_1(p.\ q) = \frac{1}{(p+c)^2(q+c)^2(p+q)}.$$

Applying the inversion formula for two-dimensional Laplace transforms [2], we find that the correlation function

$$K_1(t.\ t_1) = \frac{1}{4c^3}\, e^{-c(t-t_1)}\left[1 + c(t-t_1) - e^{-2ct_1}(1 + ct + ct_1 + 2c^2tt_1)\right]$$

corresponds to the image $\Phi_1(p, q)$ for $t \geq t_1$.

2. A multiplier by 1/t. The correlation function of the signal at the output of the second unit is given by the expression

$$K_2(t.\ t_1) = \frac{1}{4c^3tt_1}\, e^{-c(t-t_1)}\left[1 + c(t-t_1) - e^{-2ct_1}(1 + ct + ct_1 + 2c^2tt_1)\right].$$

The function $k_2(t, t_1)$ has the image

$$\Phi_2(p.\ q) = \int_p^\infty \int_q^\infty \frac{du\, du_1}{(u+c)^2(u_1+c)^2(u+u_1)}.$$

3. A unit with transfer function p+c. The formula (30) is now equivalent to

$$\Phi(p.\ q) = (q+c)(p+c)\,\Phi_2(p.\ q),$$

therefore

$$K_y(t.\ t_1) = \left(\frac{\partial}{\partial t_1} + c\right)\left[\left(\frac{\partial}{\partial t} + c\right)K_2(t.\ t_1)\right].$$

By carrying out the operation we find for $t \geq t_1$

$$K_y(t.\ t_1) = \frac{e^{-c(t-t_1)}}{4c^3t^2t_1^2}\,(2c^2t_1^2 - 2ct_1 + 1 - e^{-2ct_1}).$$

The value of a correlation function, when $t \leq t_1$ can be determined from its symmetry about the line $t = t_1$.

LITERATURE CITED

1. V. S. Pugachev, Teoria Sluchainykh Funktsii i ee Primenenie k Zadacham Avtomatichsekovo Upravleniya, (Gostekhizdat,(1957).
2. V. A. Ditkin and A. P. Prudnikov, Operatsionnoe Ischislenie po Dwum Peremennym i evo Prilozhenie, (Fizmatgiz, 1958).
3. Ed. V. V. Solodovnikov, Osnovy Avtomaticheskovo Regulirovaniya. Theory (Mashgiz, 1954).
4. M. F. Gardner and J. L. Barnes, Transients in Linear Systems (John Wiley & Sons, Inc. 1949) (Russian translation).
5. V. L. Lebedev, Sluchainye Protsessy w Elektricheskikh i Mekhanicheskikh Sistemakh (Fizmatgiz, 1958).
6. A. N. Skl'yarevich, O predstavlenii nestatsionovo lineinovo differential'novo operatora-polinoma vide summy statsionarnykh operatorov, Avtomatika i Telemekhanika 22, No. 3 (1961) (English translation available).*

*See English translation.

STRUCTURE TRANSFORMATION OF LINEAR VARYING-PARAMETER SYSTEMS

A. V. Solodov

(Moscow)

Translated from Avtomatika i Telemekhanika, Vol. 22, No. 5,
pp. 577-588, May, 1961
Original article submitted September 22, 1960

Block-diagrams of varying-parameter systems containing two kinds of generalized units are considered, viz. the lag and the phase-lead unit. Transformation rules are given of these block-diagrams obtained by the application of linear differential operators. The results are illustrated by an example.

1. Introduction

A block-diagram of a system represents usually, in a conventionally accepted manner, the interconnections of elements or units constituting the whole system, and being differentiated only by their dynamic properties. A system with variable parameters can also be represented by a block-diagram in the same way as the systems with constant parameters; the system will only contain four different types of units, called elementary units: the integrator, the differentiator, the adder, and the multiplier with a variable gain coefficient. In many cases, however, such a detailed breakdown may not prove appropriate, and it may prove sufficient to represent the system as consisting of bigger blocks. Reflecting the block-diagram structure there will be equations describing the motion of the system and establishing the connections between the input and the output signals. Only a block-diagram, however, will clearly display the interconnections between the blocks as well as the propagation path of the signals in the system; this enables one to penetrate deeper and to get a true insight into the working either of an element or of the system as a whole.

It is well known that the block-diagram method in automatic control systems with constant coefficients has been used for some time and that it has developed considerably (for example, see [1]). The difficulty in constructing a corresponding apparatus for varying-parameter systems lies primarily in the fact that it is not possible to algebraize, in the general case, the differential equations which, of course, prevents one also from obtaining simple rules as was the case in systems with constant parameters. A way of tackling this problem was outlined in [2].

There are three main problems for which the transformation rules for block-diagrams representing varying-parameter systems can be used.

First of all, by using the method and the rules of block-diagram transformations one is able to find, for practically all feasible combinations, the sequence of operations leading from one system to the other one previously given. This indicates, that by taking into consideration the corresponding differential equations, an algorithm for transforming one system of equations into another one can be established.

Further, in synthetizing linear optimem systems one has to construct a block-diagram of the optimum system such that it is actually realizable in spite of an unavoidable presence of certain elements and connections given beforehand. This problem arises in the synthesis of compensating circuits.

Finally, as an actual system represents a combination of units and elements, some of which may be complete assemblies, the necessity arises, when investigating the system, of transferring similar elements to other places leaving their structure intact.

The resulting block-diagram transformations are of course equivalent to the corresponding transformation results on differential equations and so the result cannot be simple unless appropriate approximations are used. As the latter are only feasible when actually solving practical problems, we shall not be able to consider them.

Transformations of such block-diagrams shall be considered below – those containing only two different types of generalized units: the lagging or the phase-leading one.

The general case of a linear system with variable parameters can be described by the equation

$$\sum_{i=0}^{n} a_i t \frac{d^i x_{out}}{dt^i} = \sum_{j=0}^{m} b_j(t) \frac{d^j x_{in}}{dt^j} \tag{1}$$

where x_{in} is the input signal, x_{out} the output signal $a_i(t)$ and $b_j(t)$ are given functions of time t.

We shall say that a block-diagram element is lagging if the relation between the input and the output signals is

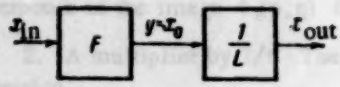

Fig. 1

$$\sum_{i=0}^{n} a_i(t) \frac{d^i x_{out}}{dt^i} = x_0 \tag{2}$$

where x_{out} is the output and x_0 the input signal of the element.

These units will be denoted by $\frac{1}{L}$ on the block-diagrams.

An elements of the block-diagram shall be said to be leading if the input and the output signals are related by

$$y = \sum_{j=0}^{m} b_j(t) \frac{d^j x_{in}}{dt^j} \tag{3}$$

where y is the output and x_{in} is the input signal of the element.

The notation adopted for these units on the block-diagrams is the symbol F.

When $y = x_0$, the expressions (2) and (3) give jointly the equation (1). Therefore, a block-diagram of a varying-parameter system can be represented by the introduced units; the simplest way is to represent it by a leading unit whose output is connected in series with a lagging one (Fig. 1).

The above introduced units can be found in block-diagrams representing automatic control systems in various combinations and with differing parameters, in forward and feedback networks and are both of main and compensatory character. When opening the feedback network of a varying parameter system, we obtain a system of elements in series whose joint dynamic behavior depends on the point of opening, which is not true for a system with constant parameters. In other words, the units of a varying-parameter system are not commutative. This implies that with two feedback contours consisting of identical elements but connected in a different order, different transformation rules are necessary.

2. Transforming Block-Diagrams with the Aid of Linear Operators

The equation (1) of a linear varying-parameter system can be written in its operational form as

$$V_1 x_{out} = V_2 x_{in} \tag{4}$$

where

$$V_1 = \sum_{i=0}^{n} a_i(t) p^i. \quad V_2 = \sum_{j=0}^{m} b_j(t) p^j$$

are linear differential operators and $p = d/dt$.

In agreement with the previously introduced definitions, the equation of the lag element is written in the form

$$L x_{out} = x_0 \tag{5}$$

and of the phase-leading element as

$$y = F x_{in} \tag{6}$$

where L and F are the respective linear differential operators.

The transformation rules of block-diagrams considered below boil down in the end to finding some new operators which are the results of transformations of the original ones.

Let there be two lag units with their equations

$$L_1 x_1 = x_0. \quad L_2 x_2 = x_1.$$

Required to find the operator representing their operation in tandem. Substituting the second into the first equation, we have

$$L_1 [L_2 x_2] = x_0.$$

The left-hand side of this equation should be regarded as operation L_1 acting on the operator L_2 but not as their product. That is why we introduce a special symbol

$$L_0 = L_1 * L_2$$

to denote this operation. Thus the result shall be written in the form

$$L_0 x_2 = [L_1 * L_2] x_2 = x_0.$$

An operator operating on another one constitutes the basic tool in block-diagram transformations. It is given by the formula

$$V_1 * V_2 = \sum_{l=0}^{n} \frac{\partial^l V_1}{\partial p^l} V_2 \frac{p^l}{l!} \tag{7}$$

where

$$V_1 = \sum_{i=0}^{n} a_i(t)\, p^i. \quad V_2 = \sum_{j=0}^{m} b_j(t)\, p^j$$

or

$$V_0 = V_1 * V_2 = \sum_{q=0}^{n+m} A_q(t)\, p^q \tag{8}$$

where

$$A_q(t) = \sum_{i=0}^{n} a_i(t)\, N_{iq} \tag{9}$$

$$N_{iq} = \sum_{j=0}^{q} C_i^{j-q+i} p^{j-q+i} b_j(t). \tag{10}$$

The differentiation symbol p in these formulas only relates to the functions which follow it directly. The formulas have of course all the properties resulting from the linearity of these operators.

Without pausing to give simple examples of transformations which follow directly from the above formulas, we shall proceed to consider transformation rules for block-diagrams with feedbacks.

Lead-lag block with a follow-up. From the block-diagram, Fig. 2a, we obtain

$$Lx_2 = F\varepsilon, \quad \varepsilon = x_0 - x_2$$

and hence

$$[L - F]\, x_2 = F x_0. \tag{11}$$

Thus the obtained lead-lag block has its variable lagging part operator equal to L − F (Fig. 2, b).

Lag block in network with feedback containing a lag block. From the block diagram Fig. 2, c, we have

$$L_1 x_2 = \varepsilon. \quad L_2 x_1 = x_2. \quad \varepsilon = x_0 + x_1$$

and hence

$$[L_2 * L_1 - 1] = L_2 x_0. \tag{12}$$

Thus a feedback network of the above type can be represented as a lag-leading block with respective operators as in Fig. 2, d.

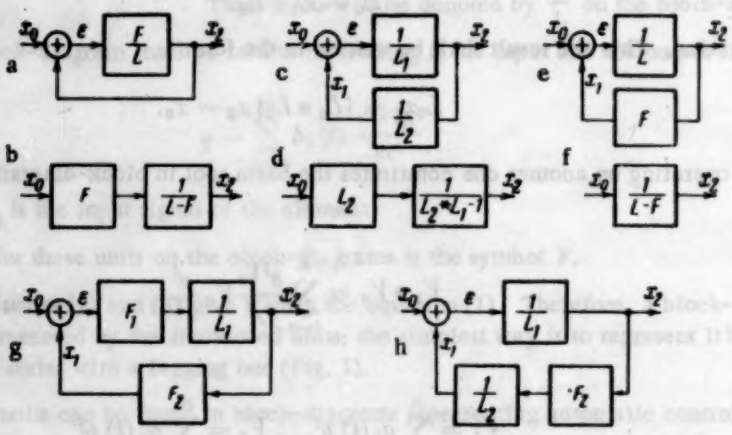

Fig. 2

Lag block in a network with feedback containing a leading block. From the block-diagram Fig. 2, e, we obtain

$$Lx_2 = \varepsilon, \quad x_1 = Fx_2, \quad \varepsilon = x_0 + x_1$$

and hence

$$[L - F]\, x_2 = x_0. \tag{13}$$

Consequently, the considered network can be made equivalent to a leading block with the operator L - F (Fig. 2,f).

Lag-lead block in a network with feedback containing a leading block. From the block-diagram in Fig. 2, g, we obtain

$$L_1 x_2 = F_1 \varepsilon. \quad x_1 = F_2 x_2. \quad \varepsilon = x_0 + x_1$$

and hence

$$[L_1 - F_1 * F_2]\, x_2 = F_1 x_0. \tag{14}$$

We thus obtain again a lag-lead block but with a different lag operator.

Lag block in a network with feedback containing a lag-lead block. From the block diagram in Fig. 2,h we obtain

$$L_1 x_2 = \varepsilon. \quad L_2 x_1 = F_2 x_2. \quad \varepsilon = x_0 + x_1$$

and hence

$$[L_2 * L_1 - F_2]\, x_2 = L_2 x_0. \tag{15}$$

The studied network is therefore transformed into a lag-lead one with appropriate operators.

The discussed block-diagram transformations illustrate adequately in what manner the linear differential operators are used. Other relations could be obtained in a similar way. The resulting new operators are easily obtained by using the formula (7). One does easily notice, however, that in all our examples we have managed to eliminate the intermediate variables by performing appropriate substitutions. If the latter cannot be carried out, a transformation of a block-diagram by our worked out methods does not prove possible. For example, in the equations

$$L_1 x_1 = x_0. \quad L_2 x_1 = x_2 \tag{16}$$

one cannot eliminate the intermediate x_1 by our methods.

In order to solve the problems in which more complicated block-diagrams occur, when it is required to eliminate such intermediate variables for which the equations are not solved, a method is used which shall be called the equalizing operators method. Operating on the left- and the right-hand sides of the expression (16) with some, still undetermined operators U_1 and U_2, we have

$$[U_1 * L_1]\, x_1 = U_1 x_0. \quad [U_2 * L_2]\, x_1 = U_2 x_2 \tag{17}$$

and we demand that it be true identically

$$U_1 * L_1 = U_2 * L_2. \tag{18}$$

Then the left-hand sides of the expressions in (17) are equal to one another, and we obtain

$$U_1 x_0 = U_2 x_2.$$

In this manner the intermediate variable has been eliminated.

Now it is necessary to find the operators U_1 and U_2, which would ensure the equality of the left-hand sides of the expression (17). We note, first of all, that for the operators to be equal it is necessary that their orders as well as the coefficients of the same order be equal. Consequently, if in the expression (18) the operator L_1 is of the order n and the operator L_2 of the order m, the orders ν and μ of the operators U_1 and U_2 respectively should be such that the equality

$$\nu + n = \mu + m = r$$

be satisfied where r is the common order of the expressions (18). As r = n + m, therefore ν = m and μ = n.

By comparing the coefficient of equal powers of p in the expressions (18) of the operators $U_1 * L_1$ and $U_2 * L_2$, one obtains r + 1 linear algebraic equations between the unknown coefficients of the operators U_1 and U_2. We have shown that the operator U_1 must be of the order ν = m and it must, therefore, contain m + 1 coefficients, and similarly that the operator U_2 of the order μ = n will contain n + 1 coefficients. The total number of unknowns is therefore r + 2, and one of the coefficients either of the operator U_1 of U_2 can be assigned an arbitrary value.

Thus, let

$$L_1 = \sum_{i=0}^{n} a_i p^i. \qquad L_2 = \sum_{j=0}^{m} b_j p^j. \tag{19}$$

Then

$$U_1 = \sum_{j=0}^{m} \alpha_j p^j. \qquad U_2 = \sum_{i=0}^{n} \beta_i p^i \tag{20}$$

where the coefficients α_j and β_j are still unknown and to be determined.

The operators $U_1^* L_1$ and $U_2^* L_2$ are expressed in the form

$$U_1 * L_1 = \sum_{k=0}^{r} A_k p^k. \qquad U_2 * L_2 = \sum_{k=0}^{r} B_k p^k. \tag{21}$$

By taking also the identity (18) into account, we obtain

$$A_k = B_k \quad (k = 0.\ 1.\ 2. \ldots . r).$$

By applying the formulas (8) and (9) and from expression (19) and (20) we obtain

$$\sum_{i=0}^{m} \alpha_i N_{iq}^{\alpha} = \sum_{j=0}^{n} \beta_j N_{jq}^{\beta} \quad (q = 0.\ 1.\ 2. \ldots . r) \tag{22}$$

where the functions

$$N_{iq}^{\alpha} = \sum_{k=0}^{q} C_i^{i-q+k} p^{i-q+k} a_k. \quad N_{jq}^{\beta} = \sum_{k=0}^{q} C_j^{j-q+k} p^{j-q+k} b_k \tag{23}$$

are known because the coefficients a_i and b_j are known.

By putting $\alpha_m = 1$ in the equations (22) which is possible because the value of one unknown can be assigned arbitrarily, and by transposing the terms containing the unknowns to the left-hand side, a system of r + 1 linear algebraic equations is obtained

$$\alpha_0 N_{0q}^{\alpha} - \beta_0 N_{0q}^{\beta} + \alpha_1 N_{1q}^{\alpha} - \beta_1 N_{1q}^{\beta} + \ldots + \alpha_{m-1} N_{(m-1)q}^{\alpha} - \beta_n N_{nq}^{\beta} = - N_{mq}^{\alpha}$$
$$(q = 0.\ 1.\ 2. \ldots . r). \tag{24}$$

whose solution will provide the sought coefficients α_i and β_j of the equalizing operators U_1 and U_2.

We shall now consider block-diagram transformations in which the above described method should be used.

Moving a leading block behind a lag block. From the block diagram shown in Fig. 3, a, we obtain

$$F_1 x_1 = x_{in}. \quad x_{out} = F_1 x_1.$$

Operating with equalizing operators

$$[U_1 * L_1]\, x_1 = U_1 x_{in}. \quad [U_2 * F_1]\, x_1 = U_2 x_{out}$$

we obtain

$$U_2 x_{out} = U_1 x_{in} \tag{25}$$

provided that

$$U_1 * L_1 = U_2 * F_1. \tag{26}$$

The transformed block-diagram is shown in Fig. 3,b.

Lag-leading blocks with feedback containing another lag block. From the block-diagram Fig. 3,c, we obtain the equations

$$L_1 x_2 = F_1 x_0 + F_1 x_1 \qquad L_2 x_1 = x_2.$$

By applying the equalizing operators we get

$$[U_1 * L_1]\, x_2 = [U_1 * F_1]\, x_0 + [U_1 * F_1]\, x_1. \quad [U_2 * L_2]\, x_1 = U_2 x_2$$

and in view of the identity

$$U_1 * F_1 = U_2 * L_2 \tag{27}$$

we finally obtain

$$[U_1 * L_1 - U_2]\, x_2 = [U_1 * F_1]\, x_0. \tag{28}$$

The resulting block-diagram is shown in Fig. 3, d.

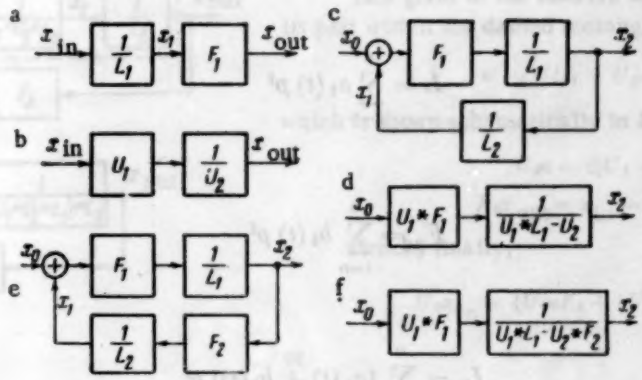

Fig. 3

Lag-leading block in a network with feedback containing a lag-leading block. For the block-diagram shown in Fig. 3,e, the following equations are valid:

$$L_1 x_2 = F_1 x_0 + F_1 x_1. \quad L_2 x_1 = F_2 x_2.$$

By applying the equalizing operators and performing transformations similar to those in the preceding case, we obtain

$$[U_1 * L_1 - U_2 * F_2]\, x_2 = [U_1 * F_1]\, x_0 \tag{29}$$

$$U_1 * F_1 = U_2 * L_2. \tag{30}$$

The resulting block-diagram takes the form shown in Fig. 3, f.

The preceding examples lead to transformation rules for other types of diagrams. The derived formulas and transformations enable one to "convolve" the elements of any given system so that it will be transformed to any previously given type of system; in particular, this can be done when a single equation connects the input and the output. In the case of a constant-parameter system, the respective operators representing the components are formally identical with complex Laplace transforms expressions. All our formulas and results of transformations are, of course, also valid in the constant-parameter case, but in addition the formula (7) then takes a particularly simple form

$$V_1 * V_2 = V_1 V_2 = V_2 V_1.$$

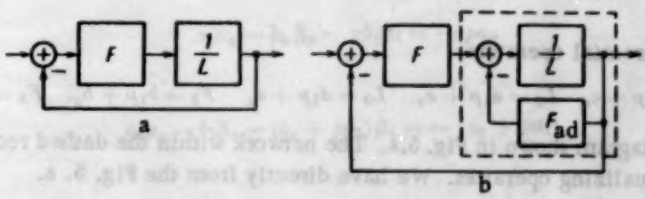

Fig. 4

When constructing automatic control systems with varying-parameter components it is useful sometimes to make the whole system into a filter with constant parameters. To achieve this, it is obviously necessary to find the corresponding matching complementary blocks together with their mode of connection in such a way that the required result is obtained. Let, for example, the block-diagram of a servo be, as shown in Fig. 4,a with block F of a constant-parameter type. It is required to obtain additional elements in such a way that the complete new system becomes a constant-parameter filter. We join the lag block $\frac{1}{L}$ to a negative feedback containing a leading block F_{ad} (Fig. 4,b). The operator of the new block within the dashed lines is equal to

$$L_0 = L + F_{ad}.$$

Further, assuming that

$$L = \sum_{i=0}^{n} a_i(t)\, p^i$$

then, by putting

$$F_{ad} = \sum_{i=0}^{n} b_i(t)\, p^i$$

we obtain

$$L_0 = \sum_{i=0}^{n} [a_i(t) + b_i(t)]\, p^i.$$

When the condition

$$a_i(t) + b_i(t) = \text{const}$$

is fulfilled, the operator L_0 has constant coefficients as required. Such an approach is advantageous as one can obtain the values of the coefficients of the operators L_0 by a suitable selection of the functions $b_i(t)$ such that they be equal, for example, either to the mean values of the coefficients $a_i(t)$ or, say, to their maximum values. In this way the dynamic characteristics of the new block can be made to become close to those of the old one at certain fixed values of its parameters. It is obvious that with several blocks with variable parameters, the above method can be applied to each block independently; moreover, it is even possible to find one big feedback including all the blocks with variable parameters. In order to achieve this, we must perform a transformation in accordance with the rules previously described, thus reducing the system to one with one or two blocks.

Example. Given a system described by the equations:

$$a_1(t)\frac{dx_2}{dt} + a_0(t)\, x_2 = x_1$$

$$x_3 = b_1(t)\frac{dx_2}{dt} + b_0(t)\, x_2$$

$$c_2(t)\frac{d^2x_1}{dt^2} + c_1(t)\frac{dx_1}{dt} + c_0(t)\, x_1 = x_{in} - x_3 - x_4$$

$$d_1(t)\frac{dx_{out}}{dt} + d_0(t)\, x_{out} = x_1. \quad x_4 = e_1(t)\frac{dx_{out}}{dt} + e_0(t)\, x_{out}$$

Required a transformation such that the connection between the input and the output signal be described by a single equation.

By introducing the differential operators

$$L_1 = c_2p^2 + c_1p + c_0 \quad L_2 = a_1p + a_0. \quad L_3 = d_1p + d_c. \quad F_2 = b_1p + b_0. \quad F_3 = e_1p + e_0 \tag{31}$$

we can construct the block-diagram shown in Fig. 5,a. The network within the dashed rectangle can easily be transformed with the aid of the equalizing operators. We have directly from the Fig. 5, a.

$$L_1x_1 = \varepsilon - x_3. \quad L_2x_2 = x_1. \quad x_3 = F_2x_2.$$

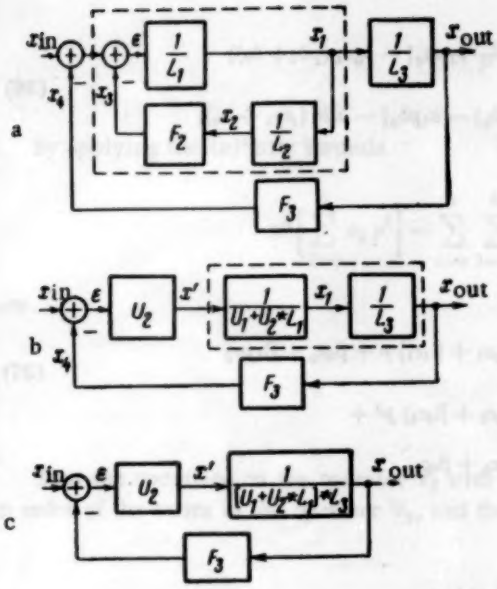

Fig. 5

Introducing the equalizing operators we obtain

$$[U_1 * L_2]\, x_2 = U_1 x_1. \quad [U_2 * F_2]\, x_2 = U_2 x_3$$

and hence

$$U_2 \varepsilon = [U_1 + U_2 * L_1]\, x_1 \tag{32}$$

as

$$U_1 * L_2 = U_2 * F_2. \tag{33}$$

This gives us the network shown in Fig. 5,b. Transforming its part within the dashed rectangle, we obtain

$$x' = \{[U_1 + U_2 * L_1] * L_3\}\, x_{\text{out}}$$

which is shown schematically in Fig. 5,c. Then, we obtain

$$U_2 \varepsilon = \{[U_1 + U_2 * L_1] * L_3\}\, x_{\text{out}}$$

$$F_3 x_{\text{out}} = x_{\text{in}} - \varepsilon, \quad x_{\text{in}} - F_3 x_{\text{out}} = \varepsilon.$$

Hence, finally,

$$U_2 x_{\text{in}} = \{U_2 * F_3 + [U_1 + U_2 * L_1] * L_3\}\, x_{\text{out}} \tag{34}$$

or

$$U_2 x_{\text{in}} = L_0 x_{\text{out}} \quad L_0 = U_2 * F_3 + [U_1 + U_2 * L_1] * L_3. \tag{35}$$

In order to find explicitly the operator expressions (35), it is necessary to determine, first of all, the operators U_1 and U_2. In view of (33) and (31), these operators must be of the form

$$U_1 = \alpha_1 p + \alpha_0. \quad U_2 = \beta_1 p + \beta_0$$

and the operators $U_1 * L_2$ and $U_2 * F_2$ are both of the order r = 2.

From the (23) formulas, we obtain:

when q = 0

$$N^{\alpha}_{00} = 0. \qquad N^{\beta}_{00} = b_0$$
$$N^{\alpha}_{10} = pa_0. \quad N^{\beta}_{10} = pb_0;$$

when q = 1

$$N^{\alpha}_{01} = a_1 \qquad N^{\beta}_{01} = b_1$$
$$N^{\alpha}_{11} = a_0 + pa_1 \qquad N^{\beta}_{11} = b_0 + pb_1$$

when q = 2

$$N^{\alpha}_{02} = 0 \qquad N^{\beta}_{02} = 0$$
$$N^{\alpha}_{12} = a_1 \qquad N^{\beta}_{12} = b_1.$$

Applying the formulas (24) and putting $\alpha_1 = 1$ gives:

when q = 0

$$a_0\alpha_0 - b_0\beta_0 - pb_0\beta_1 = -pa_0$$

when q = 1

$$a_1\alpha_0 - b_1\beta_0 - (b_0 + pb_1)\beta_1 = -(a_0 + pa_1)$$

when q = 2

$$0\alpha_0 + 0\beta_0 - b_1\beta_1 = -a_1.$$

By solving these simultaneous equations we obtain the required coefficients of the operators U_1 and U_2:

$$\alpha_0 = \frac{1}{b(a_0b_1 - b_0a_1)}\{b_1[a_1pb_0 + b_0(pa_1 + a_0) - b_1pa_0] - b_0a_1(pb_1 + b_0)\}$$
$$\beta_0 = -\frac{1}{b_1(a_0b_1 - b_0a_1)}\{a_1[b_1pa_0 + a_0(pb_1 + b_0) - a_1pb_0] - a_0b_1(pa_1 + a_0)\} \quad (36)$$
$$\beta_1 = \frac{a_1}{b_1}. \quad \alpha_1 = 1.$$

Now applying the formulas (7) we obtain

$$U_2 * F_2 = U_2F_2 + \frac{\partial U_2}{\partial p}F_2p = \beta_1e_1p^2 + (\beta_1pe_1 + \beta_0e_1 + \beta_1e_1)p + \beta_0e_0 + \beta_1pe_0 \quad (37)$$
$$U_2 * L_1 = U_2L_1 + \frac{\partial U_2}{\partial p}L_1p = \beta_1c_2p^3 + (\beta_1pc_2 + \beta_0c_2 + \beta_1c_1)p^2 +$$
$$+ (\beta_1pc_1 + \beta_0c_1 + \beta_1c_0)p + \beta_1pc_0 + \beta_0c_0.$$

We have further

$$U_1 + U_2 * L_1 = a_{43}p^3 + a_{42}p^2 + a_{41}p + a_{40}$$

where

$$a_{43} = \beta_1c_2. \quad a_{42} = \beta_1pc_2 + \beta_0c_2 + \beta_1c_1. \quad a_{41} = \beta_1pc_1 + \beta_0c_1 + \beta_1c_0 + \alpha_1 \quad (38)$$
$$a_{40} = \beta_1pc_0 + \beta_0c_0 + \alpha_0.$$

Applying again the formula (7) we obtain

$$L_4 * L_3 = L_4L_3 + \frac{\partial L_4}{\partial p}L_3p + \frac{\partial^2 L_4}{\partial p^2}L_3\frac{p^2}{2} + \frac{\partial^3 L_4}{\partial p^3}L_3\frac{p^3}{6} = \quad (39)$$
$$= b_{44}p^4 + b_{43}p^3 + b_{42}p^2 + b_{41}p + b_{40},$$

where

$$b_{44} = a_{42}d_1$$
$$b_{43} = 3a_{43}pd_1 + \frac{1}{2}a_{42}d_1 + a_{42}d_0$$
$$b_{42} = 3a_{43}pd_0 + \frac{1}{2}a_{42}d_0 + a_{41}d_1 + a_{42}pd_1 + 3a_{43}p^2d_1 \quad (40)$$
$$b_{41} = a_{41}d_0 + a_{42}pd_0 + 3a_{43}p^2d_0 + a_{40}d_1 + a_{41}pd_1 + a_{42}p^2d_1 + a_{43}p^3d_1$$
$$b_{40} = a_{40}d_0 + a_{41}pd_0 + a_{42}p^2d_0 + a_{43}p^3d_0.$$

By substituting the expressions (37) and (39) into (35) we finally obtain

$$L_0 = b_{44}p^4 + b_{43}p^3 + (b_{42} + \beta_1e_1)p^2 +$$
$$+ (b_{41} + \beta_1pe_1 + \beta_0e_1 + \beta_1e_1)p + b_{40} + \beta_0e_0 + \beta_1pe_0. \quad (41)$$

The coefficients of the operators L_0 and U_2 can be computed with the aid of the expressions (36), (38) and (40).

APPENDIX

We shall now find a formula expressing the result of the operation of one operator on another

Given operators

$$V_1 = \sum_{i=0}^{n} a_ip^i \qquad V_2 = \sum_{j=0}^{m} b_jp^j.$$

Consider the following differential equation

$$p^k \circ V = p^k \Big[\sum_{i=0}^{n} a_i p^i\Big].$$

By applying the Leibnitz formula

$$p^k \Big[\sum_{i=0}^{n} a_i p^i\Big] = \sum_{i=0}^{n} \sum_{\lambda=0}^{k} C_k^\lambda (p^\lambda a_i)\, p^{k-\lambda+i} = \sum_{\lambda=0}^{k} C_k^\lambda (p^\lambda V)\, p^{k-\lambda} \tag{42}$$

where

$$p^\lambda V = \sum_{i=0}^{n} (p^\lambda a_i)\, p^i.$$

Thus the operation on the operator V_2 with the operator V_1 is equivalent to successive differentiation up to the n-th order of the terms of the operator V_2, and the multiplication by the coefficients a_i

$$V_1 \circ V_2 = \sum_{i=0}^{n} a_i (p^i \circ V_2)$$

as the elimination of the intermediate variable x_1 in the equations

$$V_1 x_1 = x_0. \quad V_2 x_2 = x_1$$

leads exactly to the relation

$$[V_1 \circ V_2]\, x_2 = x_0.$$

When applying the formula (42) to the operator V_2 we obtain

$$p^i \circ V_2 = \sum_{\lambda=0}^{i} C_i^\lambda (p^\lambda V_2)\, p^{i-\lambda}.$$

We multiply both sides of the last relation by $a_i(t)$ and add

$$\sum_{i=0}^{n} a_i (p^i \circ V_2) = V_1 \circ V_2 = \sum_{i=0}^{n} \sum_{\lambda=0}^{i} C_i^\lambda a_i (p^\lambda V_2)\, p^{i-\lambda}$$

or, changing the summation index

$$V_1 \circ V_2 = \sum_{i=0}^{n} \sum_{l=0}^{i} C_i^{i-l} a_i p^{i-l} V_2 p^l. \tag{43}$$

Considering the sum

$$\sum_{i=0}^{n} C_i^{i-l} a_i p^{i-l}$$

we note that

$$\frac{1}{l!} \frac{\partial^l V_1}{\partial p^l} = \sum_{i=0}^{n} C_i^{i-l} a_i p^{i-l}$$

and this gives us the formula (7):

$$V_1 \cdot V_2 = \sum_{l=0}^{n} \frac{\partial^l V_1}{\partial p^l} V_2 \frac{p^l}{l!}.$$

By substituting the value of the operator V_2 into (43), we obtain

$$V_0 = V_1 \cdot V_2 = \sum_{i=0}^{n} \sum_{l=0}^{i} \sum_{j=0}^{m} C_i^{i-l} a_i p^{i-l} b_j p^{l+j}.$$

The order of this operator is obviously determined by the exponent of p^{l+j}, and it is equal to n+ m. This implies that the operator V_0 contains n + m + 1 powers of p with corresponding coefficients, and it can be represented in the form

$$V_0 = \sum_{q=0}^{n+m} A_q(t)\, p^q.$$

The expressions for these coefficients can easily be written if it is taken into account that the power with the exponent q is obtained by varying the index l from zero to q and the index j from q to 0 in such a way that l + j always equals q. Then

$$V_0 = \sum_{i=0}^{n} \sum_{q=0}^{i+j} \sum_{j=0}^{m} a_i C_i^{i-q+j} p^{i-q+j} b_j p^q$$

and

$$A_q(t) = \sum_{i=0}^{n} \sum_{j=0}^{q} a_i C_i^{i-q+j} p^{i-q+j} b_j.$$

We introduce the notation

$$N_{iq} = \sum_{j=0}^{q} C_i^{i-q+j} p^{i-q+j} b_j. \tag{44}$$

Then

$$A_q(t) = \sum_{i=0} a_i N_{iq}. \tag{45}$$

The expressions (44) and (45) determine fully the formulas (8) and (9).

LITERATURE CITED

1. Ed. V. V. Solodovnikov, Osnovy Avtomaticheskovo Regulirovaniya. Theory (Mashgiz, 1954).
2. L. A. Zadeh, Circuit analysis of linear varying-payameter networks, J. App. Phys. vol. 21 (1950).

THE ANALYSIS OF NONLINEAR AND EXTREMAL PULSE SYSTEMS BY APPLYING THE INCREMENTAL PHASE PLANE METHOD

V. M. Kuntsevich

(Kiev)

Translated from Avtomatika i Telemekhanika, Vol. 22, No. 5,
pp. 589-598, May, 1961
Original article submitted October 17, 1960

The analysis is carried out of certain nonlinear and extremal pulse systems in the incremental phase plane. The incremental-phase-plane method is made more precise and further developed. The boundaries of the switching regions are determined, and systems with delay and systems with nonlinear and pulse correction are investigated.

Nonlinear pulse systems, and in particular, relay pulse systems, were investigated in [1-6].

For the investigation of nonlinear pulse systems with amplitude modulation, J. Aseltine in [6] proposed the application of the incremental phase plane, in which the coordinates were the variable itself and its first difference. By the application of this method, which is, in our opinion, the most illuminating and convenient of those at present available, we carry out below the analysis of certain types of extremal and relay pulse systems. We will also make more precise and develop to a certain extent some applications of this method, namely: the determination of the boundaries of the switching regions, the investigation of systems containing loops with a delay and circuits with nonlinear and pulse corrections, and the investigation of pulse systems of the third order.

1. The Investigation of the Simplest Extremal Pulse Systems

The principle of operation of extremal systems, including step systems, is well known (see, for example, [7]), and so we turn directly to the consideration of certain very simple extremal pulse systems. We will analyse the transitional processes in these systems for impulse perturbations (or for nonlinear initial conditions), assuming as in [8,9] that, as a result of the perturbation impulse, the extremal characteristic is displaced and occupies some new quasi-motionless position, which for simplicity of calculation will be taken to be the origin for the analysis. The structural scheme of the system is shown in Figure 1, a.

We write the equations of a section of the system as

$$\mu = \alpha_1 u \tag{1}$$

$$\tau_1 \dot{x} + x = \alpha_2 \mu \tag{2}$$

$$\varphi = -\alpha_3 x^2. \tag{3}$$

With the assumption that the coordinate x can be measured directly, or in the opposite case with the assumption that a model is available of the linear part of the object of control, the equation for extremal control of the relay type* can be written in the form

$$u = \begin{cases} \operatorname{sign} \Delta\varphi_{n-1}\, \Delta x_{n-1} & \text{for } n \leqslant \bar{t} \leqslant n+\gamma \\ 0 & \text{for } n+\gamma \leqslant \bar{t} \leqslant n+1 \end{cases} \tag{4}$$

where $\bar{t} = \frac{t}{T}$, T = const, $\gamma \ll 1$.

*In [8] a system with proportional control was studied.

When we solve (3) and (4) simultaneously, we obtain

$$u_n = -\operatorname{sign}(x_n + x_{n-1}). \tag{5}$$

Further, the simultaneous solution of (1), (2), and (5) yields the equation for the dynamics of the system in the form

$$\Delta^2 x_n + \left(1 - e^{-\frac{1}{\tau}}\right)\Delta x_n = -\alpha\left(1 - e^{-\frac{1}{\tau}}\right)u_{n+1} \tag{6}$$

where

$$u_{n+1} = -\operatorname{sign}(x_{n+1} + x_n) \qquad \alpha = \alpha_1' \alpha_2 \alpha_3 \qquad \tau = \frac{\tau_1}{T} \qquad \alpha_1' = \alpha_1 T.$$

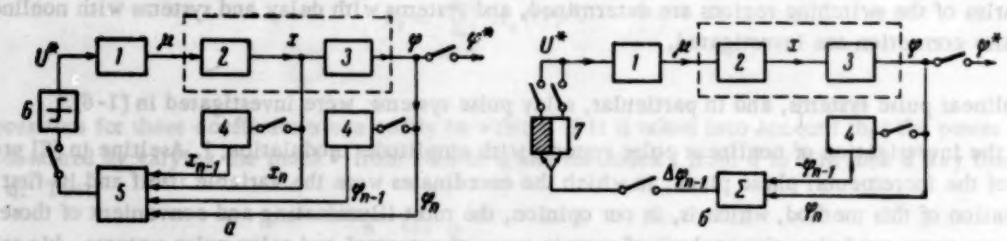

Fig. 1. a. Block diagram of an extremal pulse system with direct coupling for the coordinate x (or with a model of the linear part of the object of control); b. block diagram of an extremal pulse system without a model of the linear part of the object of control: 1) executive drive; 2) linear part of the object of control; 3) link with the extremal characteristic; 4) memory unit; 5) unit for calculation according to the formula (4); 6) relay element; 7) trigger unit, carrying out the calculation for the formula (13).

We now introduce the new variable $y = \Delta x$. Then, as was shown in [6], the equation of the phase trajectories corresponding to (6) is

$$x = x_0 - \frac{y - y_0}{1 - e^{-\frac{1}{\tau}}} \pm \frac{\alpha}{\left(1 - e^{-\frac{1}{\tau}}\right)}\left\{\left[-\frac{1}{\tau}\ln\left|1 \mp \frac{1 - e^{-\frac{1}{\tau}}}{\alpha} y\right| + \frac{1}{\tau}\ln\left|1 \mp \frac{1 - e^{-\frac{1}{\tau}}}{\alpha} y_0\right|\right]\right. \tag{7}$$

where x_0 and y_0 are the initial conditions.

If we start from only the difference equations of pulse systems, which determine the coordinates of the system only for discrete instants of time, then the equations of the phase trajectories, obtained by J. A. Aseltine in [6], generally speaking also only determine discrete points in the phase plane. We denote by $x_{n-\epsilon}$ and $y_{n-\epsilon}$ the coordinates of the system displaced by an arbitrary time $\epsilon (0 \leq \epsilon \geq 1)$ relative to the discrete instants n. The value of $x_{n-\epsilon}$ can be determined for a given transfer function of the continuous part of the system, by using the D-transformation [10] or the modified Z-transformation [11]. When we substitute $x_{n-\epsilon}$ and $y_{n-\epsilon}$ in (7), it is easily seen that for any value of ϵ, all the values of $x_{n-\epsilon}$ and $y_{n-\epsilon}$ will also lie on the trajectory defined by (7). Thus the equation obtained in [6] determines at every instant of time the position of the representative point in the plane.

For constructing the phase trajectories of the system, it is sufficient to have the equation (7), but these calculations are more easily performed, and the properties of the system become clearer, if we consider the boundaries (or at least one of the boundaries) in the phase plane. With the aim of simplifying the further exposition, we introduce a definition. We will call the expression after "sign" the switching function F.

The equation of one boundary of the switching region can be obtained by equating the switching function to zero, since it is evident that switching can not occur before F passes through zero. Consequently, one boundary, in the system being considered, is given by the equation

$$x_{n+1} + x_n = 0.$$

But since $x_{n+1} = y_n + x_n$, the final equation of the boundary MN of the switching region (see Fig. 2, a) is obtained as

$$y = -2x. \tag{8}$$

Another boundary of the switching region can be obtained as follows. We choose values of x_0 and y_0 lying on the boundary $F = 0$ of the switching region using the phase-trajectory equations (7), and then calculate the value y_1 corresponding to $x_1 = x_0 + y_0$. The equation (7) is transcendental, and we solve it graphically. Starting from values of x_0 and y_0, we locate point by point a second boundary EOF of the switching region (see Fig. 2, a), the configuration and size of which is determined not only by the form of the switching function F, but also by the parameters of the linear part of the system.*

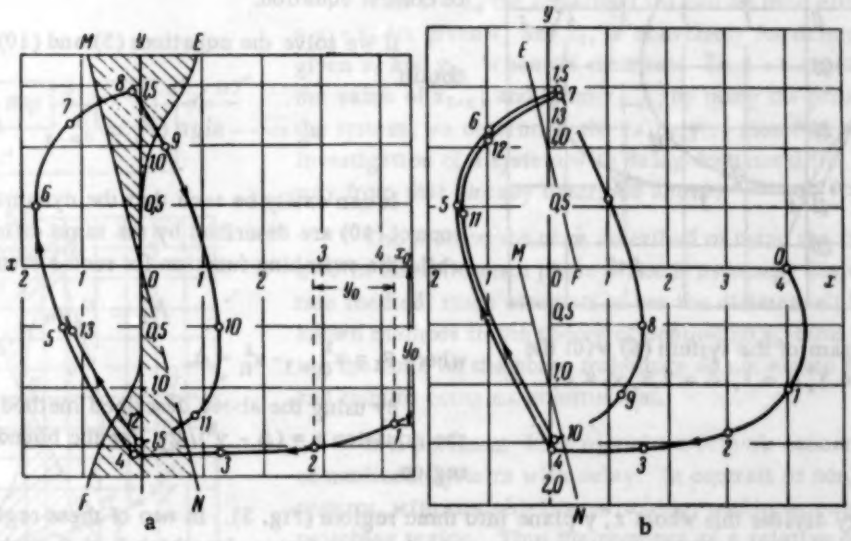

Fig. 2. a. The phase representation of the system (6) with the control (4) for $\tau = 1$, $x_0 = 4.2$, $y_0 = -1.35$; b. phase representation of the system (6) with the control (9) for $\tau = 1$, $\alpha = 1$, $\Delta = 1$, $x_0 = 4$, $y_0 = 0$.

If we know the character of the variation of the coordinate x, and use the equation (3), we can obtain the variation of the output φ of the object in control.

In Fig. 2, b, we show phase trajectories for a system with the switching function

$$F = x_{n+1} + x_n - \Delta \operatorname{sign} y_n \tag{9}$$

i.e., for a system in which the nonlinear element is a relay element with hystersis loop 2Δ. The equation of one pair of boundaries of the switching region is obtained by setting (9) equal to zero:

$$y = \begin{cases} -2x - \Delta & \text{for} \quad y > 0 \\ -2x + \Delta & \text{for} \quad y < 0. \end{cases}$$

As can be seen from Fig. 2, b, oscillations with period $T_x = 8T$ occur in the system.

---

*There is no difficulty in principle in obtaining the switching region. In this connection, the method of investigating the problem in which the switching points located inside a certain region uniquely determined by the parameters of the system are considered as random variables [5], unnecessarily complicates the work, and is not adequate for the present work.

We will analyze further the transitional processes in extremal pulse systems for the case that is most interesting in practice, namely when the coordinate x is not measurable in the control system and there is no model of the linear part of the system (see Fig. 1, b).

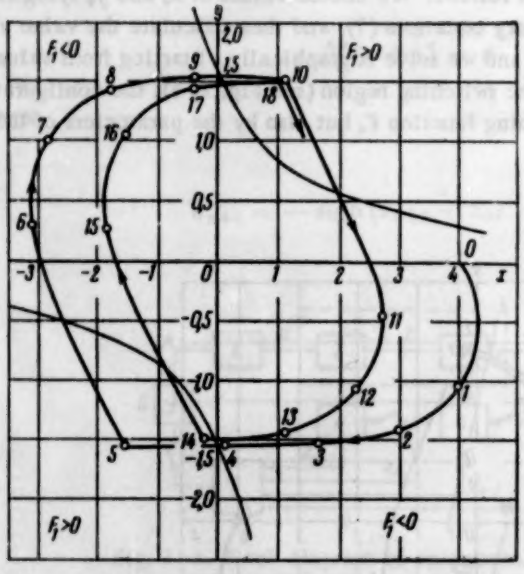

Fig. 3. Phase diagram of the system (6) with the control (10) for $\tau = 1$, $\alpha = 1$, $\Delta = 2.5$, $x_0 = 4$, $y_0 = 0$.

Let the continuous part of the system be given by the equations (1) - (3) as before. The equation for extremal control can be written in the form

$$u_n = \operatorname{sign}(\Delta\varphi_{n-1} + \Delta)\, u_{n-1} \qquad (10)$$

where Δ takes into account the effect of friction in the trigger.

We remark that extremal pulse controls, tested under the conditions occurring in industry, and rather well developed structurally (see, for example [12,13]) actually have this type of control equation.*

If we solve the equations (3) and (10) simultaneously, we obtain

$$u_n = -\operatorname{sign}(x_n^2 - x_{n-1}^2 - \Delta)\, u_{n-1}. \qquad (11)$$

It can easily be seen that the dynamics of a system with control (10) are described by the same difference equation (6), while the switching function for such a system is

$$F_2 = F_1 u_n \qquad (12)$$

where $F_1 = x_{n+1}^2 - x_n^2 - \Delta$.

By using the above described method, we obtain from (12) the equation $x = (\Delta - y^2)/2y$ for the boundary of the switching region.

This boundary divides this whole x, y plane into three regions (Fig. 3). In two of these regions, $F_1 > 0$, and so in these two regions, by (11) or (12), switching occurs. In the third region, for which $F_1 < 0$, a change in sign of the controlling quantity u is not possible.

The diagram in Fig. 3 shows that the control system we are considering is also perfectly efficient; its stationary operating regime is self-oscillating. The oscillation period of the system is determined by its parameters and the initial conditions. The greatest difference between these systems lies in the fact that when the representative point moves downwards in the region where $F_1 > 0$, more than one switching can take place in a system with the control described by (11), but only one can occur in the case of (5). Since the sign of the controlling parameter for the system (11) is determined by the product of two quantities, multiple switching can occur parameters fixed relative to one another.

The choice of parameters to ensure that no multiple switching will take place (the presence of which will entail losses in hunting) can be made in the following way. We start with values of x_0 and y_0 that can occur in practical conditions and that lie on the boundary of the switching region ($F_1 = 0$), and use the method of successive approximation to find parameters (α, τ) for the linear part of the system, such that the system leaves the region $F_1 > 0$ after a change of sign in u corresponding to a single switching.

2. Nonlinear Pulse Systems Containing a Unit with Delay

We will now use the difference phase plane to analyze the behavior of nonlinear pulse systems with delay. In order to simplify the description of the method of investigating such systems, we will use a concrete example (see Fig. 4, a). On the basis of what has been discussed above, we can write the equations

* It is not difficult to prove from the equations (1) - (3) and (10) that for $T \to \infty$ (corresponding to $e^{1/\tau} \to 0$) and for $\Delta = 0$, the systems with controls described by (4) and (10) become identical.

$$\Delta^2 x_n + \left(1 - e^{-\frac{1}{\tau}}\right)\Delta x_n = \alpha\left(1 - e^{-\frac{1}{\tau}}\right)\operatorname{sign} x'_{n+1} \tag{13}$$

$$x'_n = x_{n-\epsilon}. \tag{14}$$

As can be seen from (14), an analysis of a pulse system with delay in the difference phase plane requires the knowledge of the values of x and y at the time $t = n - \epsilon$, or, to be more precise, it is sufficient to know only the value of $x_{1-\epsilon}$ and $y_{1-\epsilon}$, since all the subsequent values of $x_{n-\epsilon}$ and $y_{n-\epsilon}$ can be determined from the phase trajectory. For the example under consideration, during the interval $0 \leq \bar{t} \leq 1$ the change in the coordinate $x(\bar{t})$, which is the reaction of the system with transfer function W(q) to an impulsive disturbance of $\pm a$, is given by the expression

$$x(\bar{t}) = \pm a\left(1 - e^{-\frac{\bar{t}}{\tau}}\right) + x_0 + \frac{1}{\tau}\dot{x}_0\left(1 - e^{-\frac{\bar{t}}{\tau}}\right). \tag{15}$$

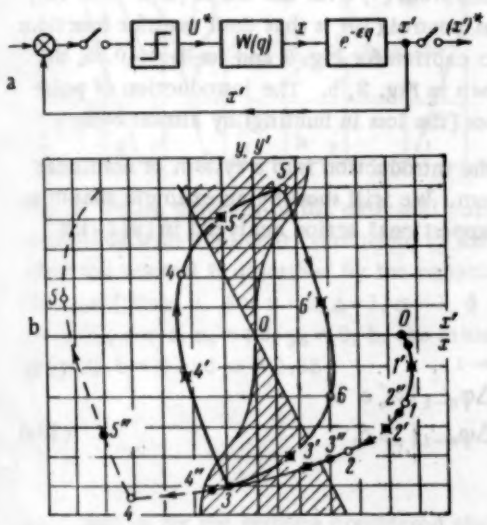

Fig 4. a. Block diagram of a nonlinear pulse system with delay; b. phase plane of a nonlinear pulse system with delay. Circles denote the x-coordinates and dots with crosses the x'-coordinates for $\epsilon = \epsilon'$, while dots denote the x'-coordinates for $\epsilon = \epsilon''$; the broken curve is the phase diagram of the system for $\epsilon = \epsilon''$.

With $\bar{t} = 1$, the equation (15) can be used either for finding $y_0 = x_1 - x_0$ for given x_1 and x_0, or conversely for determining x_0 for given x_0 and y_0. When we substitute $\bar{t} = 1 - \epsilon$ in (15), we obtain the value of $x_{1-\epsilon}$, and from $x_{1-\epsilon}$, by using the phase trajectory of the system, we determine the value $y_{1-\epsilon}$ (see Fig. 4, b). The further investigation of a system with delay does not differ in any essential way from that already described above.

The method we have described of using the time designation $n - \epsilon$ in the difference phase plane is evidently the only possible accurate method, since attempts to use the difference phase plane for known methods in the theory of continuous systems [15] for determining the time on the phase trajectory do not ensure sufficient accuracy, and require complex construction.

It is pertinent here to make a remark concerning the properties of nonlinear systems with delay. In contrast to nonlinear continuous systems, with straight-line switching, nonlinear pulse systems have a switching region. Thus the presence of a relative delay ϵ (for Fig. 4, b, $\epsilon \leq \epsilon''$) displacing a representative point in the phase plane within the limits of the switching region does not influence the period or "amplitude" of the self-oscillations. This peculiarity of nonlinear pulse systems with delay, as far as we can determine, has not been previously noted.

The advantage of investigating nonlinear pulse systems in the difference phase plane in comparison with investigating them in the usual phase plane is particularly striking in systems with delay, since in these systems we must have recourse to rather cumbersome methods of designating the time in the phase plane.

3. Nonlinear Pulse Systems with Impulse and Nonlinear Corrections

Both continuous correction and pulse-correction methods can be used in the case of relay pulse systems. Despite differences in the schematic realization of these two correction methods, their action reduces essentially to that of altering the locating (and configuration) of the switching region in the x, y plane so that the dynamic properties of the pulse system are improved. The influence of continuous correction on a relay pulse system in a concrete case is described in [6].

In many cases, especially for systems with high inertia, the practical realization of continuous correction often meets with considerable difficulties, because of the necessity of carrying out the differentiation of slowly varying functions. In such cases it is therefore preferable to use the impulse correction method, the practical realization of which can be shown to be simpler because only a definite number of memory elements are necessary.

We now consider the influence of pulse correction on the extremal system considered above.*

Let the continuous linear part of the system have the transfer function

$$W(q) = \frac{\alpha}{q(\tau q + 1)}. \tag{16}$$

and let the nonlinear characteristic of the object of control be described by the equation (3). The equation of extremal control can be written

$$u_n = \operatorname{sign}[\Delta\varphi_{n-1} + \beta\Delta\varphi_{n-2} + \Delta]\, u_{n-1}. \tag{17}$$

The simultaneous solution of (3) and (17) yields

$$u_n = -\operatorname{sign}[x_n^2 - (1-\beta)x_{n-1}^2 - \beta x_{n-2}^2 - \Delta]\, u_{n-1}. \tag{18}$$

The phase trajectories of the system under consideration are obtained from (7) with the use of (18). The only difference between the system we are considering and the system with the control (10) is that their transfer functions are different. Thus, for example, for parameters the same as those in the caption for Fig. 3 and for $\beta = -0.55$, the phase diagram of the system with the control (18) is identical to that shown in Fig. 2, b. The introduction of pulse correction thus permits a decrease in the amplitude of the self-oscillations (the loss in hunting) by almost 50%.

From the theory of continuous nonlinear systems, it is known that the introduction into a system of nonlinear correcting links permits the improvement of the quality of a control system. We will show by an example that this remains true for pulse systems. We use the extremal pulse system with proportional action analyzed in [9] (with pulse-width modultion).

The extremal-control equation for this system is

$$\operatorname{sign} u_n = \operatorname{sign}(\Delta\varphi_{n-1} + \Delta)\, u_{n-1} \tag{19}$$

$$|u_n| = \begin{cases} \delta + b|\Delta\varphi_{n-1}|, & \text{if} \quad \delta + b|\Delta\varphi_{n-1}| \leqslant c \\ c = \text{const}. & \text{if} \quad \delta + b|\Delta\varphi_{n-1}| \geqslant c. \end{cases} \tag{19a}$$

The limitation on the absolute value of the control parameter u_n is introduced to prevent any great over-regulation in the system.

A rather simple method of realizing such a control was described in [13].

By taking (3) into account, we rewrite (19) in the form

$$\operatorname{sign} u_n = -\operatorname{sign}(x_a^2 - x_{n-1}^2 - \Delta)\, u_{n-1} \tag{20}$$

$$|u_n| = \begin{cases} \delta + b|x_n^2 - x_{n-1}^2| & \text{if} \quad \delta + b|x_n^2 - x_{n-1}^2| \leqslant c \\ c = \text{const} & \text{if} \quad \delta + b|x_n^2 - x_{n-1}^2| \geqslant c. \end{cases} \tag{20a}$$

The dynamics of the system we are now considering are described by the equations (6) and (20). We have used (7) and (20) to construct the phase diagram of the system in Fig. 5. For comparison, the same diagram shows the transition process for a system with the control (10). The difference in the character of the two systems clearly shows the advantage of the system with the nonlinear correcting element.

We will consider briefly the properties of the system in question for $\delta = 0$. We note at once that the practical realization of such systems for $\Delta \neq 0$ is not particularly difficult. A characteristic feature of the system for $\delta = 0$ is that for a certain setting there is no self-oscillation in the system. This self-oscillation is unavoidable in extremal systems with constant steps.

---

* The application of impulse correction methods in extremal pulse systems was proposed by O. M. Kryzhanovskii in [13]. One of the variants of the practical realization of such systems was also introduced in this work.

A further improvement in the dynamic properties of extremal pulse systems (increasing the rapidity of action of the system and decreasing the overcontrol) is obtained by the simultaneous application of both pulse and nonlinear corrections. To confirm this fact, we will analyze an extremal sy em with the control given by the equations (17) and (19a).

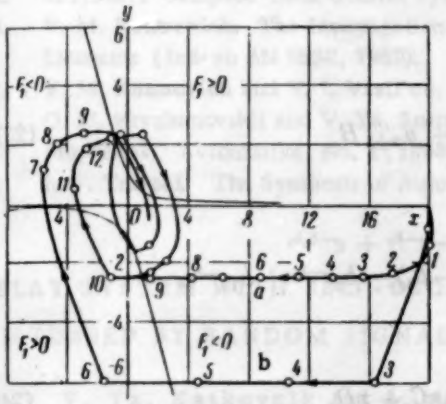

Fig. 5. Phase diagram of the extremal pulse system (6) with nonlinear correction, in the case when the control is described by the equations (20) and (20a): a. For $\tau = 1, \Delta = 1, \alpha = 1, \delta = 1$, $b = 0.05$, $c = 4$, $x_0 = 20$, $y_0 = 0$; b. the same, but with $b = 0$ and $\alpha = 1.58$

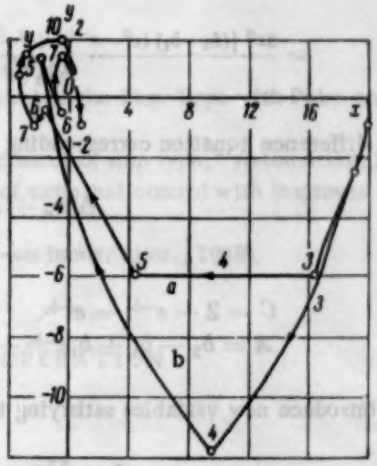

Fig. 6. Phase diagram of the extremal pulse system (6) with nonlinear and pulse correction, in the case when the control is described by the equations (19) and (21a): a. For $\tau = 1$, $\Delta = 1$, $\alpha = 1$, $\delta = 1$, $c = 4$, $b = 0.05$, $\beta = -0.25$, $x_0 = 20$, $y_0 = 0$; b. the same, but with $\beta = -0.06$ and $c = \infty$ (without any limitations on the absolute value).

Just as for the systems considered above, the continuous part of such a system is described by the difference equation (6), where u is obtained from (18) and (20a).

In Fig. 6 we show the phase diagrams of the system with the control described by the equations (18) and (20a). These diagrams were drawn from results obtained from (7) for two different adjustments of the system. It can be seen by comparing Fig. 5 with Fig. 6 that the simultaneous use of both pulse and nonlinear correction permits a significant improvement in the quality of operation of a pulse control system. The introduction of pulse correction with larger coefficients (see curve b in Fig. 6, for which $\beta = 0.06$) makes it unnecessary to impose restrictions on the absolute value of u_n*.

The example given above of the investigation of systems with pulse and nonlinear correction confirm the effectiveness of introducing such correction methods in pulse extremal systems, and they also show that the study of such systems in the difference phase plane is not basically complex.

4. Nonlinear Pulse Systems of the Third Order in the Difference Phase Plane

We consider in conclusion the possibility of extending the application of the difference-phase-plane method of investigating nonlinear pulse systems to pulse systems of the third order. The analysis of the motion of pulse systems of the third order, generally speaking, requires the consideration of the three-dimensional phase space of $\Delta^2 x$, Δx and x. The investigation of such systems can, however, be reduced to a two-dimensional analysis. To do this, a method can be used that is similar to that used for the same purpose in the study of continuous systems. We con-

*It should be noted that it is not implied that there is no necessity of imposing limitations on the absolute value of u_n in the presence of random perturbations in the control input.

sider the system shown in Fig. 4, a. Let its continuous part have the transfer function

$$W(q) = \frac{\alpha}{q(q+b_1)(q+b_2)}. \tag{21}$$

Then we can write

$$X^*(q) = \frac{\alpha e^q [(b_2-b_1)(e^q-e^{-b_1})(e^q-e^{-b_2})-b_2(e^q-1)(e^q-e^{-b_2})+b_1(e^q-1)(e^q-e^{-b_1})]}{b_1b_2(e^q-1)(e^q-e^{-b_1})(e^q-e^{-b_2})} U^*(q). \tag{22}$$

The difference equation corresponding to (22) is

$$\Delta^3 x_n + \Delta^2 x_n C + \Delta x_n D = u_{n+2} A + u_{n+1} B \tag{23}$$

where

$$C = 2 - e^{-b_1} - e^{-b_2}. \qquad D = 1 - e^{-b_1} - e^{-b_2} + e^{-b_1 b_2}$$
$$A = b_2 - b_1 + b_1 e^{-b_2} - b_2 e^{-b_1}. \qquad B = e^{-b_1 b_2}(b_2 - b_1) - b_2 e^{-b_2} + b_1 e^{-b_1}.$$

We introduce new variables satisfying the equations

$$z = \Delta^2 x. \quad v = \Delta x. \quad w = \Delta^2 x + \Delta x C + x D. \tag{24}$$

Then the equation (23) can be replaced by the equivalent equations

$$\Delta^2 v_n + \Delta v_n C + v_n D = u_{n+2} A + u_{n+1} B \quad (z = \Delta v) \tag{25a}$$
$$\Delta w_n = u_{n+2} A + u_{n+1} B. \tag{25b}$$

The investigation of the system is thus reduced to that of the difference equation of the second order (25a), the solution of which can be obtained by known methods. The variation of the coordinate w with time is easily obtained from a recurring formula obtained from (25b):

$$w_{n+1} = w_n + u_{n+2} A + u_{n+1} B. \tag{26}$$

SUMMARY

It is shown in the present article that the difference-phase-plane method can be used in the analysis of a wider class of systems than was originally proposed in [6]. A further development of this method has made it possible to investigate transitional processes in nonlinear pulse systems with delay in the simplest extremal systems, and also in systems using nonlinear and pulse correction. A method is indicated of determining the "switching region," which is analagous to the switching lines for continuous relay systems. A generalization of this method for investigating nonlinear pulse systems of the third order is described.

LITERATURE CITED

1. V. P. Kazakov, "An investigation of the dynamics of relay-pulse systems of automatic control" Avtomatika i Telemekhanika 18, No. 1 (1957).*
2. W. Oppelt, "The stability of discontinuous controls", Elektrotechnik, Vol. 2, No. 5 (1948).
3. F. J. Mullin and E. J. Jury, A Phase Plane Approach to Relay Sampled-Data Feedback Systems, AIEE, Application and Industry, No. 40 (1949).
4. R. E. Andin, The Analysis of Pulse Systems Containing Nonlinear Elements, Proceedings of the first IFAK Congress in Moscow, 1960.
5. K. Izava, Relay Systems of Control with Pulse Operation, Proceedings of the first IFAK Congress in Moscow, 1960.
6. J. A. Aseltine, The Investigation of Nonlinear Pulse Systems by the Difference-Phase-Plane Method, Proceedings of the first IFAK Congress in Moscow, 1960. (See also J. A. Aseltine and R. A. Nesbit, The Incremental

*See English translation.

Phase Plane for Nonlinear Sampled-Data Systems. Space Technology Laboratories, Inc. University of California, Los Angeles, March, 1960.)
7. A. G. Ivakhnenko, Technical Cybernetics, Gostekhizdat, UkSSR, Kiev, 1959.
8. O. M. Kryzhanovskii and V. M. Kuntsevich, "Periodic processes in extremal control systems," Izv. AN SSSR, OTN, "Energetika i avtomatika," No. 3 (1959).
9. V. M. Kuntsevich, "Some questions on the theory of extremal systems of the step type," Izv. AN SSSR, OTN, "Energetika i automatika," No. 5 (1960).
10. Ya. Z. Tsypkin, The Theory of Pulse Systems (Fizmatgiz, 1959).
11. E. I. Jury, Sampled-Data Control Systems, (John Wiley and Sons, 1958).
12. V. M. Kuntsevich, The Investigation of Systems of Extremal Control of the Step Type with Pulse and Digital Elements (Izd-vo AN SSSR, 1960).
13. V. M. Kuntsevich and V. I. Vasil'ev, "New designs of extremal control of step type," Avtomatika, No. 3(1960).
14. O. M. Kryzhanovskii and V. Ya. Soltyk, "Discontinuous systems of extremal control with improved dynamic properties," Avtomatika, No. 4 (1960).
15. J. G. Traksel, The Synthesis of Automatic Control Systems (Izv-vo Inostr. Liter., 1959).

RELAY SYSTEM WITH SELF-OSCILLATING MODE OF OPERATION DISTURBED BY RANDOM SIGNALS

V. Ya. Katkovnik and A. A. Pervozvanskii

(Leningrad)

Translated from Avtomatika i Telemekhanika, Vol. 22, No. 5, pp. 599-604, May, 1961
Original article submitted September 19, 1960.

A basic problem in the theory of automatic systems is precise performance in the presence of random effects. Accuracy evaluation is based on the analysis of system motion under the effect of forces and random disturbances.

The object of the present work is to investigate the dynamics of a self-oscillating system having relay-type nonlinearities.

Fig. 1 shows the block diagram of such a system.

The problem is solved by the method of adjustment [1]. The effect of small random forces is investigated for a system with an oscillating mode of operation. Discussing the problem of small fluctuations of a system, it is natural to assume the undisturbed mode to be that periodic process which the method of adjustment describes qualitatively.

The equations of motion of the system have the form

$$x = \frac{1}{p} K(p)\, y, \quad y = f(\sigma, \dot{\sigma}), \quad \sigma = x + \zeta \qquad \left(K(p) \equiv \frac{P(p)}{Q(p)}, \quad p \equiv \frac{d}{dt}\right) \tag{1}$$

where $\zeta(t)$ is a stationary random process (with $M\{\zeta\} = 0$ and $M\{\zeta^2\} = \sigma_\zeta^2$; $f(\sigma, \dot{\sigma})$ is a relay characteristic with hysteresis loop and current brace (Fig. 2).

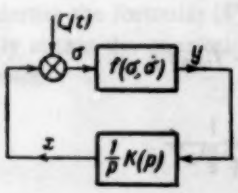

Fig. 1

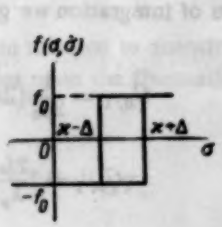

Fig. 2

Let us introduce the new variables

$$z_0 = \frac{y}{p} \qquad z_\rho = \frac{y}{p - \lambda_\rho} \quad (\rho = 1, 2, \ldots, n) \tag{2}$$

where $\lambda_\rho (\rho = 1, 2, \ldots, n)$ are the roots of polynomial Q(p), which for ease of computation are assumed to be dissimilar (Re $\lambda_\rho < 0$). Let us write equation (1) in the canonical form [1]:

$$z_0 = y. \; z_\rho - \lambda_\rho z_\rho = y. \; x = \sum_{\rho=0}^{n} \beta_\rho z_\rho. \quad y = f(\sigma, \dot{\sigma}). \quad \sigma = x + \zeta. \tag{3}$$

Here,

$$\beta_0 = \frac{P(0)}{Q(0)}. \; \beta_\rho = \frac{P(\lambda_\rho)}{\lambda_\rho Q(\lambda_\rho)}.$$

We examine the initially undisturbed mode ($\zeta = 0$). Integration of system (2), at $y = f_0$, yields

$$z_0(t) = f_0 t + C_0. \quad z_\rho(t) = C_\rho e^{\lambda_\rho t} - \frac{f_0}{\lambda_\rho}.$$

Let us denote the coordinates of the system which describe a motion under the effect of signal f_0, and a motion under the effect of signal $-f_0$, through subscripts 1 and 2, respectively. T_1 and T_2 are the corresponding time intervals.

Using the continuity and periodicity conditions of the process in the system (the time count starts from the moment of the last switch of the relay), we write

$$z_{\rho,1}(0) = z_{\rho,2}(T_2), \quad z_{\rho,1}(T_1) = z_{\rho,2}(0) \quad (\rho = 0, 1, \ldots, n). \tag{4}$$

Then follows the systems of relations:

$$C_{0,1} = -f_0 T_2 + C_{0,2} \qquad f_0 T_1 + C_{0,1} = C_{0,2}$$
$$C_{\rho,1} - \frac{f_0}{\lambda_\rho} = C_{\rho,2} e^{\lambda_\rho T_2} + \frac{f_0}{\lambda_\rho} \qquad C_{\rho,1} e^{\lambda_\rho T_1} - \frac{f_0}{\lambda_\rho} = C_{\rho,2} + \frac{f_0}{\lambda_\rho}. \tag{5}$$

By adding the relay performance conditions

$$x_1(0) = \varkappa + \Delta. \quad x_2(0) = \varkappa - \Delta$$

to relations (5) we get a system of equations with the unknowns T_1, $T2$, $C_{0.1}$, $C_{0.2}$, $C_{\rho,1}$, $C_{\rho,2}$. From the first pair of conditions(5) follows

$$T_1 = T_2 = T.$$

The self-oscillation period is determined from the transcendental relation

$$\frac{\beta_0 T}{2} + \sum_{\rho=1}^{n} \frac{\beta_\rho}{\lambda_\rho} \operatorname{th} \frac{\lambda_\rho T}{2} = -\frac{\Delta}{f_0}. \tag{6}$$

For the constants of integration we get

$$C_{0,1} = \frac{1}{2\beta_0}(2\varkappa - f_0 \beta_0 T) \qquad C_{0,2} = \frac{1}{2\beta_0}(2\varkappa + f_0 \beta_0 T) \tag{7}$$
$$C_{\rho,1} = \frac{2f_0}{\lambda_\rho} \frac{1}{1 + e^{\lambda_\rho T}} \qquad C_{\rho,2} = -\frac{2f_0}{\lambda_\rho} \frac{1}{1 + e^{\lambda_\rho T}}.$$

The magnitude of period T_2 is independent of the $\varkappa$-shift in the relay characteristics, because $\varkappa$ affects only the values of constants $C_{0.1}$ and $C_{0.2}$. It is necessary to verify the value of T, obtained from equation (6) with the aid of the condition for an adequate direction of switching

$$\dot{x}(0) = \beta_0 f_0 + \sum_{\rho=1}^{n} \beta_\rho \lambda_\rho C_{\rho.1} > 0.$$

Let us now analyze the disturbed mode of operation.

Denote through T_k ($k = 1,2,\ldots$) the consecutive time cells ("half-periods") during each of which the relay output signal, y, is constant (takes the form f_0 or $-f_0$). Let us assume for definiteness that the disturbance $\zeta(t)$ is applied across the system beginning with the instant t_0 (within the time cell T_1) during which $y = f_0$. Denote through ζ_k the value for $\zeta(t)$ at the end of interval T_k, i.e., at the moment of switching.

Let us further introduce the subscript k to denote the processes involved in the variation of all the variables over the interval T_k.

Then

$$z_{0.k} = C_{0.k} + (-1)^{k-1} f_0 t. \quad z_{\rho.k} = C_{\rho.k} e^{\lambda_\rho t} + (-1)^k \frac{f_0}{\lambda_\rho} \quad (\rho = 1, 2, \ldots, n).$$

(Time t is counted from the beginning of each interval.)

The continuity conditions

$$z_{\rho\ k}(T_k) = z_{\rho.k+1}(0) \quad (\rho = 0, 1, \ldots, n)$$

yield the recurrent relations

$$\begin{aligned} C_{0.k} + (-1)^{k-1} f_0 T_k &= C_{0.k+1}, \\ C_{\rho.k} e^{\lambda_\rho T_k} + (-1)^k \frac{f_0}{\lambda_\rho} &= C_{\rho.k+1} + (-1)^{k+1} \frac{f_0}{\lambda_\rho} \quad (\rho = 1, 2, \ldots, n). \end{aligned} \tag{8}$$

Introduce the values which characterize a deviation from the undisturbed mode:

$$\Delta T_k = (-1)^k (T - T_k). \qquad \Delta C_{\rho.k} = C_{\rho.k} - C^*_{\rho.k}$$

where T is determined from the period equation (6), while

$$C^*_{\rho.k} = \frac{2 f_0}{\lambda_\rho} \frac{(-1)^{k-1}}{1 + e^{\lambda_\rho T}} = C_\rho (-1)^{k-1} \quad (\rho = 1, 2, \ldots, n),$$

$$C^*_{0.k} = \begin{cases} C_{0.1} & \text{at} \quad k = 2m-1 \\ C_{0.2} & \text{at} \quad k = 2m. \end{cases}$$

Furthermore, let us assume that the disturbances ζ_k are small compared to the amplitude values of the input signal, x(t), in the undisturbed mode of operation. Then, on account of the stability of the said mode, the values ΔT_k, $\Delta C_{\rho,k}$ ($\rho = 0, 1, \ldots, n$), speaking generally, are also small compared to the corresponding values of T, C_ρ.

Using relations (5), we linearize the discontinuity conditions (8) as follows:

$$\Delta C_{0.k} = \Delta C_{0.k-1} + f_0 \Delta T_{k-1}. \quad \Delta C_{\rho.k} = e^{\lambda_\rho T} \Delta C_{\rho.k-1} + C_\rho e^{\lambda_\rho T} \Delta T_{k-1}. \tag{9}$$

Considering the formulas (9) to be first-order difference equations in relation to quantities $\Delta C_{\rho,k}$ ($\rho = 0, 1, \ldots, n$), we readily obtain the expressions for the dependence of these quantities upon the fluctuations of the half-periods ΔT_k, as follows:

$$\Delta C_{0.k} = f_0 \sum_{i=1}^{k-1} \Delta T_i. \quad \Delta C_{\rho.k} = C_\rho \sum_{i=1}^{k-1} e^{\lambda_\rho T (k-i)} \Delta T_i. \tag{10}$$

Let us now use the switching conditions

$$x_k(0) = (-1)^{k-1}\Delta + x - \zeta_{k-1} \tag{11}$$

or

$$\Delta x_k(0) = -\zeta_{k-1}. \tag{12}$$

At the same time

$$\Delta x_k(0) = \sum_{\rho=0}^{n} \beta_\rho \Delta z_{\rho,k}(0) = \sum_{\rho=0}^{n} \beta_\rho \Delta C_{\rho,k}. \tag{13}$$

Substitution of (10) into relation (13) yields the following infinite system of linear equations for the determination of ΔT_k:

$$\beta_0 f_0 \sum_{i=1}^{k-1} \Delta T_i + \sum_{\rho=0}^{n} \beta_\rho C_\rho \sum_{i=1}^{k-1} e^{\lambda_\rho T(k-i)} \Delta T_i = -\zeta_{k-1} \quad (k = 2.3.\ldots). \tag{14}$$

By subtracting the (k - 1) equation from each k-equation, the system is brought to the form:

$$\sum_{i=1}^{k} a_i \Delta T_i = -\zeta_k + \zeta_{k-1} \tag{15}$$

where

$$a_1 = f_0\beta_0 + \sum_{\rho=1}^{n} \beta_\rho \lambda_\rho C_\rho e^{\lambda_\rho T}$$

$$a_i = \sum_{\rho=1}^{n} \beta_\rho \lambda_\rho C_\rho (e^{\lambda_\rho T} - 1) e^{(i-1)\lambda_\rho T} \quad (i = 2.3.\ldots.k).$$

It is obvious that the coefficients a_i decrease rapdily with increasing subscript i. Their physical meaning is quite simple. The quantity a_i constitutes the difference between the values at the moments iT and (i - 1)T of the response of the linear group of the system to pulse disturbance; however, not at zero initial conditions, where it would be the impulse function that corresponds to the operator $\frac{1}{p}K(p)$, but for conditions which provide for the continuity and periodicity of the processes in the undisturbed system.

The solution of the system (15) is not too complicated because the matrix of the a-coefficient is triangular, and the quantities ΔT_k can be expressed in sequence through all the $\zeta_i (i \leq k)$. For an arbitrary k we have

$$\Delta T_k = -\sum_{i=1}^{k} A_i \zeta_{k-i+1} \tag{16}$$

where the coefficients A_k are defined from the recurrent relation

$$A_k = -\frac{1}{a_1} \sum_{j=1}^{k-1} A_j a_{k-j+1} \quad (k \geqslant 3) \tag{17}$$

it being evident that

$$A_1 = \frac{1}{a_1}. \quad A_2 = -\left(\frac{1}{a_1} + \frac{a_2}{a_1^2}\right)$$

(the validity of relation (17) is readily proved from induction).

Speaking generally, equation (16) fully determines the disturbed mode of operation. Substituting (16) into (10) and changing the order of summation, we get

$$\Delta C_{0,k} = -f_0 \sum_{j=1}^{k-1} \zeta_{k-j} \sum_{i=1}^{j} A_i$$

$$\Delta C_{\rho,k} = -C_\rho \sum_{j=1}^{k-1} \zeta_{k-j} \sum_{i=1}^{j} A_j e^{(j-i+1)\lambda_\rho T}. \tag{18}$$

The fluctuations of signal x(t) are determined from formula

$$\Delta x_k(t) = \beta_0 \Delta C_{0.k} + \sum_{\rho=1}^{n} \beta_0 e^{\lambda_\rho t} \Delta C_{\rho.k}$$

or, if we allow for (12), from

$$\Delta x_k(t) = \zeta_{k-1} - \sum_{\rho=1}^{n} \beta_\rho (1 - e^{\lambda_\rho t}) \Delta C_{\rho.k}.$$

The first item in the last expression characterizes the direct effect of disturbance in k-switching, while the remaining items characterize the effect of the fluctuations of the preceding half-periods, weakened due to system attenuation. Finally we write

$$\Delta x_k(t) = \sum_{j=1}^{k-1} \zeta_{k-j} D_j(t) \tag{19}$$

where

$$D_j(t) = \begin{cases} 1 - A_1 \sum_{\rho=1}^{n} \beta_\rho C_\rho (1 - e^{\lambda_\rho t}) e^{\lambda_\rho T} & \text{для } j = 1 \\ -\sum_{i=1}^{j} A_i \sum_{\rho=1}^{n} \beta_\rho C_\rho (1 - e^{\lambda_\rho t}) e^{(j-i+1)\lambda_\rho T} & \text{для } j = 2.3.\ldots \end{cases}$$

Let $\zeta(t)$ be a stationary random process with an assembly average equal to zero, and a correlation function

$$R_\zeta(\tau) = \sigma_\zeta^2 \rho_\zeta(\tau).$$

It is obvious that the assembly average of the period fluctuations and the signal x(t) is also equal to zero. The dispersion of the period is given by formula

$$\sigma_{T_k}^2 = M\{\Delta T_k^2\} = \sigma_\zeta^2 \sum_{i=1}^{k} \sum_{j=1}^{k} A_i A_j \rho_\zeta[(i-j)T] \tag{20}$$

and the dispersion of signal x(t) is given by formula

$$\sigma_{x_k}^2(t) = \sigma_\zeta^2 \sum_{i=1}^{k-1} \sum_{j=1}^{k-1} D_i(t) D_j(t) \rho_\zeta[(i-j)T]. \tag{21}$$

If the random disturbance is a wide-band disturbance and

$$\rho_\zeta[(i-j)T] \ll 1 \quad \text{при} \quad i \neq j$$

the simpler relations

$$\sigma_{T_k}^2 = \sigma_\zeta^2 \sum_{i=1}^{k} A_i^2 \tag{22}$$

$$\sigma_{x_k}^2 = \sigma_\zeta^2 \sum_{i=1}^{k-1} D_i^2 \tag{23}$$

can be obtained.

In a similar manner it is possible to find the correlation coefficient between the half-periods

$$M\{\Delta T_k \Delta T_m\} = \sigma_\zeta^2 \sum_{i=1}^{k} \sum_{j=1}^{m} A_i A_j \rho_\zeta [(i - j + m - k) T]. \tag{24}$$

The relation for the stable value σ_T is found from (20) or from (22), provided that the upper summation limit is extended to infinity.

The fluctuations of signal x(t) are of a nonstationary nature. However, the change $\Delta x(t)$ over the period T_k is fully defined by the fluctuations of the initial values $\Delta C_{\rho,k} (\rho = 0, 1, \ldots, n)$, which constitute elements of random sequences, each of which has a stable character in the case of sufficiently large k. In these terms, it is possible to speak of the stable fluctuations, $\overline{x}_k(t)$, as of fluctuations over a period that is sufficiently distant from the initial moment at which the random disturbance $\zeta(t)$ was applied. For the dispersion of the stable fluctuations we have the following expression

$$\sigma_{\bar{x}}^2(t) = \sigma_\zeta^2 \sum_{i=1}^{\infty} \sum_{j=1}^{\infty} D_i(t) D_j(t) \rho_\zeta [(i - j) T]. \tag{25}$$

and at small correlation, the expression

$$\sigma_{\bar{x}}^2(t) = \sigma_\zeta^2 \sum_{i=1}^{\infty} D_i^2(t). \tag{26}$$

In spite of their apparent bulkiness, the given formulas are not too tedious in computation since the coefficients A_j and D_j diminish rapidly with increasing number as a direct consequence of mode stability.

As an example, let us examine the following application of the technique described. Let operator K(p) have the following form:

$$K(p) = -\frac{1}{(\tau_1 p + 1)(\tau_2 p + 1)}$$

and let the relay have no hysteresis loop ($\Delta = 0$). A half-period of the oscillations is defined by the expression

$$\frac{\beta_0 T}{2} + \sum_{\rho=1}^{2} \frac{\beta_\rho}{\lambda_\rho} \operatorname{th} \frac{\lambda_\rho T}{2} = 0.$$

At $\tau_1 = 1$ sec, $\tau_2 = 2$ sec, $\lambda_1 = -1$ sec^{-1}, $\lambda_2 = -0.5$ sec^{-1}, $\beta_0 = -1$, $\beta_1 = -1$, $\beta_2 = 2$, we have $T = 4.6$ sec.

The computation of a_k may be limited to the three terms:

$$a_1 = -0{,}656\, f_0, \quad a_2 = -0{,}326\, f_0, \quad a_3 = -0{,}0328\, f_0.$$

Let us use the values obtained for a_1, a_2, a_3 to calculate several values for the A_k-coefficients:

$$A_1 = \frac{1}{f_0} 1.53. \quad A_2 = -\frac{1}{f_0} 2.29. \quad A_3 = \frac{1}{f_0} 1.06. \quad A_4 = -\frac{1}{f_0} 0.414. \quad A_5 = \frac{1}{f_0} 0.153.$$

When the noise correlation function is approximated by the exponent

$$R_\zeta(\tau) = \sigma_\zeta^2 e^{-\alpha|\tau|}$$

from (13), we get

$$\sigma_T = 0{,}84 \frac{1}{f_0} \sigma_\zeta \text{ для } \alpha = 0.01. \qquad \sigma_T = 1.6 \frac{1}{f_0} \sigma_\zeta \text{ для } \alpha = 0.1.$$

In the case of white noise ($\rho_\zeta(\tau) = \delta(\tau)$), we have

$$\sigma_T = 3{,}0\frac{1}{f_0}\sigma_\zeta.$$

The wider the band of white Gaussian noise, the larger the spread in values of the oscillation parameters; at a very-low-frequency random effect, the standard deviation of the half-period diminishes.

The discussed procedure, practically unchanged, may be used to investigate the disturbances in other periodic modes of relay systems. In principle, it may be extended to cover piecewise-linear systems [2]; it seems, however, that the impediment of the excessive computational labor involved can be circumvented in the practice only for systems of low order.

LITERATURE CITED

1. A. I. Lur'e, "Certain nonlinear problems in the theory of automatic control," (State Press for Technical and Theoretical Literature, 1951).
2. S. M. Rytov, "On the theory of fluctuations in self-oscillating systems with piecewise-linear characteristics," Izv. Byssh. Uchebn. Zaved., Radiofizika 2, 1 (1959).

COMPENSATION OF DELAY IN A RELAY SYSTEM

N. A. Korolev

(Moscow)

Translated from Avtomatika i Telemekhanika, Vol. 22, No. 5,
pp. 605-612, May, 1961
Original article submitted October 19, 1960

A method of stabilizing a lagging automatic control system employing relays is explained, using a second-order system as an example. The method is based on compensation of the lagging by introduction of an anticipatory signal by a feedback to the system input from the output of the element that causes the delay. The transient processes in such a system are calculated and plotted. The control function is computed, taking into account the derivatives of the quantity to be controlled. Compensation of the hysteresis loop in a static relay characteristic is examined.

1. Fundamental Equation of the System

Control systems with relays, as a rule, have a time delay, originating in the relay components, which noticeably lowers the quality of the operation, increases the time during which transients are prevailing, and sometimes lead to instability of the control system.

R. W. Bass [1,2] has offered a method for compensation of the lagging in relay operated systems by the addition of a special feedback. In the present paper, an attempt is made to evaluate this method by means of an example of its application to an actual relay operated tracking system; the circuit diagram of this system is shown in Fig. 1, a, and a function block diagram of it is in Fig. 1, b.

The output shaft (ultimate power application) must reproduce the movements of the control or pilot shaft. The amplifier y provides a gain k_y; the polarized relay Пр has a zone of insensitivity $\varkappa$, the repeater relay—a lag T. The transfer function of the motor is taken to be:

$$K_M(p) = \frac{k_M}{p(Mp+1)} \tag{1}$$

and that of the repeater relay:

$$K_П(p) = k_P e^{-pT}. \tag{2}$$

Hence, the transfer function of the linear part of the system is:

$$K(p) = K_M(p)\,K_П(p) = \frac{k_M k_P}{p(Mp+1)}\,e^{-pT}. \tag{3}$$

The characteristic of the polarized relay is presented in Fig. 2 and is expressed mathematically as follows:

$$y = \Phi(k_y x) = \begin{cases} 1 & \text{at} \quad k_y x > \varkappa. \\ 0 & \text{at} \quad \varkappa > k_y x > -\varkappa. \\ -1 & \text{at} \quad -\varkappa > k_y x. \end{cases} \tag{4}$$

Now we can write down the equation of the complete system in the open loop state: setting $k_M k_P = k$, this equation is:

$$M\ddot{\psi}(t) + \dot{\psi}(t) = k\Phi[k_y x(t-T)]. \tag{5}$$

The equation for closing the loop is:

$$\psi_r(t) - \psi(t) = x(t). \tag{6}$$

In general $\psi_r(t)$ (the reference input setting) can be any function of time, but we shall consider here only the particular case when this function represents a stepwise disturbance, that is, a sudden instantaneous change of the control angle setting by a constant value. For the sake of simplicity, we assume to have at $t = 0$: $\psi(0) = \psi_0$ and $\psi_r = 0$. Then substituting (6) into (5), and introducing θ as the independent variable, we obtain the equation of the system in the closed loop condition:

$$\ddot{\varphi}(\theta) + \dot{\varphi}(\theta) = -\Phi_\tau[\varphi(\theta)], \tag{7}$$

where

$$\varphi(\theta) = \frac{1}{kM}\psi(t), \quad \theta = \frac{t}{M} \qquad \tau = \frac{T}{M}$$

$$-\Phi_\tau[\varphi(\theta)] = \Phi_\tau[-\varphi(\theta)] = \Phi[-\varphi(\theta-\tau)],$$

$$\Phi(\varphi) = \begin{cases} 1 & \text{at} \quad \varphi > \varepsilon. \\ 0 & \text{at} \quad \varepsilon > \varphi > -\varepsilon. \\ -1 & \text{at} \quad -\varepsilon > \varphi. \end{cases} \tag{8}$$

When $k_y\psi = \varkappa$ we have $\varphi = \epsilon$. Hence:

$$\varepsilon = \frac{1}{k_y k_M}\varkappa. \tag{9}$$

For any of the possible values of the function $\Phi(\varphi)$, the solution of equation (7) will have the following form:

$$\begin{aligned}\ddot{\varphi} &= -[\Phi_\tau(\varphi) + \dot{\varphi}_0]e^{-\theta}\\ \dot{\varphi} &= -\Phi_\tau(\varphi) + [\Phi_\tau(\varphi) + \dot{\varphi}_0]e^{-\theta}\\ \varphi &= \varphi_0 - \theta\Phi_\tau(\varphi) + [\Phi_\tau(\varphi) + \dot{\varphi}_0](1 - e^{-\theta})\end{aligned} \tag{10}$$

where $\varphi_0 = \varphi(0)$ and $\dot{\varphi}_0 = \dot{\varphi}(0)$.

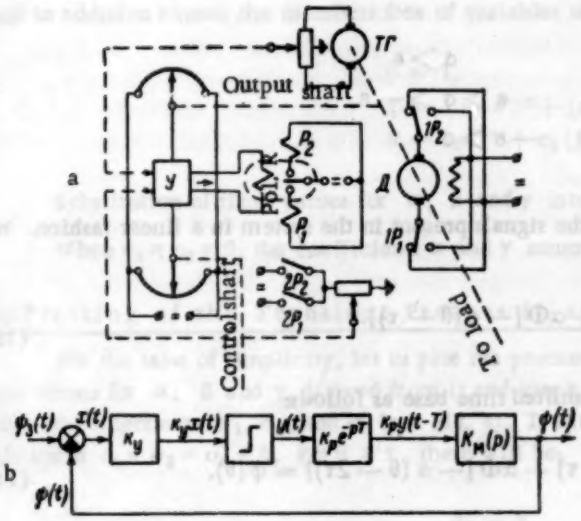

Fig. 1

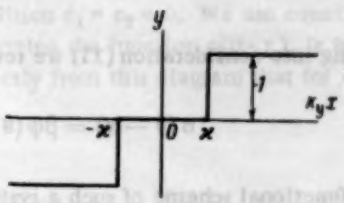

Fig. 2

2. Compensation of Lagging

Using known techniques [3], it is possible to determine and plot the transient processes in the closed loop system described by equation (7). In Fig. 3 are shown two curves representing the transient process, one in a system with time lag (I), the other in a system without time lag (II). Both curves were computed for a system having the following parameters: M = 0.02 sec, k_y = 30 ma/deg, k_M = 4 deg/v·sec, k_p = 25v, $\varkappa$ = 3 ma, $\psi(0)$ = -1 deg. It is evident that lagging makes the effect of the transient process very much worse.

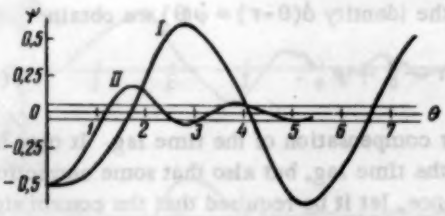

Fig. 3

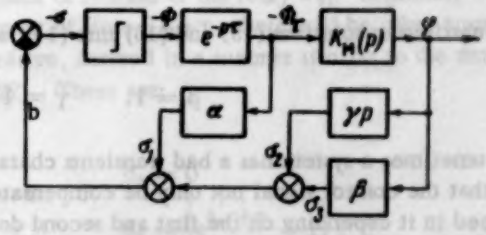

Fig. 4

The compensation method described in [1,2] is based on a simple idea: in a relay operated system, the reaction of the linear part due to the operation of the relay component is well known. Therefore, it is possible to create at the systems input, after time τ has elapsed, a controlling command action $\sigma(\theta - \tau)$, which will completely compensate for the time lag, or, in other words, to introduce in the original command function (reference input) $\varphi(\theta)$ a forward shift of the time count reference point by τ. We thus have:

$$\sigma(\theta - \tau) = \varphi(\theta) \quad \text{или} \quad \sigma(\theta) = \varphi(\theta + \tau) \tag{11}$$

where $\varphi(\theta)$ is the command function of the system without time lag. Obviously, to make this possible it is necessary that the time interval between consecutive switching operations of the relay be greater than τ.

The equation of the system with lag compensation is obtained from (7) by substituting for the control function $\varphi(\theta)$ the function $\sigma(\theta-\tau)$. We then have:

$$\ddot{\varphi}(\theta)+\dot{\varphi}(\theta)=-\Phi_{\tau}[\sigma(\theta)] \tag{12}$$

where

$$\Phi(\sigma)=\begin{cases}1 & \text{at} \quad \sigma>\varepsilon\\ 0 & \text{at} \quad \varepsilon>\sigma>-\varepsilon\\ -1 & \text{at} \quad -\varepsilon>\sigma.\end{cases}$$

Let us find the control action $\sigma(\theta)$ by combining all the signals present in the system in a linear fashion. We then have:

$$\sigma(\theta)=\beta\varphi(\theta)+\gamma\dot{\varphi}(\theta)+\alpha\Phi[-\sigma(\theta-\tau)]. \tag{13}$$

Taking into consideration (11) we rewrite (13) for the shifted time base as follows:

$$\sigma(\theta-\tau)=\beta\varphi(\theta-\tau)+\gamma\dot{\varphi}(\theta-\tau)+\alpha\Phi[-\sigma(\theta-2\tau)]=\varphi(\theta). \tag{14}$$

The functional scheme of such a system is shown in the block diagram of Fig. 4.

Let us determine the coefficients α, β and γ by solving equation (12) for the time interval between two consecutive switchovers of the relay. Setting

$$\Phi_{\tau}[-\sigma(\theta)]=1$$

we obtain from (10):

$$\varphi(\theta)=\varphi_0-1+\theta+e^{-\theta}. \tag{15}$$

Shifting our variable (argument) θ by τ, we have:

$$\varphi(\theta-\tau)=\varphi_0-1+\theta-\tau+e^{\tau}e^{-\theta}. \tag{16}$$

Substituting solutions (15) and (16) into (14), and making use of the identity $\dot{\sigma}(\theta-\tau)=\dot{\varphi}(\theta)$ we obtain:

$$\beta=1. \qquad \gamma=1-e^{-\tau}. \qquad \alpha=\tau-1+e^{-\tau}. \tag{17}$$

Sometimes a system has a bad transients characteristic even after compensation of the time lag. It may be required that the control signal not only be compensated with respect to the time lag, but also that some correction be introduced in it depending on the first and second derivative. For instance, let it be required that the control signal have the following form:

$$\lambda(\theta-\tau)=\varphi(\theta)+c_1\dot{\varphi}(\theta)+c_2\ddot{\varphi}(\theta) \tag{18}$$

where c_1 and c_2 are predetermined coefficients.

Leaving the functional scheme of Fig. 4 unchanged, and taking into consideration that feedback α produces a signal which is proportional to the second derivative of φ, we can rewrite (14) as follows:

$$\lambda(\theta-\tau)=\beta\varphi(\theta-\tau)+\gamma\dot{\varphi}(\theta-\tau)+\alpha\Phi[-\lambda(\theta-2\tau)]=$$
$$=\varphi(\theta)+c_1\dot{\varphi}(\theta)+c_2\ddot{\varphi}(\theta). \tag{19}$$

The new values of coefficients α, β and γ are determined in a similar manner as before. We use the solutions for equation (12) within the time interval T_0 between switchovers of the relay (provided $T_0 > 2\tau$), that is (15) with the original variable and (16) with the shifted by τ variable, and obtain from (19) the following equation:

$$\lambda(\theta-\tau)=\beta[\varphi_0-1+\theta-\tau+e^{\tau}e^{-\theta}]+\gamma(1-e^{\tau}e^{-\theta})+\alpha=$$
$$\varphi(\theta)+c_1\varphi(\theta)+c_2\varphi(\theta)=\varphi_0-1+\theta+e^{-\theta}+c_1(1-e^{-\theta})+c_2e^{-\theta}. \quad (20)$$

This equation must be satisfied for any value of θ. Let us substitute in it for θ the variables $\theta \to \infty$, and $\theta = 0$, and in addition equate the members free of variables on both sides. We then obtain:

$$\begin{aligned}\beta &= 1,\\ \gamma &= 1-e^{-\tau}+(c_1-c_2)e^{-\tau},\\ \alpha &= c_2e^{-\tau}+c_1(1-e^{-\tau})+e^{-\tau}+\tau-1.\end{aligned} \quad (21)$$

Substitution of these values for α, β and γ into (20) turns it into an identity.

When $c_1 = c_2 = 0$, the coefficients α and γ assume the values given above in (17).

3. Plotting of the Transient Process in a Compensated System

For the sake of simplicity, let us plot the process $\varphi(\theta)$ at the condition $c_1 = c_2 = 0$. We use equation (14), and the values for α, β and γ derived from it and given in (17). To determine the function $\sigma(\theta-\tau)$, it is necessary to find its components σ_1, σ_2, and σ_3 (see Fig. 4). It can be deduced directly from this diagram that for $\theta < \tau$, there always is $\sigma_1 = \sigma_2 = \sigma_3 = 0$. For $\theta \geq \tau$, there will be:

$$\begin{aligned}\sigma_1 &= \alpha\\ \sigma_2 &= \gamma(1-e^{\tau}e^{-\theta}) = \gamma(1-e^{-\theta_0})\\ \sigma_3 &= \beta(\theta_0-1+e^{-\theta_0})\end{aligned} \quad (22)$$

where $\theta_0 = \theta - \tau \geq 0$. Relationships (22) are valid until the effect of the next switchover of the relay comes through. Suppose that σ reaches the threshold value for throwing over the relay $\sigma = -\epsilon_0$ at the moment of time θ'_{01}. Hence, expressions (22) are valid when θ varies within the limits of $0 \leq \theta_0 \leq \theta'_{01}+\tau$.

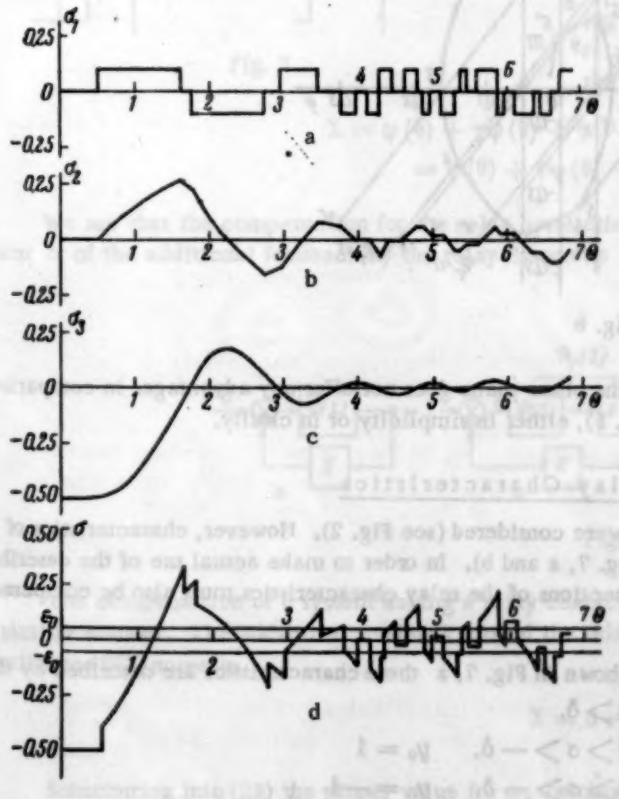

Fig. 5

In figure 5,a, b, and c the components σ_1, σ_2 and σ_3 are plotted, and in Fig. 5d, the sum obtained as a result of their addition (graphically or by tabulation and arithmetic). The point of intersection of the curve σ with the horizontal straight line $-\epsilon_0$ corresponds to the moment of release of the relay θ'_{01}. Beginning with the moment of time $\theta'_{01}+\tau$, there will be other equations operative, derived in a manner similar to the derivation of (22). These are:

$$\begin{aligned}\sigma_1 &= 0\\ \sigma_2 &= \left(e^{\theta'_{01}+\tau}-1\right)e^{-\theta}\\ \sigma_3 &= \theta'_{01}-\left(e^{\theta'_{01}}-1\right)e^{-\theta}.\end{aligned} \quad (23)$$

Equations (23) will be valid within the limits of $\theta'_{01}+\tau \leq \theta_0 \leq \theta_{01}+\tau$ where θ_{01} is the moment at which $\sigma(\theta_0)$ crosses the straight line $\sigma = +\varepsilon_0$ the second threshold value, corresponding to the reverse switching operation of the relay. These quantities are determined graphically. Further, equations for the next operational sections are made up, similar to (22) and (23). The values obtained for σ_1, σ_2, σ_3 and σ are shown in Fig. 5.

We are interested in the output parameter $\sigma_3(\theta)$ of the system, which represents the degree of completion of the course run by function $\varphi(\theta)$. Comparing Fig. 5,c with curve II of Fig. 3, we see that at the beginning a complete compensation of the lagging is taking place (no shift by τ present). After that, however, some difference is observed between these two curves, and from there on, the control action $\sigma(\theta)$ assumes the character of undamped oscillations. This is due to the fact that one of the conditions for achievement of complete compensation is not satisfied, namely, the requirement that the time interval between consecutive switching operations of the relay must be greater than the lag time τ: already the time between the first and second switchover of the relay is smaller than τ. During the transient process this incongruity is repeated many times, and finally exerts a predominant influence. During this time the output function σ_3 fluctuates with a small amplitude and at a relatively high frequency. The latter fact is in contradiction with the statements of the author of papers [1] and [2]: the suggested method of stabilization does not eliminate the problem of wear of the relay contacts.

An attempt to investigate compensation of time lag by the phase plane method in a manner, similar to the investigation of the lag itself, as for instance in [4], does not lead to desired results: the basic virtue of the phase plane method—easier determination of operational complexes of a system by means of graphical construction and plotting of switchover lines and point loci transformations—can not be made use of in the present case, because the control operation if governed to a great extent by whichever derivative of the system happens to be the "dominant" derivative, and it is not known a priori which derivative that is; this can be determined only by studying a whole family of switchover curves, and selecting the one having the proper crossover with the curve of the point loci, which in turn is dependent upon the initial conditions. The only thing left to do is to use the method of sectional curve fitting, that is, to solve the equations of motions in several consecutive sections for which the initial conditions are given

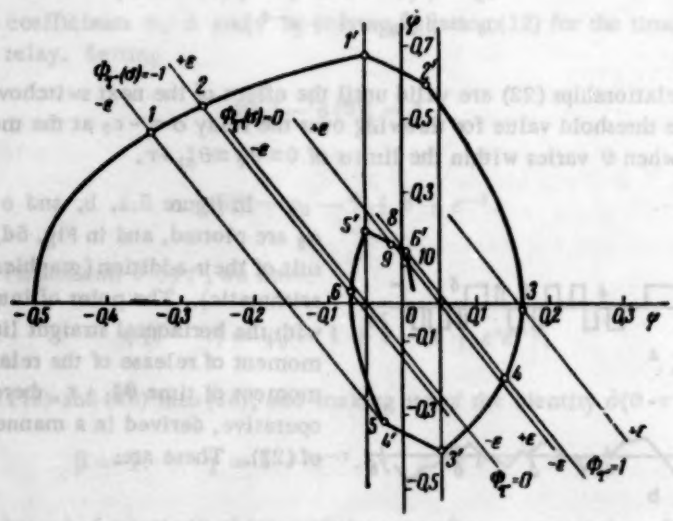

Fig. 6

(Fig. 6). Therefore, representations of this operation on the phase plane does not offer any advantages in comparison with the representation by an explicit time function (Fig. 5), either in simplicity or in clarity.

4. Compensation for Hysteresis Loop of Relay Characteristics

Until now only single valued relay characteristics were considered (see Fig. 2). However, characteristics of actual relays have sections consisting of hysteresis loops (Fig. 7, a and b). In order to make actual use of the described stabilization against timelag effects, the hysteresis loop sections of the relay characteristics must also be compensated for.

Let us examine first the characteristics of a relay shown in Fig. 7, a these characteristics are described by the following equation:

$$y = \Phi(\sigma) = \begin{cases} 1 \begin{cases} \sigma > \delta. \\ \delta > \sigma > -\delta. \quad y_0 = 1 \end{cases} \\ -1 \begin{cases} \delta > \sigma > -\delta. \quad y_0 = -1 \\ -\delta > \sigma, \end{cases} \end{cases} \tag{24}$$

where y_0 is the value of y just prior to one of the switching over operations of the relay. Let us introduce a new variable χ acting at the input to the relay and subject to the following condition:

$$\chi = \sigma - \delta \operatorname{sign} \Phi(\chi) = \sigma - \delta\Phi(\chi). \tag{25}$$

which expresses the fact that there is a rigid feedback provided from the output (Fig. 8a). The operational threshold of the relay is $\pm\delta$ (Fig. 7a): that is, the value of χ must fall to at least $\chi = -\delta$, or rise to at least $\chi = +\delta$ for the relay to carry out a switching operation. In either case, until this threshold is reached, σ will equal zero (Fig. 7, b). However, such a compensation of the hysteresis loop by a simple rigid feedback across the relay itself results in faulty operation of the latter, because, as is well known, at the moment of the switchover the input signal also is subject to a jump, which moreover is equal to $\pm 2\delta$.

In order to avoid contact chattering during the makes and breaks of the relay, it is sufficient to introduce in the feedback circuit a small delay action. Inasmuch as there is already a time delay τ present in the system, it appears advantageous to make use of it for this purpose. To do this, if the component causing the time delay is in the circuit after the relay, part of the signal is fed back to the relay input from the output of the time delay component (Fig. 8, b); if the time delay element precedes the relay in the circuit, the feedback goes from the output of the relay to the input of the time delay component (Fig. 8, c). It must be noted, that complete compensation for the hysteresis loop will take place only in case the interval between successive switching operations of the relay is not less than τ. When feedback not across the relay itself is used, but across the relay plus the other delay causing component, equation (25) takes the following form:

$$\chi = \sigma - \delta\Phi_\tau(\chi), \tag{26}$$

where the subscript τ, at Φ symbolically designates that now the delayed by τ value is used as the independent variable in function Φ, that is $\Phi[\chi(\theta-\tau)] = \Phi_\tau(\chi)$.

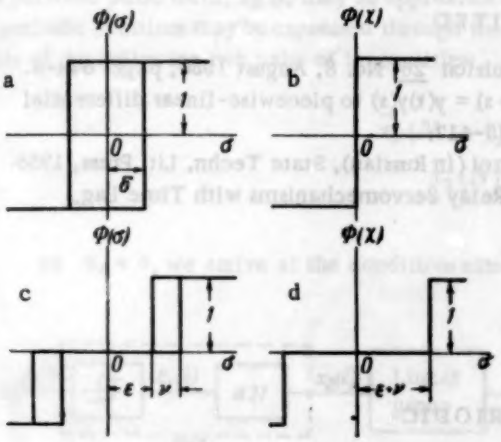

Fig. 7

Substituting into (26) the value of σ from (13) and taking into account (17) and also the fact that to the input of the relay now the signal $-\chi$ instead of $-\sigma$ is applied, we obtain the following:

$$\chi = \varphi(\theta) + \gamma\varphi(\theta) + \alpha\Phi_\tau(-\chi) + \delta\Phi_\tau(-\chi) = \\ = \varphi(\theta) + \gamma\dot{\varphi}(\theta) - (\alpha+\delta)\Phi_\tau(\chi). \tag{27}$$

We see that the compensation for the relay hysteresis loop, mathematically, is due to an increase of the coefficient α of the additional feedback by the relay hysteresis δ (see Fig. 7, a).

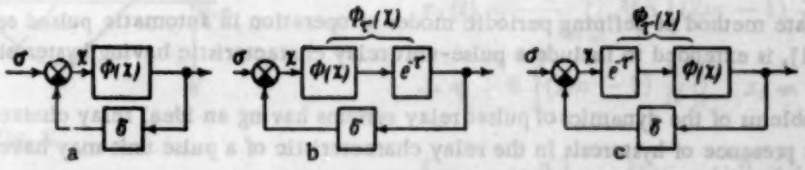

Fig. 8

The compensation of a system having a relay characteristic of a more general type (Fig. 7, c) is carried out in a similar manner. The additional feedback around the relay and the delay components is expressed by an equation similar to (26), namely:

$$\chi = \sigma - \nu\Phi_\tau(\chi). \tag{28}$$

Substituting into (28) the proper value for σ, we obtain:

$$\chi = \varphi(\theta) + \gamma\varphi(\theta) - (\alpha + \nu)\Phi(\chi). \tag{29}$$

We see that the compensation for relay hysteresis amounts to an increase of the feedback coefficient α by the value of the relay hysteresis ν. The effective dead area of the relay (when the input to it is below the threshold) with this hysteresis compensation is equal to $\epsilon + \nu$. It should be noted that in [1] it is erroneously stated that the feedback coefficient is decreased by the amount of hysteresis, and that the dead area is increased not by ν, but by $\nu/2$.

SUMMARY

An effective system for stabilization of relay systems subject to time delays is described which was suggested by R. W. Bass [1,2]. The time lag of the system and also the effects of the hysteresis loop sections in the relay characteristic are compensated by additional control action of a kind specifically developed for this purpose.

The method is applicable to a wide variety of relay systems, and particularly in cases where the delay is an inherent property of the relay itself. The wearing out of the relay contacts, however, may be increased by this method.

LITERATURE CITED

1. R. W. Bass, "Improved on-off missile stabilization," Jet Propulsion 26, No. 8, August 1956, pages 644-8.
2. R. W. Bass, "A generalization of the functional relation $\gamma(t+s) = \gamma(t)\gamma(s)$ to piecewise-linear differential equations," Quart. Appl. Math. 14, No. 4, Jan. 1957, pp. 415-417.
3. Ya. Z. Tsypkin, Theory of Relay Systems in Automatic Control (in Russian), State Techn. Lit. Press, 1955.
4. V. V. Petrov and V. Yu. Rutkovskii, Theory of the Simplest Relay Servomechanisms with Time Lag, Izvest. Akad. Nauk SSSR, OTN No. 4, 1956.

INFLUENCE OF HYSTERESIS ON THE MODE OF PERIODIC PROCESSES IN PULSED RELAY SYSTEMS

V. P. Kazakov

(Moscow)

Translated from Avtomatika i Telemekhanika, Vol. 22, No. 5, pp. 613-617, May, 1961
Original article submitted November 12, 1960

The approximate method of defining periodic modes of operation in automatic pulsed relay systems described in [1], is extended to include a pulse-unit relay characteristic having hysteresis.

Some of the problems of the dynamics of pulsed relay systems having an ideal relay characteristic have been examined in [1]. The presence of hysteresis in the relay characteristic of a pulse unit may have a marked effect upon the mode of the processes occurring in such systems.

The dynamics of pulsed relay systems having both hysteresis and a second-order linear group have been investigated in [2] by the phase plane method.

In the present work, a method is outlined in which the effect of hysteresis upon the periodic-mode parameters of pulsed relay systems is taken into account irrespective of the complexity of the phase plane. Fig. 1 shows the schematic diagram of the pulsed relay system investigated. The pulse unit of such a system can be represented in the form of a two-position relay with hysteresis, series connected to an amplitude-modulated pulse unit.

Let the system have simple self-oscillations with a relative half-period N, where N is an integer. Then, in analogy with continuous relay systems [3], the conditions for the existence of periodic solutions in a pulsed relay system may be written in the following form:

$$\begin{aligned} &\tilde{x}_3(\bar{t}_0) = \varkappa_0 \quad \text{at} \quad (N-1) < \bar{t}_0 \leqslant N \\ &\dot{\tilde{x}}(\bar{t}_0) > 0 \quad \text{at} \quad (N-1) < \bar{t}_0 < N \\ &\tilde{x}_3(\bar{t}) \leqslant \varkappa_0 \ \text{ and } \ \tilde{x}_1(\bar{t}) = -1 \quad \text{at} \quad 0 \leqslant \bar{t} < N. \end{aligned} \tag{1}$$

Here, $\varkappa_0$ is the half-width of the hysteresis zone; $\bar{t} = t/T_p$ is the relative time; $\bar{t}_0$ is the moment of switching, that is the moment at which occurs the intersection of $\tilde{x}_3(\bar{t})$ with the line $\varkappa_0$; N is equal to T/T_p; T is a half-period of the oscillations; and T_p is the repetition rate of the pulse unit.

The relations (1) constitute the conditions for the proper moment and direction of switching as well as the conditions for the absence of switching throughout a half-period. It is assumed that the linear group of the system has the properties of a low-frequency filter and, hence, the stable response of the linear group to the first harmonic of the periodic pulse train, $\tilde{x}_3(t)$, may in approximation be substitued for $\tilde{x}_3(\bar{t})$. Here, the conditions for the existence of periodic solutions may be expressed through the values of $\tilde{x}_3(\bar{t})$ and $\dot{\tilde{x}}_3(t)$ in the discrete points N - 1 and N, in the form of the following two pairs of inequalities:

$$\begin{aligned} &\tilde{x}_3(N-1) \leqslant \varkappa_0, \quad \dot{\tilde{x}}_3(N-1) \geqslant 0 \\ &\tilde{x}_3(N) \geqslant \varkappa_0, \quad \dot{\tilde{x}}_3(N) \geqslant 0. \end{aligned} \tag{2}$$

At $\varkappa_0 = 0$, we arrive at the conditions cited in [1].

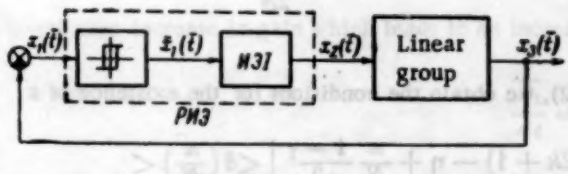

Fig. 1

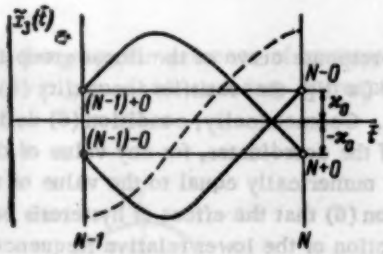

Fig. 2

Fig. 2 illustrates the two end positions of the $\tilde{x}_3(\bar{t})$ curve relative to the pulse-period moments N-1 and N, which provide for the existence of a periodic mode with a half-period N = 1. It may be seen from the figure that the first pair of inequalities (2) is indicative of the existence of a periodic solution for the case where the $\tilde{x}_3(\bar{t})$ curves are located on the left side of the dotted curve; the second pair of inequalities defines a given periodic mode for the case where the $\tilde{x}_3(\bar{t})$ curves are on the right side of the dotted curve. The existence of periodic solutions with a half-period $N \geq 2$ is defined by the complete set of inequalities (2). As has been shown in [1], the output of the system and its first derivative have the form:

$$\tilde{x}_3(\bar{t}) = \frac{4k_u}{\pi} \sum_{m=1}^{\infty} MK\left[(2m-1)\frac{\pi}{N}\right] \sin\left\{(2m-1)\frac{\pi}{N}\bar{t} + \psi + \theta\left[(2m-1)\frac{\pi}{N}\right]\right\} \quad \dot{\tilde{x}}_3 = \frac{4k_u}{N} \sum_{m=1}^{\infty} (2m-1)\, MK \left[(2m-1)\frac{\pi}{N}\right] \cos\left\{(2m-1)\frac{\pi}{N}\bar{t} + \psi + \theta\left[(2m-1)\frac{\pi}{N}\right]\right\}$$

where

$$M = \frac{1}{2m-1} \frac{\sin(2m-1)\frac{\pi}{2N}\gamma}{\sin(2m-1)\frac{\pi}{2N}} \quad \text{and} \quad \psi = (2m-1)\frac{\pi}{2N}(1-\gamma).$$

Hence, their first harmonics are:

$$\tilde{x}_3(\bar{t}) = \frac{4k_u}{\pi}\,\frac{\sin\frac{\pi}{2N}\gamma}{\sin\frac{\pi}{2N}}\,K\left(\frac{\pi}{N}\right)\sin\left[\frac{\pi}{N}\bar{t} + \frac{\pi}{2N}(1-\gamma) + \theta\left(\frac{\pi}{N}\right)\right] \tag{3}$$

$$\dot{\tilde{x}}_3(\bar{t}) = \frac{4k_u}{N}\,\frac{\sin\frac{\pi}{2N}\gamma}{\sin\frac{\pi}{2N}}\,K\left(\frac{\pi}{N}\right)\cos\left[\frac{\pi}{N}\bar{t} + \frac{\pi}{2N}(1-\gamma) + \theta\left(\frac{\pi}{N}\right)\right]. \tag{4}$$

where k_u is the simplification factor of the pulse unit; γ is the relative duration of the pulses acting at the output of the pulse unit; $K(\pi/N)$ is the frequency response modulus of the linear group of the system, and $\theta(\pi/N)$ is the linear-group phase.

Substituting the time values $\bar{t} = N-1$ and $\bar{t} = N$ into expressions (3) and (4), we get

$$\begin{aligned}
\tilde{x}_3(N-1) &= A\sin\left[\frac{\pi}{N}\frac{1+\gamma}{2} - \theta\left(\frac{\pi}{N}\right)\right]\\
\tilde{x}_3(N) &= A\sin\left[-\frac{\pi}{N}\frac{1-\gamma}{2} - \theta\left(\frac{\pi}{N}\right)\right]\\
\dot{\tilde{x}}_3(N-1) &= -\frac{\pi}{N}\cos\left[\frac{\pi}{N}\frac{1+\gamma}{2} - \theta\left(\frac{\pi}{N}\right)\right]\\
\dot{\tilde{x}}_3(N) &= -\frac{\pi}{N}\cos\left[-\frac{\pi}{N}\frac{1-\gamma}{2} - \theta\left(\frac{\pi}{N}\right)\right].
\end{aligned} \tag{5}$$

where $A = \frac{4k_u}{\pi}\,\frac{\sin\frac{\pi}{2N}\gamma}{\sin\frac{\pi}{2N}}\,K\left(\frac{\pi}{N}\right)$.

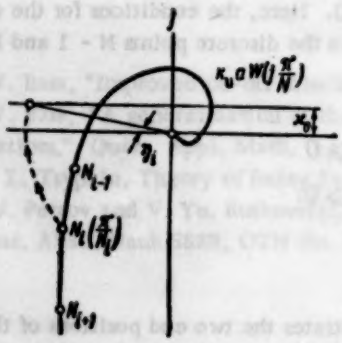

Fig. 3.

By subordinating the equations (5) to the inequalities (2), we obtain the conditions for the existence of a periodic solution for an arbitrary N, as follows:

$$\begin{aligned}
-\left[\pi(2k+1) - \eta + \frac{\pi}{N}\frac{1-\gamma}{2}\right] &< \theta\left(\frac{\pi}{N}\right) <\\
&< -\left[\pi(2k+1) - \eta - \frac{\pi}{N}\frac{1+\gamma}{2}\right] \qquad (k = 0.1.2.\ldots.\infty).
\end{aligned} \tag{6}$$

Here, η = arc sine $\varkappa_0/A$.

From this inequality it follows that if the point on the frequency-response curve of the linear group that corresponds to a certain value of the relative frequency π/N_i has a phase $\theta(\pi/N_i)$ that satisfies inequality (6), then the system will have a periodic solution with a relative half-period $N = N_i$. Geometrically, condition (6) defines the vectors on the complex plane which have their vertices at the origin of the coordinates, for any value of the relative half-period N (or the relative frequency $\frac{\pi}{N}$). The angle of sector β is numerically equal to the value of the relative frequency $\frac{\pi}{N}$ for which it is plotted. It can be seen from expression (6) that the effect of hysteresis becomes apparent in a deflection of each sector through an angle η_i in the direction of the lower relative frequences (larger N).

Since at $\varkappa_0$ = const. the angle η is a function of the amplitude of the first harmonic $\tilde{x}_3(\bar{t})$, which for given γ and k_u is dependent on frequency $\frac{\pi}{N}$ alone, each sector will be turned anti-clockwise through its angle η_i.

Fig. 3 shows a method of determining η_i graphically directly from the frequency response of the system's linear group expressed in values of N. The frequency response modulus is multiplied by the coefficient $k_u a$, where $a = 4/\pi\,[(\sin\pi/2N)\gamma / \sin\pi/2N]$. Values for a calculated for various γ and N, are given in [1].

Since the position of the sectors depends upon the amplitude of the periodic mode of the system, a variation in circuit gain—as distinct from a system employing an ideal relay—will cause a change in frequency of the periodic process, this change being of a discrete nature. An angular position of the sector that determines the existence

in the system of a periodic mode with a half-period $N = N_i$ can vary in the positive direction through an angle a_1, and in the negative direction through an angle a_2 without affecting the frequency of the periodic mode involved (Fig. 4). Thus, a change in system gain over a certain range will not affect the frequency of the periodic process. At larger gain variations in one or the other direction, the oscillation frequency of the system will vary in a jump-like manner. Let us denote by $\eta_i^* = \eta_i + a_1$ the limit value of angle η at which the system transfers from the existing periodic mode to another, lower-frequency mode. Here, it is necessary always to observe the condition $\eta_i^* \leq \frac{\pi}{2}$, which expresses the fact that the amplitude of the periodic mode may not be less than x_0. Bearing in mind that

$$\eta_i^* = \arcsin \frac{x_0}{A_i^*} = \arcsin \frac{x_0}{A_i} + \alpha_1$$

where A_i^* is the amplitude value of the oscillations having a relative half-period $N = N_i$, at which there occurs a change in frequency, we find the corresponding change in system gain which provides for the occurrence of a periodic mode with a relative half-period larger than N_i. This change is equal to

$$\frac{A_i^*}{A} = \frac{x_0}{x_0 + A_i \sin \alpha_1}.$$

From condition $\eta_i^* \leq \pi/2$ it follows that the magnitude of angle α_1 must obey the inequality

$$\alpha_1 \leqslant \arcsin\left(1 - \frac{x_0}{A_i}\right).$$

The boundary condition η, at which the frequency of the periodic mode increases, we will denote through $\bar{\eta}_i = \eta_i - \alpha_2$, with the restriction that an increase in gain does not render the angle η smaller than zero, i.e., $\bar{\eta}_i \geq 0$. Since

$$\bar{\eta}_i = \arcsin \frac{x_0}{A_i} = \arcsin \frac{x_0}{A_i} - \alpha_2$$

the relative increase in gain which leads to an increase in periodic-mode frequency is equal to

$$\frac{\bar{A}_i}{A_i} = \frac{x_0}{x_0 - A_i \sin \alpha_2}.$$

The feasibility of such change is limited by the condition

$$\alpha_2 \leqslant \eta_i.$$

In this way, the presence of hysteresis in the pulse-unit relay characteristic, in the case of a limited value of open-system gain, leads to a drop in frequency of the periodic mode, and makes it dependent of the gain value selected.

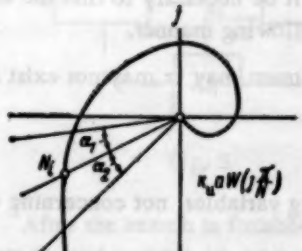

Fig. 4

LITERATURE CITED

1. V. P. Kazakov, "Investigation of the dynamics of automatic-control pulsed relay systems," Avtomatika i Telemekhanika 18, 1 (1957).*
2. K. Izawa and L. E. Weaver, Relay-Type Feedback Control Systems with Dead Time and Sampling, Application and Industry, No, 42 (1959).
3. Ya. Z. Tsypkin, "Theory of automatic-control relay systems," State Press for Technical and Theoretical Literature, 1955.

*See English translation.

ON ONE METHOD OF AUTOMATIC SEARCH FOR THE EXTREMUM OF A FUNCTION OF MANY VARIABLES

K. B. Norkin

(Moscow)

Translated from Avtomatika i Telemekhanika, Vol. 22, No. 5,
pp. 618-623, May, 1961
Original article submitted October 14, 1960

Three variations of an automatic search method using sufficient conditions for the extremum are described. Sufficient conditions for the extremum are found which are suitable for use in computers.

In solving problems about the automatic search for the extremum of a function of several variables, methods which involve the necessary conditions for the extremum are ordinarily used (see, for example [1-3]). The search ceases at point M_0 if each variable individually has an extremum at this point. This condition is necessary, but not sufficient. Such methods give the desired results for a large class of functions, but they are, strictly speaking, applicable only to the case $n = 1$ (n is the number of variables). Even when $n = 2$, convergence to a saddle or crest of a function Q, for which the extremum is sought, is possible. This happens because certain search methods, which theoretically converge strictly to the true extremum point if the function is continuously differentiable, in practice do not converge to the extremum since they use a finite step. This proves that if the step is finite, it is impossible to consider the convergence of the method used only for the case of continuously differentiable functions. Practice shows that it is better to consider the function Q continuous, but differentiable only almost everywhere, and to use only those analysis results which are justified for such functions. For example, Fig. 1, a shows the movement of an automatic search system for two methods: the Gauss-Zeidel method (heavy solid line), and the gradient method (heavy dashed line). The light lines designate equal levels of the function Q. The search converges to points K_1 and K_2, respectively. There is an extremum for each of the variables individually at each of these points. The points are not extremum, however, since the sufficient conditions for the extreme are not met for the aggregate of the variables.

Methods are described in the literature which permit one to overcome this difficulty to a greater or lesser degree [4].

Three variations of one search method are described below, which ensure convergence to the point M_0, at which the sufficient conditions for the extremum for the aggregate of variables are met, and which hold for a broad class of functions.

The essence of the simplest variation will be explained by an example. Let it be necessary to find the extremum of a function $Q = Q(x_1, x_2, \ldots, x_n)$ of n variables. We will proceed in the following manner.

1. We will seek the extremum of Q in the usual manner. However, an extremum may or may not exist at the convergence point of the search.

2. We will fix the variable x_1.

3. We will seek, by any known method, the extremum of Q for the remaining variables, not concerning ourselves about meeting the sufficient conditions.

4. We will remember the value of Q at the point found.

5. We will change x_1 by a small amount Δx_1, leaving all the other coordinates unchanged.

6. We will repeat the search for the extremum of Q with this new value of x_1.

7. We will compare the former and newly found values of Q. On the basis of this comparison, we will make the next change in x_1 in such a way that Q changes in the desired direction. The path of movement for the case of two variables is given in Fig. 1, b.

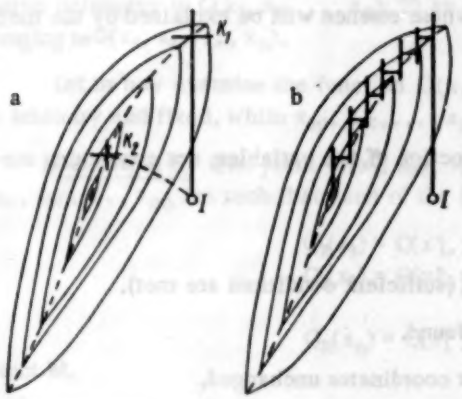

Fig. 1

This method can be called "the method of fixed coordinates." It can be shown that this method converges to the point M_0, which is extremal for a certain class of functions Q in which the convergence points of the search in n-1 variables form curves in the coordinate space, for different values of x_1, regardless of whether M_0 lies in the domain of the given function or on the boundary.

The block diagram of a system which operates according to the method described is given in Fig. 2. The output of object O is fed to two automatic optimizers: a multichannel optimizer AO_2, and a single-channel optimizer AO_1. The variable x_1 is set by optimizer AO_1 after optimizer AO_2 finishes its search. The remaining variables $x_2, x_3, \ldots, x_n$ are set by optimizer AO_2. AO_1 is a step optimizer; it takes a step on command from AO_2, which acts after the completion of a search. If changes in x_1 in one direction cause undesirable changes in Q, optimizer AO_1 changes x_1 in the other direction. AO_1 can be any single-channel optimizer. The simplest circuit of such an optimizer is shown in Fig. 3.

To explain the operation of the circuit, let us first assume that capacitor C_1 and the circuit with P_3 are not present, and that R_1 is very small. P_1 is a two-winding neutral polarized relay, connected so that the passage of current through coil A causes contact $1P_1$ to close, operates P_2, and transfers the moving contact $1P_2$ to position B. Current now flows through winding B of relay P_1. This causes contact $1P_1$ to open, etc. A pulse pair is obtained as a result. If R_1 is increased, the pulse-pair oscillations will cease when a certain value of R_1 is reached. If a short positive pulse is fed through C_1, one pulse pair will occur, and the process will once more stop. The contact $2P_2$ changes its position in this manner. The first positive pulse switches contact $1P_3$, for example to +E; and the second to -E. Contacts $1P_p$ and $2P_p$ are closed by optimizer AO_2 when a search is finished. Capacitor C_1 is charged to a voltage equal to Q, and capacitor C_3 to a voltage E. The polarized relay P_3 is connected so that the charging current does not cause it to operate. After contactz $1P_p$ and $2P_p$ drop out, there is no discharge current through C_1 (the capacitor "remembers" the value of Q), but the discharge current - C_3 flows through relay P_3 and causes contact $1P_3$ to close briefly; x_1 is increased or decreased in this case, depending on the position of $2P_3$. The search for the extremum of Q is conducted for the variables $x_2, x_3, \ldots, x_n$.

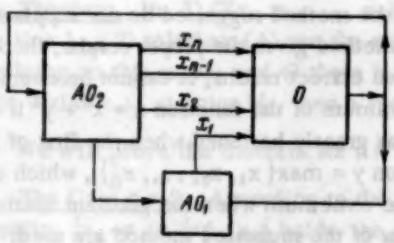

Fig. 2

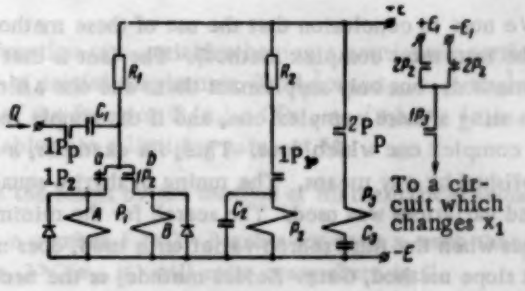

Fig. 3

After the search is finished, relay P_p, built into AO_2, operates again. If Q has decreased, no pulse pair is triggered, and contact $1P_3$ causes x_1 to change in the former direction. If, however, Q has increased, the pulse pair is triggered, and x_1 will change in a new direction after contact $2P_p$ drops out. The optimizer described was tested and "felt" a difference of $\Delta Q = 0.2$ volt. If it were necessary to search for the maximum of Q, it would be necessary to change the polarity of E and to reconnect the windings of the polarized relay.

The suggested method and the conditions of its applicability have a mathematical basis, which is given in the Appendix.

The proposed method is very simple. However, if an arbitrary variable is fixed, it does not work for all functions. It gives good results for a number of functions if the variable to be fixed is chosen correctly. In this case, the optimizer can automatically switch the output of AO_1 to the different variables $x_1, x_2, \ldots, x_n$ in turn, by means of a special commutator. Functions may be encountered, however, for which even this complication of the search (second variation) does not ensure convergence to the true extremum.

In this case, a method (third variation) can be recommended, whose essence will be explained by the method of induction.

For the Case of Two Variables

1. Using any known method, we will find the extremum of a function of two variables, not concerning ourselves about meeting the sufficient conditions.

2. We will fix the variable x_1.

3. We will find the extremum of a function of one variable, x_2 (sufficient conditions are met).

4. We will remember the value of the function Q at the point found.

5. We will change x_1 by a small amount ΔX_1, leaving all other coordinates unchanged.

6. We then repeat the search for the extremum of Q with x_2 as the variable.

7. We will compare the former and newly found values, and make the next change in x_1 in the proper direction on the basis of this comparison.

For the Case of Three Variables

The variable x_3 must be fixed, and a point sought by the above-mentioned method at which the sufficient conditions for the extremum of a function of two variables (x_1, x_2) are met. Then x_3 is changed, and the search is repeated with x_1 and x_2 as variables, and finally the effectiveness of the change in x_3 is evaluated.

For the Case of n Variables

The variable x_n must be fixed, and a point found at which the sufficient conditions of the extremum are met for the (n-1)st variable, and the value of Q found at that point must be remembered. Then x_n can be changed, the search repeated in terms of the (n-1)st variable, and the effectiveness of the change in x_n evaluated. The mathematical basis and conditions of applicability of the suggested search method can be found in the first half of the theorem in the Appendix (for the case n=2), if one considers x_2 to be a vector with coordinates $(x_2, x_3, \ldots, x_n)$. In this case, a line of extremums will exist for a very broad class of functions.

We note in conclusion that the use of these methods causes practically no increase in difficulty or search time (even the last, most complex method). The fact is that the variations of the method suggested do not supplant other search methods, but only supplement them and one another. If a simple method gives the proper results, there is no sense in using a more complex one, and if the simple method does not give correct results, it cannot be compared to a more complex one which does. Thus, for example, a search for the minimum of the function $z = x^2 + y^2$ is easily accomplished by any means. The tuning of thyrite square-law devices was greatly hastened when the first of the suggested variations was used. The search for the minimum of the function $y = \max\{x_1, x_2, \ldots, x_n\}$, which easily converges when the third search variation is used, does not converge to the extremum when the gradient method, steepest slope method, Gauss-Zeidel method, or the two simpler variations of the suggested method are used. The information presented may prove useful even in the case of manual search for the extremum.

APPENDIX

Let us find the sufficient conditions for the maximum* of a function of n variables, suitable for use in computers. The meeting of sufficient conditions for the maximum of a function of one variable is easily confirmed by an automatic machine. It is desirable to use this fact in solving the stated problem.

---

*The result is found in an analogous manner for the minimum.

In practice, it is important to find not the strict maximum, but the largest value in a certain, limited, closed region. If the function is continuous, this value may either be a maximum, or may lie on the boundary. It is desirable to combine these two cases by the term "limiting value."

Definition I. The function $Q = Q(x_1, x_2, \ldots, x_n)$, given in the region $G(x_1, x_2, \ldots, x_n)$, is said to have a limiting value at the point $M_0\{x_{10}, x_{20}, \ldots, x_{n0}\}$, if: 1) in any arbitrarily small area around the point M_0, there are points belonging to $G(x_1, x_2, \ldots, x_n)$; 2) an area around M_0 exists in which the value of $Q(M) < Q(M_0)$ at all points M belonging to $G(x_1, x_2, \ldots, x_n)$.

Let us now examine the function $Q(x_1, x_2, \ldots, x_n)$ at the point $M\{x_1^*, x_{2e}, x_{3e}, \ldots, x_{ne}\}$. Here $x_1 = x_1^*$, and is arbitrary and fixed, while $x_{2e}, x_{3e}, \ldots, x_{ne}$ are certain numbers.

Definition II. The point $M\{x_1^*, x_{2e}, x_{3e}, \ldots, x_{ne}\}$ will be called a point of partial maximums for $x_1 = x_1^*$, if $x_{2e}, x_{3e}, \ldots, x_{ne}$ are such that each of the functions:

$$Q_2(x_2) = Q(x_1^*, x_2, x_{3e}, \ldots, x_{ne}) \text{ of one variable } x_2,$$
$$Q_3(x_3) = Q(x_1^*, x_{2e}, x_3, \ldots, -x_{ne}) \text{ of one variable } x_3,$$

$Q_n(x_n) = Q(x_1^*, x_{2e}, x_{3e}, \ldots, x_n)$ of one variable x_n has a limiting value at the point M.

It is evident that

$$\begin{aligned} x_{2e} &= \varphi_2(x_1), \\ x_{3e} &= \varphi_3(x_1), \\ &\cdots\cdots\cdots \\ x_{ne} &= \varphi_n(x_1), \end{aligned} \qquad (A)$$

that is, the position of the point of partial maximums depends on x_1 and on the form of the function Q. At least one point of partial maximums corresponds to each x_1.

Definition III. The curve given by relations (A) in the region $G(x_1, x_2, \ldots, x_n)$ is called the curve of partial maximums.

A curve of partial maximums sometimes exists for continuous functions in a bounded, closed region. Another variable can be used instead of x_1 to construct the curve of partial maximums. Our proof does not depend on which particular variable is used for this construction. If a partial maximum curve does not exist for a given function (but a surface does), the theorem does not hold. We note, however, that the partial maximum curve exists for the case $n = 2$ for a very broad class of functions. This fact can easily be used as the basis for the third variation of the suggested method.

Theorem. If: 1) $Q(x_1, x_2, \ldots, x_n)$ is a continuous function of n variables having a continuous partial maximum line L_{x_1}; 2) relations (A) are the equation of a curve of partial maximums; 3) $M_0\{x_{10}, x_{20}, \ldots, x_{n0}\}$ is a point lying on this curve; and 4) there is a limiting value of the function $Q_1(x_1) = Q[x_1, \varphi_2(x_1), \varphi_3(x_1), \ldots, \varphi_n(x_1)]$ of one variable x_1 at point M_0, then a function Q of n variables has a limiting value at M_0.

We will prove the theorem for $n = 2$, and generalize the result by the method of mathematical induction.

The Case $n = 2$. According to the definition of L_{x_1}, a number $\delta_2(x_1) > 0$ exists for each x_1 such that if the inequality $|x_2 - \varphi_2(x_1)| < \delta_2(x_1)$ holds, the inequality $Q(x_1, x_{2e}) > Q(x_1, x_2)$ will exist everywhere in G.

Since $\delta_2(x_1) > 0$, it has a lower bound, that is, there is a lower bound δ_2; $\delta_2 > 0$, since $\delta_2(x_1) > 0$ for every x_1, and the region is closed.

Since $Q_1(x_1) = Q[x_1, \varphi_2(x_1)]$, and has a limiting value at M_0, a $\delta_1 > 0$ exists such that if the inequality $|x_1 - x_{10}| < \delta_1$, holds, the conditions $Q_1(x_1) < Q_1(x_{10}) = Q(x_{10}, x_{20})$.

Finally, we find that when $|x_1 - x_{10}| < \delta_1$ and $|x_2 - x_{2e}| < \delta_2$, the inequality is justified, which proves the first part of our theorem:

$$Q(x_1, x_2) < Q(x_{10}, x_{20}).$$

The case of Arbitrary n. Let us examine the function $Q^* = Q[x_1, x_2, \ldots, x_{n-1}, \varphi_n(x_1)]$ instead of Q. This is a function of the (n-1)st variable, which meets the conditions of the theorem at M_0. By induction, there exist positive $\delta_1, \delta_2, \ldots, \delta_{n-1}$ such that the condition

$$Q[x_1, x_2, \ldots, x_{n-1}, \varphi_n(x_1)] < Q(M_0)$$

will occur as soon as the inequalities

$$|x_1 - x_{10}| < \delta_1; \ |x_2 - x_{20}| < \delta_2; \ldots; |x_{n-1} - x_{(n-1)0}| < \delta_{n-1} \quad (1)$$

hold simultaneously.

Since $Q(x_1, x_2, \ldots, x_n)$ is continuous in x_n everywhere in G for the case when

$$|x_1 - x_{10}| + |x_2 - x_{20}| + \ldots + |x_{n-1} - x_{(n-1)0}| > 0 \quad (2)$$

according to the lemma about the conservation of sign, a $\delta_n(x_1, x_2, \ldots, x_{n-1})$, can be found such that if relations (1), (2), and $|x_n - x_{n0}| < \delta_n$, hold simultaneously, the inequality

$$Q(x_1, x_2, \ldots, x_n) < Q(x_{10}, x_{20}, \ldots, x_{n0}) \quad (3)$$

also holds.

Here $\delta_n > 0$ – the lower bound for $\delta_n(x_1, x_2, \ldots, x_{n-1})$ exists, since $\delta_n(x_1, x_2, \ldots, x_{n-1}) > 0$ and the region is closed. If the condition

$$|x_1 - x_{10}| + |x_2 - x_{20}| + \ldots + |x_{n-1} - x_{(n-1)0}| = 0$$

occurs instead of (2), then a δ_n^* can be found according to the definition of L_{x_1}, such that (3) always holds when $|x_n - x_{n0}| < \delta_n^*$.

Thus, the existence of an area around point M_0 in which (3) holds everywhere is proven. The bounds of this area are defined by relations (1), and $|x_n - x_{n0}| < \min\{\delta_n, \delta_n^*\}$. The theorem has been completely proven.

LITERATURE CITED

1. A. A. Fel'dbaum, "An automatic optimizer" (in Russian), Avtomatika i Telemekhanika, Vol. XIX, No. 8 (1959).*
2. O. V. Kirillov, "An automatic minimizer for low duty-cycle operation" (in Russian), in the Collection, Theory and Application of Discrete Automatic Systems, published by the Academy of Sciences Press, USSR, 1960.
3. A. B. Shubin, "Ten-channel automatic electromechanical optimizer" (in Russian), Avtomatika i Telemekhanika, Vol. XXI, No. 5 (1960).*
4. R. T. Stakhorskii, "Multichannel automatic optimizer for solving variation problems" (in Russian), Avtomatika i Telemekhanika, Vol. XX, No. 11 (1959).*

*See English translation.

A SERVOMECHANISM WITH A TWO-PHASE ASYNCHRONOUS MOTOR WHOSE CONTROL WINDING IS POWERED BY A CURRENT GENERATOR

N. P. Vlasov

(Gor'kii)

Translated from Avtomatika i Telemekhanika, Vol. 22, No. 5,
pp. 624-629, May, 1961
Original article submitted September 2, 1960

A servomechanism with an asynchronous motor operating on alternating current is examined, in which the control winding is powered by a current generator. An expression is found for the output magnitude of the open-loop system, taking initial conditions into account, and also for the transfer function. The stability of the system is studied with certain simplifying assumptions.

In AC servomechanisms, the actuating element is often a two-phase motor with a squirrel-cage rotor. One of the stator windings—the excitation winding—is connected to a voltage of constant amplitude; the other winding—the control winding—is part of the control circuit of the servo system. It is ordinarily assumed that the excitation winding resistance is small in comparison with the inductive reactance.

The control winding can be powered by a controllable power amplifier having a sufficiently small resistance (from a voltage generator). It is then assumed that the control winding circuit can be neglected, and only the inductive reactance considered. Servomechanisms with asynchronous motors operating under these conditions have been examined more than once [1-3].

The control winding can also be powered by a power amplifier with a high resistance, so high that the inductive reactance can be neglected in the control winding circuit. This kind of power amplifier is a current generator. A servomechanism with an asynchronous motor powered by a current generator will be discussed in this article.

1. Motion Equation and Transfer Function of the Servo System

Let us examine the servo system whose diagram is shown in the figure. In this diagram, I is a measuring element, M is a modulator, 1, 2, 3, are linear passive four-pole networks, A is an asynchronous motor, TG is an asynchronous tachometer generator, and P is a gear box. Using these designations, we can write an equation for the measuring element

$$x(t) = \Theta_1(t) - \Theta_2(t) \tag{1}$$

an equation for the modulator

$$u_x(t) = U_m x(t) \cos(\omega_0 t + \varphi) \tag{2}$$

and one for the voltage across the tach generator output

$$u_S(t) = \frac{k_S}{\omega_0} U_{S\,m} \sin(\omega_0 t + \alpha) \frac{d\Theta_2}{dt}. \tag{3}$$

Neglecting the resistance of the excitation winding circuit, we write the equation of this winding

$$u_2(t) = U_{2m} \sin(\omega_0 t + \psi) = \frac{d\psi_b}{dt}. \tag{4}$$

Here ψ_b is the flux of the excitation winding.

Let the transfer functions of four-poles 1, 2, and 3 be $\overline{Y_1(p)}$, $\overline{Y_2(p)}$ and $\overline{Y_3(p)}$ respectively.

Using the diagram, we can write

$$\overline{I_c(p)} = \frac{\overline{Y_1(p)}}{R}\left[\overline{Y_3(p)}\,\overline{U_x(p)} - \overline{Y_2(p)}\,\overline{U_S(p)}\right]. \tag{5}$$

Here R is a constant having the sense and dimensions of resistance. $\overline{I_c(p)}$ is a representation of the current in the control winding. Equation (5) can be considered as the control winding circuit equation.

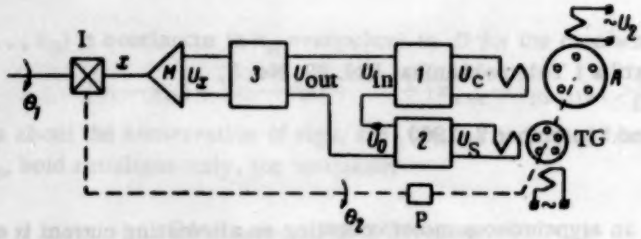

Let us write an expression for the rotor flux referred to the axis of the control winding.

$$\psi_a = Li_a + M_0 i_c. \tag{6}$$

Here L is the inductance of the rotor, M_0 is the mutual inductance between the rotor and control winding, i_a is the rotor current, referred to the control winding axis.

The rotor equations can be represented in the form

$$\frac{d\psi_a}{dt} + n\psi_B\frac{d\Theta_2}{dt} + i_a r = 0 \tag{7}$$

$$\frac{d\psi_B}{dt} - n\psi_a\frac{d\Theta_2}{dt} + i_B r = 0 \tag{7a}$$

where r is the rotor resistance, and n is the transfer coefficient (the ratio of the angular rotation of the motor shaft to that of the drive shaft, Θ_2). Equations (4, 6, 7 and 7a) are written under the assumption that one can neglect the rotor and stator leakage flux.

Let us write the equation for the rotation of the drive shaft

$$Jn^2\frac{d^2\Theta_2}{dt^2} + \frac{n}{r}\left[n(\psi_a^2 + \psi_B^2)\frac{d\Theta_2}{dt} + \psi_B\frac{d\psi_a}{dt} - \psi_a\frac{d\psi_B}{dt}\right] = -k\frac{d\Theta_2}{dt}. \tag{8}$$

Here J is the moment of inertia of the rotating mass, referred to the motor shaft, and k $d\Theta_2/dt$ is the external torque applied to the drive shaft. If the term $\psi_a^2\,(d\Theta_2/dt)$ in the left half of equation (8) is neglected, one can say that for small signals, equations (1-6, 7 and 8) form a set of linear differential equations with periodic coefficients, from which equation (5) can be written in a form suitable for Laplace transformation. This set can be solved by means of the method given in [1,3]. Writing (1-6, 7 and 8) in a form which takes initial conditions into account, and solving for $\Theta_2(p)$, discarding terms involving X and Θ_2 as functions of the operator P with arguments $p \pm j\omega_0$ on the basis of the reasoning given in [1,3], we get the following expression for $\overline{\Theta_2(p)}$:

$$\overline{\Theta_2(p)} = \left\{\frac{nM_0U_mU_{2m}}{4R\omega_0}\left\{\left[\frac{p-j2\omega_0}{r+L(p-j\omega_0)}\,\overline{Y_1(p-j\omega_0)}\,\overline{Y_3(p-j\omega_0)}\,e^{j(\psi-\varphi)}\right] + \right.\right.$$

$$\left.\left. + [\ ]^*\right\}\overline{X(p)} + \frac{k_S nM_0U_mU_{2m}}{2R\omega_0^2}\left\{\left[\frac{p-j2\omega_0}{r+L(p-j\omega_0)}\,\overline{Y_1(p-j\omega_0)}\,\overline{Y_2(p-j\omega_0)}\,e^{j\psi}\right] + \right.$$

$$\left. + [\ ]^*\right\}\Theta_2(0)\sin\alpha - \frac{n^2LU_{2m}}{2r\omega_0^2}\left\{\left[\frac{p-j2\omega_0}{r+L(p-j\omega_0)}\,e^{j\psi}\right] + [\ ]^*\right\}\Theta_2(0)\cos\psi +$$

$$+\left[Jn^2p + k + \frac{n^2U_{2m}^2}{2r\omega_0^2}(1+\cos 2\psi)\right]\Theta_2(0) + Jn^2\dot{\Theta}_2(0) +$$

$$+\frac{nU_{2m}L}{2r\omega_0}\left[Li_a(0)+M_0i_c(0)\right]\left\{\left[\frac{p-j2\omega_0}{r+L(p-j\omega_0)}e^{j\psi}\right]+[\ ]^*-\frac{2\cos\psi}{L}\right\}\left\{\left\{Jn^2p^2+\right.\right.$$

$$+kp+\frac{n^2U_{2m}}{2r\omega_0^2}p-\frac{n^2U_{2m}^2}{4r\omega_0^2}\left\{\left[\frac{L(p-j2\omega_0)}{r+L(p-j\omega_0)}\right]+[\ ]^*\right\}p+$$

$$\left.\left.+\frac{k_Snk_0U_{2m}U_{cm}}{4R\omega_0^2}\left\{\left[\frac{j(p-j2\omega_0)}{r+L(p-j\omega_0)}\overline{Y_1(p-j\omega_0)}\,\overline{Y_2(p-j\omega_0)}e^{j(\psi-\alpha)}\right]+[\ ]^*\right\}p\right\}^{-1}. \tag{9}$$

Here the designation [ ]* represents the complex conjugate of the expression included within the brackets [ ] appearing before it.

In equation (9), the operator coefficient for $\overline{X(p)}$ is the transfer function, and the remaining terms express the effect of the initial conditions. Introducing the operator $s = p/\omega_0$, and the constants

$$\delta=\psi-\varphi\quad\gamma=\psi-\alpha\quad T=\frac{\omega_0L}{r}\quad T_1=\frac{Jn^2\omega_0}{K}\quad T_2=\frac{2r\omega_0RK}{nk_0U_mU_{2m}}$$

$$T_3=\frac{n^2U_{2m}^2}{2r\omega_0^2K}\quad K_S=\frac{k_Snk_0U_{2m}U_{cm}}{2r\omega_0RK}\quad K=k+\frac{n^2U_{2m}^2}{2r\omega_0^2} \tag{10}$$

we write the transfer function of the open-loop system in the following manner:

$$\frac{\overline{\Theta_2(s)}}{\overline{X(s)}}=\frac{\frac{1}{2}\left\{\left[\frac{s-j2}{T(s-j)+1}\overline{Y_1(s-j)}\,\overline{Y_2(s-j)}e^{j\delta}\right]+\left[\ \right]^*\right\}}{T_3s\left\{T_1s+1+\frac{K_c}{2}\left(\left[\frac{j(s-j2)}{T(s-j)+1}\overline{Y_1(s-j)}\,\overline{Y_2(s-j)}e^{j\gamma}\right]+[\ ]^*\right)-\frac{T_2}{2}\left[\left(\frac{T(s-j2)}{T(s-j)+1}\right]+[\ ]^*\right)\right\}}. \tag{11}$$

Using equation (1), we can find the transfer function of the closed-loop system.

If the voltage

$$u_S(t)=\frac{k_S}{\omega_0}US_m\cos(\omega_0t+\alpha)\frac{d\Theta_2}{dt} \tag{3a}$$

is put into the feedback loop instead of (3), we get the expression

$$\frac{\overline{\Theta_2(s)}}{\overline{X(s)}}=\frac{\frac{1}{2}\left\{\left[\frac{s-j2}{T(s-j)+1}\overline{Y_1(s-j)}\,\overline{Y_2(s-j)}e^{j\delta}\right]+[\ ]^*\right\}}{T_3s\left\{T_1s+1+\frac{K_c}{2}\left(\left[\frac{s-j2}{T(s-j)+1}\overline{Y_1(s-j)}\,\overline{Y_2(s-j)}e^{j\gamma}\right]+[\ ]^*\right)-\frac{T_2}{2}\left(\left[\frac{T(s-j2)}{T(s-j)+1}\right]+[\ ]^*\right)\right\}}. \tag{11a}$$

for the transfer function of the open-loop system.

It is evident that the transfer function of the closed loop system can be found from (11a) by using equation(1).

2. Stabilization of the Servo System

Let us examine the servo without feedback, in which case the only member with an operator coefficient is the two-phase asynchronous motor.

Substituting $K_S = 0$, $\overline{Y_1(s)} = K_1$, and $\overline{Y_2(s)} = K_2$ into equation (11) or (11a), where K_1 and K_2 are amplification coefficients, and assuming for simplicity that $\psi = \varphi$, we get the following expression for the transfer function of the closed-loop system

$$\frac{\overline{\Theta_2(s)}}{\Theta_1(s)}=\frac{K_0[T(s^2+2)+s]}{s(T_1s+1)[T^2(s^2+1)+2Ts+1]+(K_0-TT_3s)[T(s^2+2)+s]}. \tag{12}$$

Here

$$K_0 = \frac{K_1 K_2}{T_3}.$$

Let us examine the case of a purely inertial load (k = 0). Then $T_3 = 1$, as follows from (10). The inequalities $T^2 \gg 1$ and $TT_1 \gg 1$ ordinarily hold well for an asynchronous motor. Keeping this in mind, and considering the approximate transfer function [2] for $|s^2| \ll 1$, we find, from (12),

$$\frac{\overline{\Theta_2(s)}}{\overline{\Theta_1(s)}} = \frac{K_0(s+2T)}{2TT_1s^3 + T^2T_1s^2 + (K_0 - T^2)s + 2TK_0}. \quad (12a)$$

Using the Routh-Hurwitz criterion, we find that the system described by equation (12a) is unstable.

Let us consider the system with feedback, under the condition that the voltage of expression (3) is introduced into the feedback loop.

Let four-poles 1, 2 and 3 be inertialess with amplification coefficients $Y_1(s) = K_1$, $Y_2(s) = K_2$, and $Y_3(s) = K_3$. Setting $\delta = \gamma = 0$ for simplicity, we find, by using (11), an expression for the transfer function of the closed-loop system

$$\frac{\overline{\Theta_2(s)}}{\overline{\Theta_1(s)}} = \frac{K_0[T(s^2+2)+s]}{s\{(T_1s+1)[T^2(s^2+1)+2Ts+1]+\mu(Ts+2)\}+(K_0 - TT_3s)[T(s^2+2)+s]}.$$

Here

$$\mu = K_S K_1 K_2. \quad (13)$$

If again we set $T_3 = 1$, $T^2 \gg 1$, $TT_1 \gg 1$, and examine the approximate transfer function for $|s^2| \ll 1$, we get

$$\frac{\Theta_2(s)}{\overline{\Theta_1(s)}} = \frac{K_0(s+2T)}{2TT_1s^3 + (T^2T_1 + \mu T)s^2 + (K_0 + 2\mu - T^2)s + 2TK_0}. \quad (13a)$$

The servo will be stable if the following conditions hold:

$$K_0 + 2\mu > T^2 \quad (14)$$

$$\mu(K_0 + 2\mu + 2TT_1 - T^2) > TT_1(3K_0 + T^2). \quad (15)$$

It is evident that inequalities (14) and (15) will hold if μ is sufficiently large.

Let the voltage of (3a) be introduced into the feedback loop. Then under the previous conditions ($\delta = \gamma = 0$; $\overline{Y_1(s)} = K_1$; $\overline{Y_2(s)} = K_2$; $\overline{Y_3(s)} = K_3$), by using equation (11a), we get an expression for the transfer function of the closed-loop system

$$\frac{\overline{\Theta_2(s)}}{\overline{\Theta_1(s)}} = \frac{K_0[T(s^2+2)+s]}{s(T_1s+1)[T^2(s^2+1)+2Ts+1]+[K_0+s(\mu - TT_3)][T(s^2+2)+s]}. \quad (16)$$

If we again set $T_3 = 1$, $T^2 \gg 1$, $TT_1 \gg 1$, and examine the approximate transfer function for $|s^2| \ll 1$, we get

$$\frac{\overline{\Theta_2(s)}}{\overline{\Theta_1(s)}} = \frac{K_0(s+2T)}{2TT_1s^3 + (T^2T_1 + \mu)s^2 + (K_0 + 2\mu T - T^2)s + 2TK_0}. \quad (16a)$$

The servo will be stable if the following conditions hold

$$K_0 + 2\mu T > T^2 \quad (17)$$

$$\mu\left[\frac{K_0}{T} + 2\mu + T(2TT_1 - T^2)\right] > TT_1(3K_0 + T^2). \quad (18)$$

It is evident that inequalities (17) and (18) will hold if μ is sufficiently large.

A comparison of conditions (14) and (17) shows that (17) will hold for smaller values of μ.

Let us now compare conditions (15) and (18). Since the right halves of the inequalities are identical, we will examine the inequality

$$\frac{K_0}{T} + 2\mu + T(2TT_1 - T^2) > K_0 + 2\mu + 2TT_1 - T^2$$

from which we find

$$2T_1 - T > \frac{K_0}{T^2}. \tag{19}$$

If (19) is to hold, it is better to introduce the voltage of (3a) into the feedback loop in order to stabilize the system.

The quality of the servo can be enhanced by putting a differentiating four-pole in the loop. Since the system is unstable without feedback, it is desirable to use feedback to gain stability, and to introduce a differentiating four-pole into the loop, thus enhancing the system quality. Let such a four-pole be the four-pole 3 (see figure) with transfer function

$$\overline{Y_3(s)} = K_3 \frac{s^2 + k_1 s + 1}{s^2 + k_2 s + 1}.$$

Let us examine a system in which the voltage of (3) is introduced into the feedback loop. We will set $\delta = \gamma = 0$ for simplicity. We then get

$$\frac{\overline{\Theta_2(s)}}{\overline{X(s)}} = -\frac{K_0[(2s + k_1)(2s + k_2)(s + 2T) - (k_2 - k_1)(Ts + 2)s^2]}{s[(T_1 s + 1)(2T_3 + T^2 + 1) + \mu(Ts + 2) - TT_3(2T + s)](2s + k_2)^2} \tag{20}$$

for the approximate transfer function of the open-loop system for $|s^2| \ll 1$

If the voltage of expression (3a) is used in the feedback loop, we get

$$\frac{\overline{\Theta_2(s)}}{\overline{X(s)}} = \frac{K_0[(2s + k_1)(2s + k_2)(s + 2T) - (k_2 - k_1)(Ts + 2)s^2]}{s[(T_1 s + 1)(2Ts - T^2 + 1) + (2T + s)(\mu - TT_3)](2s + k_2)^2} \tag{21}$$

under the same simplifications assumed for the transfer function of (20).

If the diminuend in the numerator within the square brackets of expressions (20) and (21) can be neglected, the simplified transfer functions obtained can be used for a preliminary determination of the coefficients k_1 and k_2 of the differentiating four-pole, and of the coefficient μ which characterizes the feedback.

SUMMARY

An expression for the output magnitude was found for a servomechanism operating with a two-phase AC asynchronous motor whose control winding is powered by a current generator, initial conditions being taken into account. An expression was also found for the transfer function of the system. With certain simplifying assumptions, it was shown that a system having the asynchronous motor as the only inertial element would be unstable. Stability conditions for the system were found as functions of the phase of the voltage acting in the feedback loop.

LITERATURE CITED

1. N. P. Vlasov, "Elements of the theory of AC servomechanisms, and of mixed systems" (in Russian), News of the Technical High School, Electromekhanika, No. 1 (Novocherkassk, 1958).
2. N. P. Vlasov, "Transfer functions of AC servomechanisms with certain stabilizing devices" (in Russian), News of the Technical High School, Electromekhanika, No. 12 (Novocherkassk, 1958).
3. N. P. Vlasov, "A method of finding the transfer functions of AC-operated automatic control systems" (in Russian), Avtomatika i Telemekhanika, Vol. XXI, No. 6 (1960).*

*See English translation.

INVESTIGATING A THYRATRON PULSE CONVERTER WITH A STEP MOTOR

V. M. Kolesnikov

(Moscow)

Translated from Avtomatika i Telemekhanika, Vol. 22, No. 5,
pp. 630-640, May, 1961
Original article submitted July 8, 1960

The paper presents an analytical and experimental investigation of the steady-state and transient responses involved in the conversion of discrete electrical pulses into mechanical angles of rotation in a pulsed electric drive with a three-stator step motor. Formulas are derived for choosing the optimal parameters of the system, and an analysis is made of certain of its operating modes.

In automatic control systems a converter that converts discrete electrical pulses into mechanical angles of rotation is often used as an actuating drive [1-3] (Fig. 1). The converter consists of dc source, a three-stator motor of the step type, and a network which amplifies the power in the pulses.

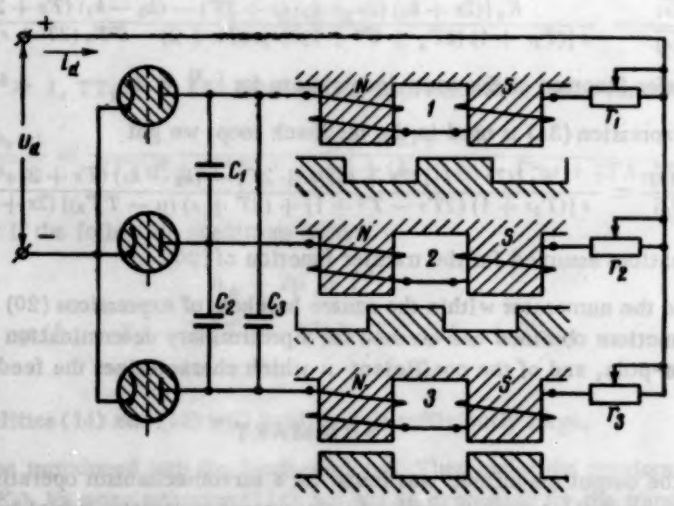

Fig. 1. Circuit diagram for the amplification and conversion of discrete pulses to angles of rotation. 1, 2, 3 are the windings and poles of the step motor; r_1, r_2, r_3 are the ballast resistors.

The converter operates as follows. As the control pulses are successively applied from the input unit to the grids of the rectifiers (at discrete instants of time) the current is switched from one winding to another; as a consequence of this the rotor rotates through a definite angle.

Each control pulse corresponds to an angle of rotation equal to $\frac{1}{3}$ of a pole division. This angle is henceforth called the "step."

In the literature, we are acquainted with [4,5] which investigate the dynamics of step motors. However, these investigations were performed from the point of view of the mechanical behavior of a rotor in a motor without taking into account the processes which occur in the pulse amplification network and the pulse conversion device.

In this paper we investigate the entire converter as a whole, taking into account both the mechanical and electromagnetic processes.

The investigation of the processes in the converter is a complex nonlinear problem in view of the presence of the thyratron rectifiers and the variable inductances of the motor windings. These inductances are in the general case a function of the current and the rotor angle of rotation. Each stator of the motor must be treated as an electromagnet operating on periodic pulses with a variable frequency.

We shall study the energy relationships in the stator for this mode of operation. We shall introduce the following quantities: ω is the angular frequency for the periodic pulses of arbitrary shape which are applied to the winding; Θ is the time in angular units measured along the curve for the periodic pulses $\Theta = \omega t$; x is the instantaneous value of the winding reactance corresponding to harmonic oscillations at a frequency equal to the frequency of the periodic pulses:

$$x = \omega L$$

where L is the instantaneous value of the motor winding inductance.

We shall assume that the reactance of the winding is a function of the current i and the angle of rotation φ of the rotor:

$$x = x(i, \varphi).$$

We shall make use of the known relationships for the voltage balance and the energy storage in the winding. Taking into account the definitions introduced above, these equations can be written as

$$u = ir + \frac{d(xi)}{d\theta},$$

$$w = \frac{1}{\omega}\int_0^{xi} id(xi) = \frac{1}{\omega}\left[i(xi) - \int_0^{i} xi\, di\right].$$

Note that in the latter equation the upper limits of the integrals, as well as the expressions in the integrand, depend on the current and the angle of rotation of the rotors.

Taking into account the fact that

$$\frac{d(xi)}{d\theta} = \frac{\partial(xi)}{\partial i}\frac{di}{d\theta} + \frac{\partial(xi)}{\partial \varphi}\frac{d\varphi}{d\theta}$$

we find the power drawn by the winding

$$s = ui = i^2 r + i\frac{\partial(xi)}{\partial i}\frac{di}{d\theta} + i\frac{\partial(xi)}{\partial \varphi}\frac{d\varphi}{d\theta}. \qquad (1)$$

Differentiating the expression for the stored energy, we obtain

$$q = \frac{dw}{dt} = \left(\frac{\partial w}{\partial i}\frac{di}{d\theta} + \frac{\partial w}{\partial \varphi}\frac{d\varphi}{d\theta}\right)\omega.$$

Since

$$\frac{\partial w}{\partial i} = \frac{1}{\omega}\frac{\partial}{\partial i}\left[i(xi) - \int_0^{i} xi\, di\right] = \frac{i}{\omega}\frac{\partial(xi)}{\partial i}$$

it follows that

$$q = i\frac{\partial(xi)}{\partial i}\frac{di}{d\theta} + \omega\frac{\partial w}{\partial \varphi}\frac{d\varphi}{d\theta}. \qquad (2)$$

By analogy with circuit theory we shall call the quantity q the instantaneous reactive power for a harmonic input. Such a definition is justified on two counts. First, Expression (2) contains the winding reactance corresponding to a definite frequency of the harmonic current. Second, this expression corresponds only to the magnetizing power producing the magnetic flux.

When there is no saturation

$$s = i^2 r + i\left(i\frac{dx}{d\varphi} + x\frac{di}{d\varphi}\right)\frac{d\varphi}{d\theta} \qquad q = i\left(\frac{i}{2}\frac{dx}{d\varphi} + x\frac{di}{d\varphi}\right)\frac{d\varphi}{d\theta}. \tag{3}$$

Studying expressions (3) simultaneously, we can write the following equation for the resistive power by analogy with circuit theory for a harmonic input:

$$p_a = i^2 r + \frac{i^2}{2}\frac{dx}{d\varphi}\frac{d\varphi}{d\theta}. \tag{4}$$

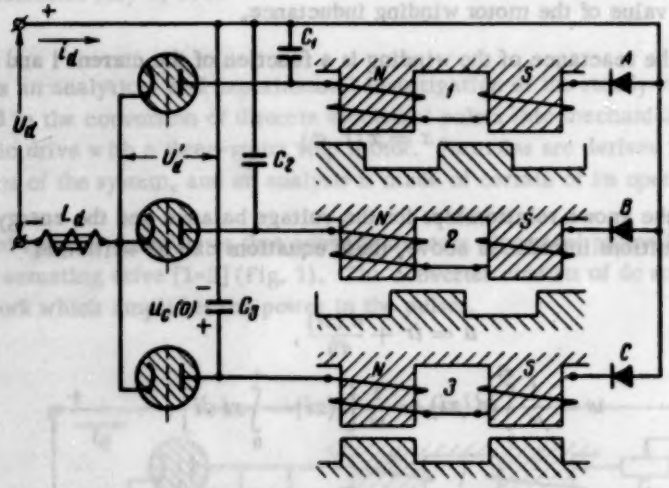

Fig. 2. Circuit for amplifying and converting discrete pulses into angles of rotation. L_d is the inductance of the cathode choke; 1, 2, 3 are the windings and poles of the step motor; A, B, C are uncontrolled diode rectifiers.

After dividing (3) and (4) by i, we obtain the corresponding expressions for the total (apparent) voltage consisting of its resistive and reactive components:

$$u_s = ir + x\frac{di}{d\theta} + i\frac{dx}{d\theta} \tag{5}$$

$$u_a = ir + \frac{i}{2}\frac{dx}{d\theta} \tag{6}$$

$$u_q = x\frac{di}{d\theta} + \frac{i}{2}\frac{dx}{d\theta}. \tag{7}$$

The resistive component of the voltage balances the voltage drop across the resistor and one half of the back emf. The reactive component of the total voltage balances the reactive quiescent voltage drop and the second half of the back emf.

Taking the analysis above into account, it is easy to arrive at analogous conclusions when saturation is present if we take into account the magnetic characteristic of the motor. The resulting expressions provide a comparatively easy means of performing an analysis of the transient responses and energy relationships in the step converter network.

The processes in the converter are studied in accordance with the circuit shown in Fig. 2. In contrast to known circuits, this circuit has an increased efficiency and better frequency characteristics; this can be explained by the absence of ballast resistors and the special connection of the capacitors and the diode rectifiers.

The results of the analysis performed below can easily be extended to apply to the circuit in Fig. 1 and its modification which is the particular case of the variant we are studying; it can also be extended to apply to analogous circuits with silicon transistors.

The reactance of the motor when the rotor turns can be expressed by the relationship (cf. Fig. 3)

$$x = x_{\min} + \frac{\Delta x}{2}(1 - \cos\alpha) \tag{8}$$

where $\alpha = 2l\varphi$, l is the number of pairs of poles, and $\Delta x = x_{max} - x_{min}$.

When (8) is taken into account

$$p_a = i^2 r + \frac{\Delta x l \vartheta i^2}{2\omega}\sin\alpha \tag{9}$$

$$q = xi\frac{di}{d\theta} + \frac{\Delta x l \vartheta i^2}{2\omega}\sin\alpha \tag{10}$$

is valid where $\vartheta = d\varphi/dt$ is the angular velocity.

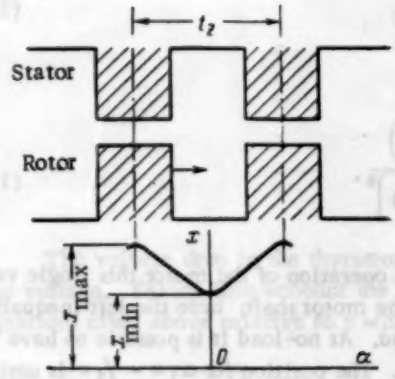

Fig. 3. Variation of the motor reactance when the rotor turns. t_z is a pole division, x_{max} and x_{min} are the maximum and minimum values of the reactance.

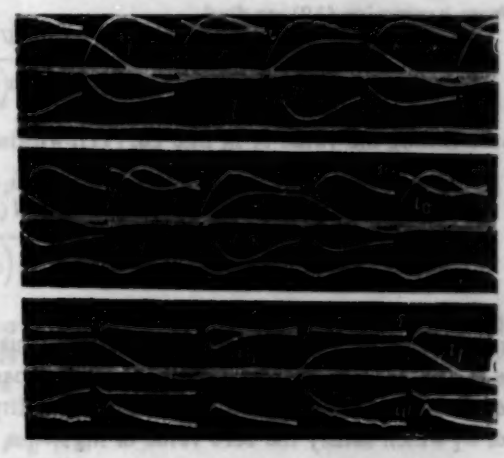

Fig. 4. i_1 is the current in the motor winding, i_a is the plate current of the thyratron; u_{ak} is the voltage across the thyratron, i_d is the rectified current, U'_d is the rectified voltage at the output of the choke; a) L_d = 7h; b) L_d = 0.5 h; c) L_d = 0, r_d = 50 ohm.

We shall study the steady-state mode. We shall assume that the instantaneous value of the current in the winding does not depend on the angle of rotation of the rotor; the duration of this value is $\Theta = \frac{2}{3}\pi$, (i.e., the current has a rectangular or almost rectangular shape).

For this case the equation

$$\theta_i = \theta_s$$

is valid where Θ_s is the time required to process a step.

From expression (9) we find that the instantaneous value of the electromagnetic power is equal to

$$p_e = \frac{\Delta x l \vartheta i^2}{2\omega}\sin\alpha.$$

Integrating this expression within the limits of a step, we obtain

$$P_e = \frac{3}{2\pi}\int_{\alpha=\alpha_1}^{\alpha=\alpha_1+\frac{2\pi}{3}} \frac{\Delta x l \vartheta i^2}{2\omega}\sin\alpha d\alpha = \frac{3\sqrt{3}\Delta x \vartheta l}{4\pi\omega} I_d^2 \sin\left(\alpha_1 + \frac{\pi}{3}\right)$$

where α_1 is the angle α corresponding to the initial instant at which a current pulse is applied to the winding of the

motor; I_d is the average value of the rectified current. The average value of the reactive power over a period is, as we know, equal to zero.

For the electromagnetic torque we have the expression

$$M_e = \frac{3\sqrt{3}\Delta x l_d^2 l}{4\pi\omega} \sin\left(\alpha_1 + \frac{\pi}{3}\right). \tag{11}$$

The resistive power drawn from the rectifier is equal to

$$P_d = I_d\, U_d = \Delta u I_d + r I_d^2 + P_e + r_d I_d^2 \tag{12}$$

where Δu is the thyratron arc drop, U_d is the choke resistance and r_d is the resistance in the winding circuit.

From expression (12) we find

$$I_d = \frac{(U_d - \Delta u)\, 4\pi\omega}{3\sqrt{3}\, l \Delta x \vartheta \sin\left(\alpha_1 + \frac{\pi}{3}\right) + 4\pi\omega (r + r_d)}. \tag{13}$$

Substituting the value of I_d into Eq. (11), we finally find

$$M_e = \frac{12\sqrt{3}\,\pi\omega\Delta x l\,(U_d - \Delta u)^2 \sin\left(\alpha_1 + \frac{\pi}{3}\right)}{\left[3\sqrt{3}\,\vartheta\Delta x l \sin\left(\alpha_1 + \frac{\pi}{3}\right) + 4\pi\omega (r + r_d)\right]^2}. \tag{14}$$

In this expression the angle α_1 is a variable quantity. For synchronous operation of the motor this angle varies over the range $^1/_6\pi \leq \alpha_1 \leq {}^2/_3\pi$, depending on the load which is applied to the motor shaft; here the left inequality corresponds to maximum load, and the right inequality corresponds to no-load. At no-load it is possible to have two values of α_1 which satisfy the zero value of M_e: $\alpha_1 = {}^2/_3$ and $\alpha_1 = -\,{}^1/_3\pi$. The position for $\alpha_1 = -\,{}^1/_3\pi$ is unstable.

Substituting $\alpha_1 = {}^1/_6\pi$ into (14), we find the expression for the maximum (stalling) torque

$$M_{max} = \frac{12\sqrt{3}\,\pi\omega\Delta x l (U_d - \Delta u)^2}{[3\sqrt{3}\,\vartheta\Delta x l + 4\pi\omega (r + r_d)]^2}. \tag{15}$$

For further loading the motor goes out of synchronism.

Expression (14) provides a simple means for finding the dependence of the angle α_1 on the load applied to the motor shaft for specified circuit reactances, motor parameters, and rotor speeds.

The derived expression (14) is valid for comparatively low frequencies of the current pulses in the motor windings. When the frequency of the pulses is increased the duration of the current in the windings increases, and the overlap of the currents in the motor windings begins to have an appreciable effect on the magnitude of the electromagnetic torque. This effect can be explained by the fact that at the instant of overlap currents exist simultaneously in two windings. These currents produce two torques which act in opposite directions, and this leads to lowering of the resultant torque on the shaft of the motor.

The equations for the converter current can be formulated in the conventional manner used in the analysis of converter circuits with rectifiers (i.e., by the method of "aligning" transient responses by segments). However, the equations for each instantaneous electromagnetic circuit which are obtained under these conditions are very complex. The problem can be simplified appreciably if we determine the degree to which the choke in the converter circuit affects the processes in the circuit and the limits for the variation of the overlap angle between the rectifier plate current.

The wave shape of the dc current as such is evidently not of interest to us. In the final analysis there is only one purpose for the choke in our case: to absorb the voltage drop in the converter at the instant when the commutation of the current occurs. In the contrary case the operation of the converter would be impossible, since there would be no guarantee that the voltage would be removed from the rectifier during the period required for deionization. This time must be less than the time corresponding to the lead angle. In the general case, the lead angle Θ_δ depends on the parameters of the entire circuit. For a specific motor and specific rectifiers the lead angle will be

determined by the magnitudes of the cathode inductance and capacitance. Here we find that in obtaining a specific lead angle an increase in the choke inductance causes a corresponding decrease in the required magnitude of the capacitors; a decrease in the capacitance causes a decrease in the overlap angles for the currents in the windings and increases the motor torque. However, the relationship here is not linear, and at a certain value the variation in the magnitude of the choke inductance ceases to affect the lead angle.

Figure 4 shows oscillograms illustrating the effect of the magnitude of the choke inductance on a) the lead angle when the remaining converter parameters remain constant, and b) the pulsations of the rectified current from a Larinov rectifier circuit. From the oscillogram it is evident that for $L_d \geq L$ it is possible to assume $I_d = \text{const.}$ within the limits of a step.

We shall demonstrate that the overlap between plate currents can also be neglected. For the commutation interval the equations for the currents and voltages can be written as follows in operator form

$$\frac{I_d}{p} = \bar{i}_1 + \bar{i}_{C_1} + \bar{i}_2 + \bar{i}_{C_2}$$

$$\bar{u} = \bar{i}_1 r + p x_{L_1} \bar{i}_1 - x_{L_1} i_1(0)$$

$$i_{C_1} = p x_{C_1} \bar{u} - x_{C_1} u_C(0)$$

$$\bar{u} = \bar{i}_2 r_2 + p x_{L_2} \bar{i}_2$$

$$\bar{i}_{C_2} = p x_{C_2} \bar{u}.$$

The voltage drop in the thyratron rectifiers can be taken into account by subtracting it from the supply rectifier voltage. Taking into account the fact that the parameters of both phases are equal, we find the solution for the equations cited above relative to $\bar{u}$ while assuming that $i_1(0) = I_d$, $u_C(0) = I_d r$:

$$\bar{u} = \frac{I_d r (p^2 x_C x_L + p x_C + 1)}{2p (p^2 x_C x_L + p x_C + 1)}.$$

Making the transition back to the original, we find

$$u = \frac{I_d r}{2}.$$

The results shows that for commutation the rectified current instantaneously makes the transition to the next rectifier without any overlap; i.e., the duration of the rectifier plate current does not exceed 120°.

The remarks made above permit us to treat each parallel circuit consisting of a motor winding and a capacitor as a certain nonlinear element of the over-all circuit which is subjected to rectangular current pulses with a duty ration equal to three.

In order to determine the lead angle Θ_δ we find the voltage across the rectifier

$$u_{ak} = u_1 - u_2$$

where u_1 is the voltage across the energized winding, u_2 is the voltage across the deenergized winding.

We shall study the general case while assuming conditionally that before the motor winding is energized the capacitor is subjected to the voltage $u_C(0)$ whose polarity is the reverse of the source polarity (cf. Fig. 2). We shall introduce the substitution

$$z' = \frac{\Delta x l \vartheta}{2\omega} \sin \alpha.$$

Then

$$u_s = ir + iz' + x \frac{di}{d\theta}.$$

The system of equations for determining the voltage u_1 is written as

$$\bar{u}_1 = (r + z')\,\bar{i} + px\bar{i}$$
$$\bar{i}_C = px_C\bar{u}_1 + x_C u_C(0)$$
$$\frac{I_d}{p} = \bar{i} + \bar{i}_C$$

whence

$$\bar{u}_1 = \frac{[I_d - px_C u_C(0)]\,[(r + z') + px]}{p\,[p^2 x x_C + p\,(r + z')\,x_C + 1]}.$$

Assuming $i(0) = I_d$ and $u_C(0) = I_d(r + z')$, we find

$$\bar{u}_2 = \frac{pxx_C(r + z') + x_C(r + z')^2 - x}{p^2 x x_C + p\,(r + z')\,x_C + 1} I_d$$

in analogous fashion.

After transition to the original

$$u_{ak} = I_d(r + z') + \frac{2I_d\rho}{\beta_1 - \beta_2}\left(\frac{\beta_2}{\beta_1}e^{-\beta_1\tau} - \frac{\beta_1}{\beta_2}e^{-\beta_2\tau}\right) + \frac{u_C(0)}{\beta_1 - \beta_2}(\beta_2 e^{-\beta_1\tau} - \beta_1 e^{-\beta_2\tau}) \quad \text{for } \sigma > 1$$

and

$$u_{ak} = (r + z')I_d + \frac{2\rho I_d}{\nu}e^{-\sigma\tau}\sin(\nu\tau + \varphi_1) - \frac{u_C(0)}{\nu}\sin(\nu\tau + \varphi_2)e^{-\sigma\tau} \quad \text{for } \sigma < 1.$$

In the expressions derived above: $\tau = \Theta/\xi$ is the dimensionless time,

$$\xi = \sqrt{xx_C}.\quad \sigma = \frac{r + z'}{2\rho}.\quad \rho = \sqrt{\frac{x}{x_C}}.\quad \beta_{1,2} = \sigma \pm \sqrt{\sigma^2 - 1}$$
$$\nu = \sqrt{1 - \sigma^2}.\quad \tan\varphi_1 = \frac{2\nu\sigma}{2\sigma^2 - 1}.\quad \tan\varphi_2 = \frac{\nu}{\sigma}.$$

Taking into account the fact that for $\tau = \tau_\delta$ we have $u_{ak} = 0$, we arrive at the following transcendental equations after certain transformations:

$$\left(\beta_2 + \frac{\beta_2}{\beta_1\sigma}\right)e^{-\beta_1\tau_\delta} - \left(\beta_1 + \frac{\beta_1}{\beta_2\sigma}\right)e^{-\beta_2\tau_\delta} = \beta_2 - \beta_1 \quad \text{for } \sigma > 1, \tag{16}$$

$$\sin(\nu\tau_\delta + \varphi_2) - \frac{1}{\sigma}\sin(\nu\tau_\delta + \varphi_1) = \nu e^{-\sigma\tau_\delta} \quad \text{for } \sigma < 1. \tag{17}$$

From this τ_δ is found using known methods.

We shall find the overlap between the currents in the windings. The current in the winding of the rectifier which is cut in is equal to

$$i_1 = I_d\left\{1 - \frac{1}{\nu}e^{-\sigma\tau}[\sin(\nu\tau + \varphi_2) - 2\sigma\sin\nu\tau]\right\} \quad \text{for } \sigma < 1$$
$$i_1 = I_d\left\{1 - \frac{1}{\beta_1 - \beta_2}[(\beta_1 - 2\sigma)e^{-\beta_2\tau} - (\beta_2 - 2\sigma)e^{-\beta_1\tau}]\right\} \quad \text{for } \sigma > 1.$$

For $\tau = \tau_\gamma$, $i_1 = I_d$. However, since beyond values i_1 the value i_1 slowly approaches I_d (especially for $\sigma > 1$), it is expedient to assume $\tau = \tau_\gamma$ for $i_1 = 0.9\,I_d$. Then τ_γ is found from the transcendental equations:

$$\sin(\nu\tau_\gamma + \varphi_2) + 2\sigma\sin\nu\tau_\gamma = 0{,}1\nu e^{\sigma\tau_\gamma} \quad \text{for } \sigma < 1 \tag{18}$$

$$(\beta_1 - 2\sigma)\, e^{-\beta_1 \tau_\gamma} - (\beta_2 - 2\sigma)\, e^{-\beta_2 \tau_\gamma} = 0{,}1\,(\beta_1 - \beta_2) \text{ for } \sigma > 1. \quad (19$$

The expressions for τ_δ and τ_γ contain only one parameter σ which takes into account all possible relationships between r, z', L and C.

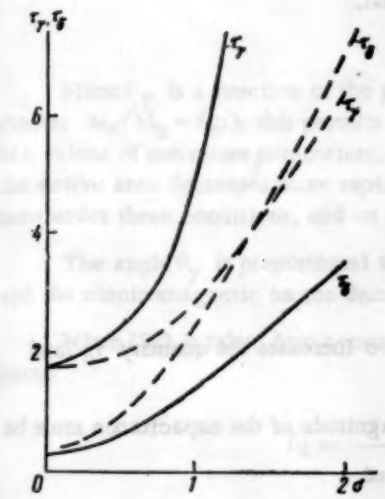

Fig. 5. The dependence of the angles of overlap and lead on the parameters of the converter in relative units. The solid lines are for $u_C(0) = 0$, and the broken lines are for $u_C(0) \neq 0$.

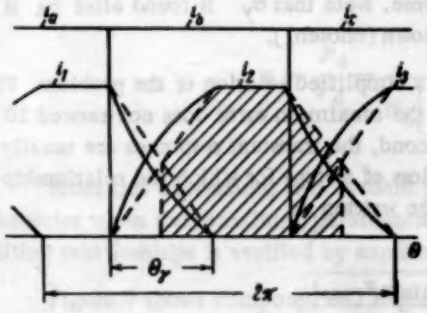

Fig. 6. Time variation of the plate and phase currents in the converter. i_a, i_b, and i_c are the plate currents of the thyratrons; i_1, i_2 and i_3 are the currents in the motor windings; θ_γ is the overlap angle for the currents in the motor windings.

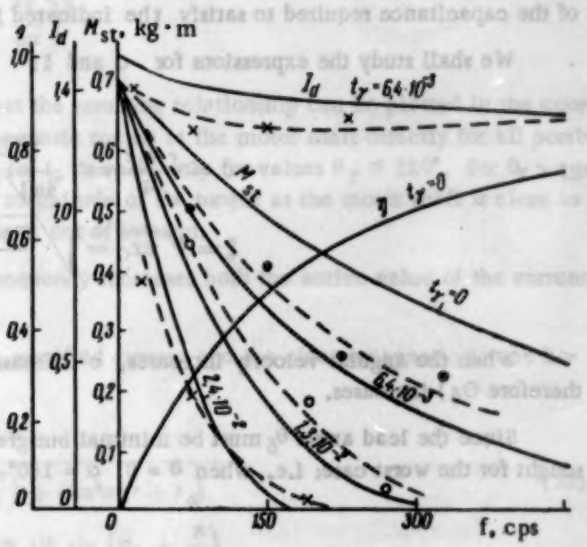

Fig. 7. The computed (the solid lines) and the experimental (the broken lines) characteristic of the drive. η is the efficiency of the converter, t_γ is the time for which the overlap between the current in the motor windings occurs, f is the frequency of the control pulses.

Figure 5 shows the functions τ_γ, $\tau_\delta = f(\sigma)$ for $u_C(0) = 0$ and $u_C(0) = I_d r$. For a specified value of σ the time τ_δ for $u_C(0) \neq 0$ is greater than the time τ_δ for $u_C(0) = 0$, and the time τ_γ for $u_C(0) \neq 0$ is less than the time τ_γ for $u_C(0) = 0$.

For stable operation of the converter the lead angle must be greater than the angle (time) for natural deionization of the rectifier as indicated by its ratings. The connection of uncontrolled diode rectifiers into the circuits of the windings for $\sigma < 1$ ($u_C(0) \neq 0$) makes it possible to assure the optimal lead angle from the point of view of stable commutation for smaller capacitances; therefore it makes it possible to operate with smaller current overlap angles in the windings and with increased torque.

It is necessary to keep in mind the fact that all of the derived expressions for voltages and currents when uncontrolled diode rectifiers are present are valid only during the initial interval of the process and permit us merely to find the angles of lead and overlap. A determination of the laws governing the variation of the current and the voltages over the entire interval requires, as we know, the solution of the problem by segments. For transition from dimensionless quantities to the angles of lead and overlap it is necessary to make use of the relationships:

$$\theta_\delta = \tau_\delta \xi \qquad \theta_\gamma = \tau_\gamma \xi.$$

Since τ_δ and τ_γ are functions of σ, it is evident that they are functions of the velocity ϑ and the angle of rotation φ. In determining the lead angle we shall base ourselves on the following.

The deionization time t_0 for the rectifier is usually specified and the lead time t_δ must be found while taking the condition $t_\delta > t_0$; this condition must be maintained for all the operating modes of the converter. The motor parameters are also specified. Since the overlap angle increases with the capacitance, it follows that the magnitude of the capacitance required to satisfy the indicated inequality must be minimal.

We shall study the expressions for σ and ξ:

$$\sigma = \frac{r + x'}{2\rho} = \frac{\sqrt{2x_C}\,[2\omega r + \Delta x l \vartheta \sin\alpha]}{4\omega\sqrt{2x_{\text{мин}} + \Delta x\,(1 - \cos\alpha)}}$$

$$\xi = \sqrt{x x_C} = \sqrt{\frac{x_C[2x_{\text{мин}} + \Delta x\,(1 - \cos\alpha)]}{2}}$$

When the angular velocity increases, σ increases. On the other hand, as σ increases the quantity τ_δ (and therefore Θ_δ) increases.

Since the lead angle θ_δ must be minimal but greater than critical, the magnitude of the capacitance must be sought for the worst case: i.e., when $\vartheta = 0$, $\alpha = 180°$ and

$$\sigma = \frac{r}{2}\sqrt{\frac{x_C}{x_{\max}}} \tag{20}$$

$$\xi = \sqrt{x_C x_{\max}}. \tag{21}$$

In order to achieve an exact determination of the overlap for the transient modes it is necessary to find $\sigma = \sigma(\vartheta, \varphi)$ and $\xi = \xi(\varphi)$. After substituting these expressions into (18) or (19), we obtain $\theta_\gamma = f(\vartheta, \varphi)$. Then, substituting this expression into the dynamics equation, we find the transient response. Note that θ_γ is found after θ_δ is determined [i.e., for the case where all of the converter parameters are known (chosen)].

However, in the majority of cases it is possible to limit ourselves to a simplified solution of the problem. First, the inequality $\Delta x/2\omega r \ll 1$ is usually valid; if we assume $\alpha = 180°$, then the maximum error does not exceed 10 to 20%, and this is an adequate approximation in practical computations. Second, the transient responses are usually determined for dynamically stable modes of motor operation (without the loss of a step) for which the relationship $\vartheta \approx \omega/l$ is valid. Under these conditions the expressions for σ and ξ can be written as

$$\sigma = \frac{r}{2}\sqrt{\frac{2x_C}{x_{\max} + x_{\min}}} \qquad \xi = \sqrt{\frac{x_C\,(x_{\min} + x_{\max})}{2}}.$$

We shall find the expressions for the currents and the electromagnetic torque while taking the overlap into account. Considering the fact that in the commutation interval

$$\frac{di_1}{d\theta} = -\frac{di_2}{d\theta}$$

it is possible to replace the curves for the decay and growth of the pulse currents with straight lines as shown in Fig. 6. The area of the pulses is not altered by this. Then, taking into account the fact that a) at the commutation instant the magnetic fluxes of two adjacent poles act in opposite directions, and b) at the instant when the commutated currents are equal to one another the resultant flux is equal to zero, it is possible to assume that the currents are also equal to zero. Thus the "active" area of each current pulse in the winding will be shaped as shown in Fig. 6 (the shaded potion). Replacing this area by a rectangle of equal size that has a duration equal to $\frac{1}{3}$ the period of the instantaneous value for the "active" current and the electromagnetic torque when the overlap is taken into account, we find

$$I = I_d\left(1-\frac{3}{8\pi}\theta_\gamma\right). \qquad M_e = \frac{3\sqrt{3}\Delta x l}{4\pi\omega} I^2 \sin\left(\alpha_1+\frac{\pi}{3}\right). \tag{22}$$

If we take the basis torque to be that corresponding to $\theta_\gamma = 0$, then

$$\frac{M_e}{M_b} = \left(1-\frac{3\theta_\gamma}{8\pi}\right)^2.$$

Since θ_γ is a function of the parameter σ, it follows that the resulting relationship can be plotted in the coordinates $M_e/M_b = f(\sigma)$; this permits us to obtain the electromagnetic torque at the motor shaft directly for all possible values of converter parameters. The resulting expression for i_γ is valid only for values $\theta_\gamma \leq 120°$. For $\theta_\gamma > 120°$ the active area decreases more rapidly as θ_γ increases. The magnitude of the torque at the motor shaft is close to zero under these conditions, and an investigation of this region is not of interest.

The angle θ_γ is proportional to frequency, and as the frequency increases both the active value of the current and the electromagnetic torque decrease.

When (22) is taken into account, the expressions for the rectified current and the electromagnetic torque become

$$I_d = \frac{49\pi^3\omega(U_d-\Delta u)}{\Delta x\theta l(8\pi-3\theta_\gamma)^2\sin\left(\alpha_1+\frac{\pi}{3}\right)+49\pi^3\omega(r+r_d)} \tag{23}$$

$$M_e = \frac{49\pi^3\omega\Delta x l[(U_d-\Delta u)(8\pi-3\theta_\gamma)]^2\sin\left(\alpha_1+\frac{\pi}{3}\right)}{[\Delta x\theta l(8\pi-3\theta_\gamma)\sin\left(\alpha_1+\frac{\pi}{3}\right)49\pi^3\omega(r+r_d)]^2}. \tag{24}$$

The limits of variation for α_1, the dependence of α_1 on the load, and the stalling torque are found by an analogous method. It is not difficult to find the converter efficiency:

$$\eta = \frac{P_e}{P_d} = \frac{8l\pi(U_d-\Delta u)(8\pi-3\theta_\gamma)^2\sin\left(\alpha_1+\frac{\pi}{3}\right)}{U_d\left[\theta l(8\pi-3\theta_\gamma)^2\sin\left(\alpha_1+\frac{\pi}{3}\right)+49\pi^3\frac{r+r_d}{\Delta L}\right]}. \tag{25}$$

From this expression, it is evident that the greater the constant $\Delta L/(r+r_d)$ the greater the efficiency of the converter when the remaining parameters stay constant. The correctness of our theoretical assumptions and the resulting relationships is verified by experiment.

Figure 7 shows computed and experimental characteristics for the drive. In performing the experiments we used a three-stator step motor with a ribbon brake. The basic parameters for the motor and for the electric circuits in the drive were the following: $\Delta L = 0.24$ h; $r = 100$ ohm; $r_d = 30$ ohm; $l = 30$; $\Delta u = 15$ v; $U_d = 215$ v.

For the chosen circuit parameters and the assumed control pulse frequency, the motor was gradually loaded for various overlap times of the winding current, and the values of the stalling torque and the currents and voltages in the circuit were fixed.

The author expresses his appreciation to A. A. Bulgakov and Ya. Z. Tsypkin for their help in performing the investigations described above.

LITERATURE CITED

1. A. E. Thomas, The Power Stepping Motor—a New Digital Actuator. Control Engineering, vol. 4, No. 1 (1957).
2. B. A. Sigov, Commutation Circuits for a Step Motor. Automation [in Russian] (Academy of Sciences Ukrainian SSR Press, No. 1, 1959).
3. I. L. Shapiro, E. M. Grossman, Yu. A. Raisov and Yu. V. Tikhvinskii, "A digital program control system for a heavy lathe," Elektrichestvo, 2 (1960).

4. B. A. Sigov, Investigating the Dynamics of a Step Motor, Automation. [in Russian] (Academy of Sciences Ukrainian SSR Press, No. 4, 1959).
5. M. L. Bykhovskii, and A. E. Kobrinskii, "Investigating the dynamics of step systems for program control of machine tools," Izvestia Vysshikh Uchebnykh Zavedenii, Mashinostroenie, 2 (1958).

THE CALCULATION OF THERMAL CONDITIONS IN TRANSISTORS

A. N. Afanas'ev

(Moscow)

Translated from Avtomatika i Telemekhanika, Vol. 22, No. 5,
pp. 641-647, May, 1961
Original article submitted December 9, 1960

A method of calculating the static thermal conditions of transistors is presented. The characteristics of a cooling plate are developed. Practical recommendations are made for cooling power transistors.

For the investigation of problems connected with the cooling of power transistors, it is convenient to employ the electrical analog method. Essentially this method depends on the principle that the equations depicting thermal and electrical processes are identical, and a thermotechnical calculation reduces to a calculation for an electrical circuit.

During the operation of a transistor, part of its power is wasted, being transformed into heat, which warms the transistor. If the power is constant in time, and is present for a long period, the temperature of the collector junction reaches a static value. In Fig. 1, a is shown the equivalent thermal circuit which reflects the process of power transmission to the surrounding medium. The thermal resistance $r_{T.int}$ representing in substance the resistance of the transistor, determines the temperature difference $\theta_J - \Theta_{cas}$ between the collector junction and the casing. It is a transistor parameter, and is called the internal resistance of the transistor.

The external resistance of the transistor (casing resistance) $R_{T.cas}$ specifies the ability of the transistor to transmit to the surrounding medium the power wasted within it.

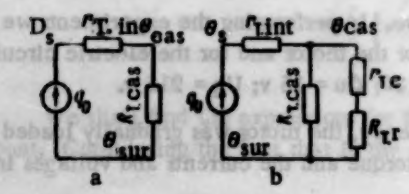

Fig. 1

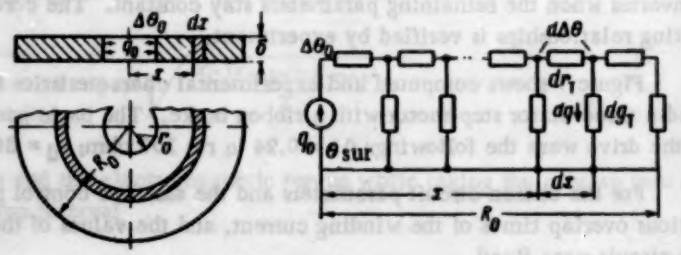

Fig. 2

The total thermal resistance of the transistor is

$$R_{T\Sigma} = r_{T.int} + R_{T.cas}. \quad (1)$$

The maximum power which the transistor can dissipate is equal to

$$q_{max} = \frac{\theta_{J\cdot max} - \theta_{sur}}{R_{T\Sigma}}. \quad (2)$$

$\theta_{j.max}$ is the maximum permissible temperature of the collector or junction for a specified collector voltage, and θ_{sur} is the temperature of the surrounding medium.

The external thermal resistance of transistors is considerably higher than the internal thermal resistance. This prevents them from being operated at their full power.

Transistor load capability can be increased with the help of a radiator. In Fig. 1, b, there is shown an equivalent circuit for a transistor cooled by means of a radiator. In this circuit, $R_{T.r}$ is the thermal resistance of the radiator, and $r_{T.c}$ is the thermal resistance of the contact which results from the imperfect matching of the transistor and radiator surfaces. Usually it amounts to 0.3-0.5°C/w. The value of $r_{T.c}$ can be lowered to 0.15-0.2 °C/w if a pad of a soft metal – for example, load 0.1-0.15 mm in thickness – is placed between the transistor and the radiator.

The external thermal resistance of a transistor cooled by a radiator is equal to

$$R_{T.ext} = \frac{R_{T.cas}(R_{T.r} + r_{T.c})}{R_{T.cas} + R_{T.r} + r_{T.c}}. \quad (3)$$

As the thermal resistance of the radiator is reduced, the power which the transistor can dissipate is increased. For $R_{T.r} + r_{T.c} \approx 0$ it reaches the limiting value

$$q_{Lim} = \frac{\theta_{J.max} - \theta_{sur}}{r_{T.int}}. \quad (4)$$

However, practically it is found unsuitable to make radiators with a thermal resistance less than the internal thermal resistance of the transistor.

The maximum temperature of the junction is directly dependent on the collector voltage; this question has been considered in detail in [1,2].

The transfer of heat from a hot body to the surrounding medium takes place by convection and thermal radiation [3].

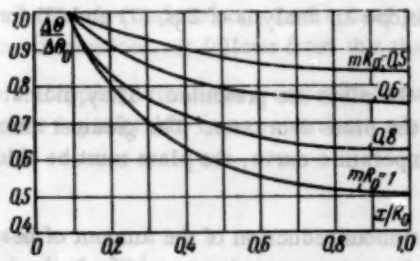

Fig. 3

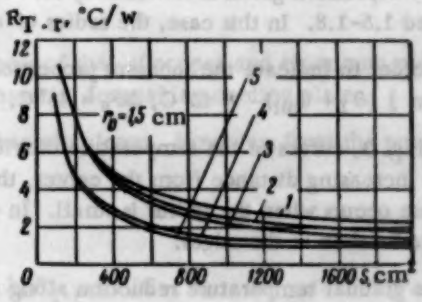

Fig. 4. (1) δ = 1 mm; (2) δ = 2 mm; (3) δ = 4 mm; (4) δ = 2 mm; (5) δ = 4 mm.

The thermal transfer coefficient of convection for a uniformly heated vertical surface with natural cooling is determined by the approximate formula

$$a_c = 1{,}4\sqrt[4]{\frac{\Delta\theta_0}{l}}, \quad (5)$$

where $\Delta\theta_0$ is the temperature difference between the hot surface and the surrounding medium in °C, and l is the height of the plate in m.

Experimentally, it has been found that thermal transfer by convection from a horizontal surface turned upwards is 30% greater than from a vertical surface. A horizontal surface turned downwards dissipates 30-40% less heat than a vertical surface.

The thermal transfer coefficient of radiation for a uniformly heated surface is equal to

$$a_r = 4{,}6\varepsilon\left(1 + \frac{\theta_{av}}{273}\right)^3 \tag{6}$$

where ϵ is the blackness coefficient of the surface, $\theta_{av} = \frac{1}{2}(\theta_1 + \theta_{sur})$, and θ_1 is the surface temperature in °C.

The simplest radiator for a transistor is a metal plate. Its thermal resistance depends on many factors, which are principally related to the geometrical dimensions, the thermal conductivity coefficient of the material, and the condition of the surface.

In Fig. 2, a circular plate is shown to which power is transmitted over a circular region of radius r_0. There is also shown in this figure an equivalent thermal circuit consisting of a long line with continuously changing parameters.

The temperature distribution along the radius of such a plate which is cooled naturally is given by the expression (see Appendix):

$$\theta = \frac{K_0(mx)\,I_1(mR_0) + K_1(mR_0)\,I_0(mx)}{K_0(mr_0)\,I_1(mR_0) + I_0(mr_0)\,K_1(mR_0)}\,\Delta\theta_0 + \theta_{sur} \tag{7}$$

where $K_0(mx)$, $I_0(mR_0)$, etc. are Bessel functions with the imaginary argument $m = \sqrt{2a/\delta\lambda}$; λ is the thermal conductivity coefficient of the material of the plate in w/m° C; $a = a_k + a_c$; δ is the plate thickness in m; r and R_0 are in m.

The thermal resistance of the plate is equal to

$$R_{T.r} = \frac{1}{2\pi r_0 \delta\lambda m\psi} \tag{8}$$

where

$$\psi = \frac{I_1(mR_0)\,K_1(mr_0) - I_1(mr_0)\,K_1(mR_0)}{K_1(mR_0)\,I_0(mr_0) + I_1(mR_0)\,K_0(mr_0)}.$$

The expression given is satisfactory for the calculation of rectangular plates where the ratio of the sides does not exceed 1.5-1.8. In this case, the radius of a circular plate of equivalent area is used for the external radius.

In order to indicate the inherent properties for a plate, we will develope an analysis of Eqs. (7) and (8) for the case when $\frac{1}{2}(\theta_1 + \theta_{sur}) = 45°C$, $\Delta\theta_0 = 45°C$.

In Fig. 3, curves of the temperature distribution along the radius of the plate are presented. They indicate that with increasing distance from the center, the surface temperature of the plate decreases. The greatest amount of decrease occurs when the radius is small. In order to straighten the temperature curve, the plate must be thicker in the middle than at the edges.

The gradual temperature reduction along the radius results in a continuous reduction of the amount of heat being transferred to the surrounding medium per unit area as the distance from the center is increased. It can be shown that there is an area above which a further increase does not produce an appreciable decrease in the thermal resistance. From the curves shown in Fig. 4 for $R_{T.r} = f(S)_{\delta = const}$ with bright (curves 1, 2 and 3) and with black anodized (curves 4 and 5) aluminum plates it is seen that there is little value in making a cooling plate with a surface area (for both sides) of more than 1000-1300 cm^2.

The surface condition of a plate has a marked effect on its thermal resistance. Thus, the thermal resistance of a black anodized aluminum plate is 25-40% less than for a bright one having the same dimensions.

In practical work there are two problems to be solved:

1) To obtain a given thermal resistance with the minimum plate area;
2) To obtain a given thermal resistance with the minimum plate volume.

The first problem is representative of the case when the plate must have minimum over-all dimensions. For a fixed area, the thermal resistance of a plate decreases with an increase in thickness, approaching the limiting value

$$R_{T.\,Lim} = \frac{1}{aS}. \tag{9}$$

It can be shown that there is a thickness beyond which a further increase does not give an appreciable reduction of the thermal resistance of a plate (Fig. 5). This occurs because for $\delta \geq 1.5a\,S/\lambda$, the temperature distribution along the surface of the plate becomes practically uniform. A uniform temperature distribution occurs for aluminum plates at thicknesses from 1 to 4 mm and a two-sided area of 300 cm^2. This is indicated by the convergence of the characteristic curves in the first part of the graph shown in Fig. 4.

The second problem arises when material costs are important. For a given quantity of material it can be shown (Fig. 6) that the thermal resistance of a plate is a minimum for $mR_0 \approx 1$. The two-sided surface of such a plate is equal to

$$S = \frac{\pi\delta\lambda}{a}. \qquad (10)$$

Let us compare two plates, one of which achieves the minimum over-all dimensions (area), and the other—the minimum material cost. The first plate uses the area efficiently, but is not economical with respect to material cost. The minimum quantity of material is used in making the second plate, but it utilizes the area inefficiently. Economy of material is achieved at the expense of area increase.

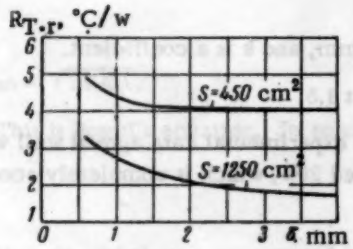

Fig. 5

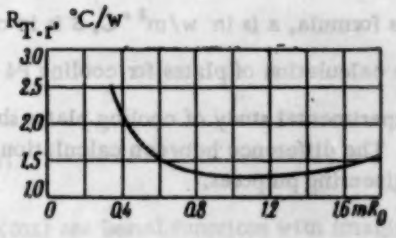

Fig. 6

The relative rating of plates made of different metals is of some interest. This can be worked out, based on the curves in Fig. 7.

The thermal resistance of a steel plate is considerably in excess of that of copper and aluminum plates of the same dimensions. It follows from this that steel is not a suitable material for making cooling plates.

Copper plates have a somewhat smaller thermal resistance than aluminum. However, from the point of view of cost, it is preferable to use aluminum plates.

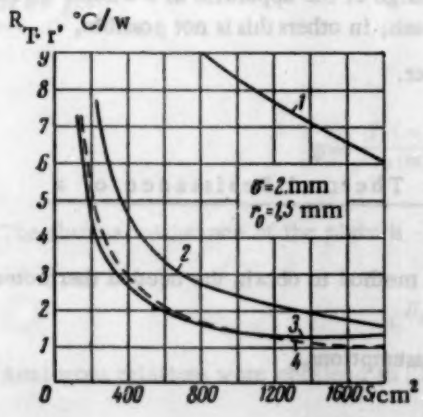

Fig. 7. 1) Steel; 2) bright aluminum; 3) anodized aluminum; 4) copper.

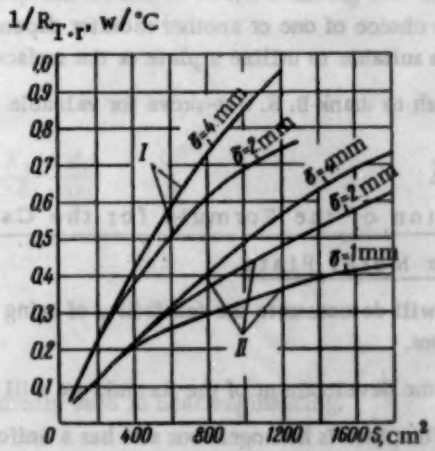

Fig. 8. I) Anodized aluminum; II) bright aluminum

Heat transfer from the surface of a plate depends both on the difference (convection) and on the absolute values (thermal radiation) of the temperatures of the surface of the plate and of the surrounding medium. Consequently, the thermal resistance of a plate is functionally connected to temperature. For an increase in the temperature difference between the surface of the plate and the surrounding medium, the thermal resistance of the plate is lowered. On the average, it can be reckoned that for a change in the temperature difference of 1°C in the interval of $\Delta\theta_0$ from 10 to 45°C, the thermal resistance changes by 0.4-0.5% with anodized plates, and by 0.5-0.6% with bright ones.

Equation (8) was given above for determining the thermal resistance of a plate. Because of the presence of Bessel functions in this expression, the calculation of cooling plates becomes cumbersome. Simplification of the calculation can be accomplished in two ways. The first method consists of constructing from Eq. (8) a curve for $R_{T.r} = f(S)_{\delta=\text{const}}$, or $1/R_{T.r} = \varphi(S)_{\delta=\text{const}}$, and finding from it the plate area needed to obtain a given thermal resistance. The standard curves for aluminum plates cooling P4 transistors (r_0 = 1.5 cm) are presented in Figs. 5 and 8.

The second method of simplifying the plate calculation consists of approximating Eq. (8) with a simpler expression. Good results for $mR_0 \leq 1.1$ are given by an approximation of the form

$$R_{T.r} = \frac{10^4}{aS} + k\sqrt{\frac{a}{\delta\lambda}}. \qquad (11)$$

In this formula, a is in $w/m^2 \cdot °C$, S is in cm^2, λ is in $w/m \cdot °C$, δ is in mm, and k is a coefficient.

In the calculation of plates for cooling P4 transistors, k is made equal ot 3.5.

An experimental study of cooling plates showed that the calculated and experimental data agreed well with each other. The difference between calculation and experiment did not exceed 20%, which is completely acceptable for engineering purposes.

SUMMARY

The load capacity of a transistor under static conditions is characterized by the maximum permissible temperature of the collector junction, the internal and external thermal resistances, and the relation of the maximum permissible voltage to junction temperature. A considerable excess of external over internal thermal resistance prevents the use of a transistor at full power

An increase in load capability is obtained for power transistors by means of auxiliary cooling with radiators, the simplest of which is a metal plate. From the point of view of cost and cooling ability, an anodized aluminum plate undoubtedly should receive preference.

The thermal resistance of aluminum plates is practically unchanged for an increase in total surface area above 1000-1300 cm^2 and a thickness above 3-4 mm.

The choice of one or another radiator depends on the structural design of the apparatus as a whole. In some cases, it is suitable to utilize a plate or the surface of the apparatus chassis; in others this is not possible.

I wish to thank B. S. Sot-skova for valuable comments on the paper.

APPENDIX

Derivation of the Formula for the Calculation of the Thermal Resistance of a Circular Metal Plate

We will demonstrate the feasibility of using the electrical analog method to obtain the needed thermotechnical relations.

For the development of the formula we will make the following assumptions.

1) The plate is homogeneous and has a uniform thickness.

2) The thickness of the plate is small compared to the outer radius; this permits us to neglect the power radiated from its end.

3) The thermal transfer coefficient is equal over the entire surface.

Separated by a distance x from the center of the plate (Fig. 2), the element dx transfers power both along the line and to the surrounding medium. The change of the temperature difference between the surface of the plate and the surrounding medium, and the change of power along the line are equal to

$$d\Delta\theta = -q\,dr_T \tag{I}$$

$$dq = -\Delta\theta\,dg_T. \tag{II}$$

Expressions for the thermal resistance of element dr_T along the line, and its thermal conductivity to the surrounding medium dg_T can be correspondingly presented in the form

$$dr_T = \frac{dx}{2\pi x\,\delta\lambda} \tag{III}$$

$$dg_T = 4\pi x a dx\,. \tag{IV}$$

From the joint solution of Eqs. (I)-(IV) we find

$$\frac{d^2\Delta\theta}{dx^2} + \frac{1}{x}\frac{d\Delta\theta}{dx} - \Delta\theta m^2 = 0 \tag{V}$$

where $m = \sqrt{2a/\delta\lambda}$.

This is Bessel's equation. Its solution will be [4]:

$$\Delta\theta = C_1 I_0(mx) + C_2 K_0(mx). \tag{VI}$$

Here C_1 and C_2 are constants of integration and $I_0(mx)$ and $K_0(mx)$ are Bessel functions with imaginary arguments.

We find the constants C_1 and C_2 from the initial conditions:

$$\Delta\theta = \Delta\theta_0 \quad \text{for} \quad x = r_0, \qquad \frac{d\Delta\theta}{dx} = 0 \quad \text{for} \quad x = R_0.$$

After transformations we obtain

$$\Delta\theta = \frac{K_0(mx)\,I_1(mR_0) + K_1(mR_0)\,I_0(mx)}{K_0(mr_0)\,I_1(mR_0) + I_0(mr_0)\,K_1(mR_0)}\,\Delta\theta_0. \tag{VII}$$

Substituting in Eq. (I) the value of $d\Delta\theta$ found from the last expression, and in addition taking into account Eq. (III) we get

$$q_0 = 2\pi r_0 \delta\lambda m \psi \Delta\theta_0,$$

where

$$\psi = \frac{I_1(mR_0)\,K_1(mr_0) - I_1(mr_0)\,K_1(mR_0)}{I_0(mr_0)\,K_1(mR_0) + I_1(mR_0)\,K_0(mr_0)}. \tag{VIII}$$

The thermal resistance of the plate is

$$R_{T_1T} = \frac{\Delta\theta_0}{q_0} = \frac{1}{2\pi r_0 \delta\lambda m\psi}. \tag{IX}$$

Analogous relations were obtained in [3,5] by a method commonly used in heat engineering.

LITERATURE CITED

1. B. S. Sot-skova, "Temperature stability and permissible values of power and voltage on the collector of a transistor," Avtomatikia i Telemekhanika 20, 11 (1959).*
2. A. A. Abdulaev, The behavior of germanium junction transistors at large power dissipations, Collecter papers, Semiconductor Apparatus and Its Use. Sov. radio press, No. 3, 1958, No. 4, 1960.
3. M. A. Mikheev, Principles of Heat Transfer [in Russian] (State Energy Press, 1956).
4. I. N. Bronshtein and K. A. Semendyaev, Handbook of Mathematics [in Russian] (State Technical Press, 1957).
5. Luft Diebold, Thermal impedance of cooling fins, Comm. and Electronics, No. 39, Nov., 1958.

A MAGNETIC - THERMISTOR TIME RELAY

O. P. D'yakov, N. M. Tishchenko and N. P. Udalov

(Moscow)

Translated from Avtomatika i Telemekhanika, Vol. 22, No. 5,
pp. 648-653, May, 1961
Original article submitted June 21, 1960

The paper proposes a time relay network that includes a pulse generator and a pulse counter. The pulse generator consists of a contactless magnetic relay (CMR) and a thermister which is used as an inertial element. A number of variants of the pulse generator circuit are given for the case where a CMR is used with directly and indirectly heated thermistors.

Time relays based on magnetic amplifiers or thermistors are usually designed on the principle of using the transient response time in one or another circuit of the unit for application of the input signal. The basic shortcoming of such units is the limitation imposed on the time interval by the inertial characteristics of the corresponding circuit.

The generator relay whose network is shown in Fig. 1a is free from this shortcoming. This network includes a pulse generator consisting of a contactless magnetic relay (CMR) and a heated thermistor (HT), as well as a pulse counter (adder). The generator produces pulses with a specified repetition frequency. The time interval is produced by adjusting the counter for a corresponding number of pulses. The error in the time interval after which the relay operates is determined basically by the generator instability which can be reduced to allowable limits.

The introduction of a CMR instead of a conventional electromagnetic relay [1] has made it possible to increase the service life and the operational reliability of the unit; this applies especially for conditions where vibrations and appreciable constant accelerations are present.

1. The Circuit Diagram

The circuit diagram of the generator time relay is shown in Fig. 1, b. The working body of a heated thermistor HT-1 is connected into the control winding of the pulse generator, and the heater is connected into the feedback winding of the CMR.

When the switch is open $B_1(I_C = 0)$ the maximum current (Fig. 1,c) flows through the heater which is the load of the CMR, and the working body of the HT is heated to the temperature $\theta_0 + \theta_{OV}$, where θ_0 is the temperature of the ambient medium and θ_{OV} is the overheating temperature of the HT corresponding to the maximum current through the heater.

When the switch is closed a current I_1', appears in the control winding; the value of this current is determined from the expression

*See English translation.

$$I_1 = \frac{U}{R(\theta_0+\theta_{ov})+r_c+r_1}, \quad (1)$$

where U is the voltage which supplies the control circuit, $R(\theta_0+\theta_{ov})$ is the HT resistance at the temperature $\theta_0+\theta_{ov}$, r_c is the resistance of the control winding, r_1 is a multiplier resistance.

The heating of the working body of the HT begins due to the current flowing through it. The magnitude of the HT resistance drops, the current I_c increases, and for $I_c = I_{rel}$ (point 2 in Fig. 2,a) the current in the heater drops abruptly; as a result the HT begins to cool, its resistance increases, and the current I_c decreases to the value I_{op} (point 3 in Fig. 2, a). For $I_c = I_{rel}$ the current through the heater again increases stepwise to a maximum and the HT is heated.

The described variations of the current in the circuit of the working body of the HT are periodic in nature.

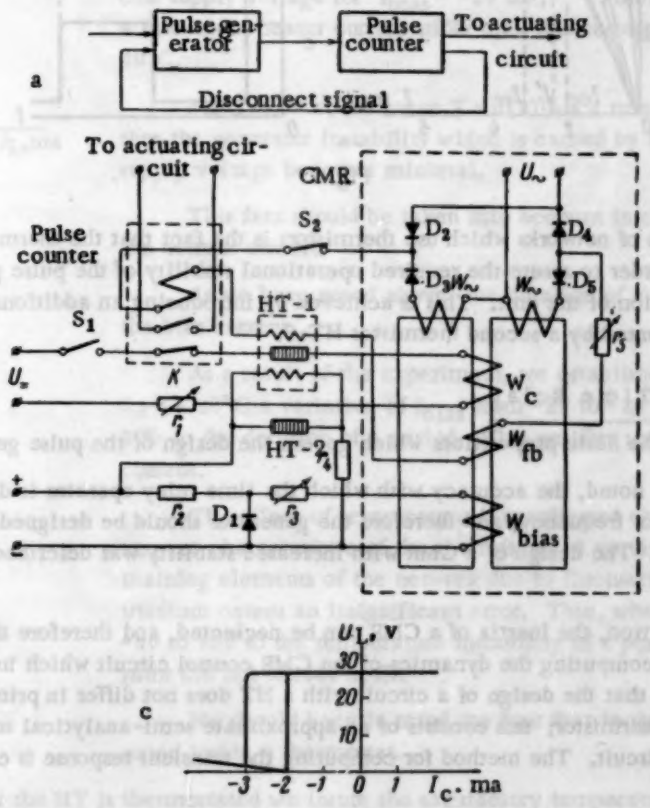

Fig. 1

The graphs showing the variation of the control and load current with time, $I_c = f(t)$ and $I_l = \varphi(t)$, are shown in Figs. 2, b and 2, c.

The repetition frequency for the pulses can be controlled by varying the resistance r_1 in the control circuit of the CMR or by varying the bias current in the CMR by means of the adjusting resistor r_3. An electromechanical pulse counter (a step motor) is used as the added; this device is characterized by relatively small dimensions and a simple construction

It is also possible to use other adders such as counters based on triggers, decatrons, ferrite elements, etc.

The winding of the pulse counter is connected as the load of the CMR. The adjustment of the counter to a specified number of pulses is achieved by switching a special switch S_2 when the control winding is disconnected ($I_c = 0$). Under these conditions a number of pulses equal to the number of times the switching-on operation is performed is applied to the counter.

When the required time interval elapses, the group of contacts K is closed (Fig. 1, b); these contacts send a signal to the control circuit and disconnect the input circuit of the pulse generator.

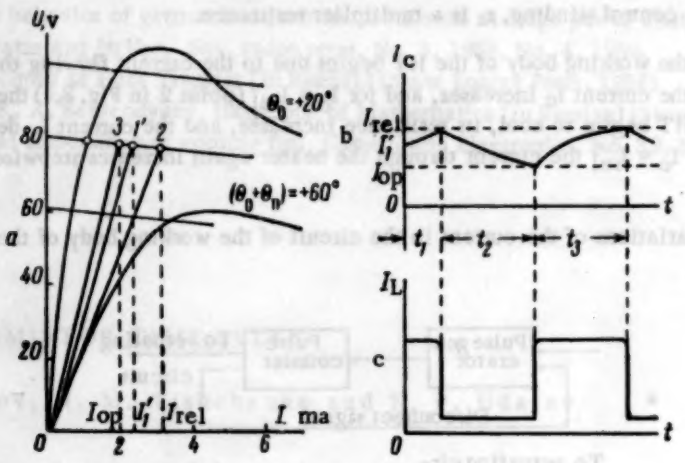

Fig. 2

An essential feature of networks which use thermistors is the fact that the thermistor parameters depend on temperature. Therefore in order to assure the required operational stability of the pulse generator it is necessary to insure temperature stabilization of the unit. This is achieved by introducing an additional heating winding for the thermistor HT-1 which is shunted by a second thermistor HT-2.

2. The Design of the Time Relay

We shall dwell on the basic propositions which govern the design of the pulse generator.

As we have already noted, the accuracy with which the time relay operates is determined chiefly by the stability of the pulse generator frequency, and therefore the generator should be designed on the basis of the requirements for increased stability. The design of a CMR with increased stability was described in [2] and therefore is not described here.

In a first approximation, the inertia of a CMR can be neglected, and therefore the computation of the duration of the pulses reduces to computing the dynamics of the CMR control circuit which includes the thermistor. We should keep in mind the fact that the design of a circuit with a HT does not differ in principle from the design of a circuitwith a conventional thermistor; this consists of an approximate semi-analytical solution of the equation for thermal equilibrium in the circuit. The method for computing the transient response is cited in [3] and therefore is omitted here.

In order to compute the dynamic characteristics of the generator it is necessary to make use of the following original data: the volt-ampere characteristics of the thermistor for θ_0 and $\theta_0+\theta_{ov}$, the heating characteristic of the thermistor, and the time constant of the thermistor.

The method for designing the thermal stabilization circuit is cited in [5].

3. The Results of an Experimental Investigation

For the purposes of performing an experimental investigation, we prepared a laboratory mock-up of a time relay designed according to the circuit shown in Fig. 1, b. We used mixed feedback in the CMR, and this permitted us to reduce the dimensions and weight of the unit.

The CMR was constructed using toroidal ribbon magnetic circuits made of "79NM" permalloy 0.08 mm thick with an outside diameter of 42 mm, and inside diameter of 30 mm, and a height of 3 mm.

The specifications for the windings were: $w_{\sim} = 3500$, $w_c = 6000$, $w_{bias} = 570$, $w_{fb} = 380$.

The experimentally determined characteristic of the CMR for a bias current of $I_{bias} = -20$ ma is shown in Fig. 1, c.

We used an HT of the type "MMT-4" which had a resistance of 100 kohm at a temperature of +20°C. Its temperature characteristic can be described by the expression $R = 3.3e^{\frac{3010}{T}}$ ohm.

The heater consisted of a coil made of nichrome wire 0.07 mm in diameter which was wound on the body of the HT; the wire was first covered with a terylene film. The resistance of the heater was 1000 ohm. The time constant of the heated thermistor was 66 seconds.

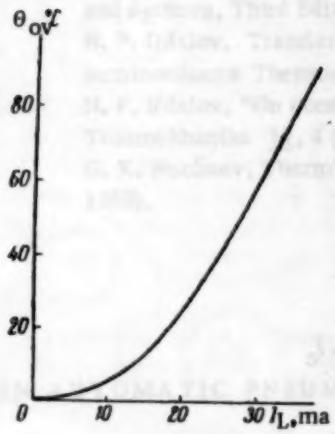

Fig. 3

The heating characteristic [4] is shown in Fig. 3. The ac circuit of the CMR was supplied from a source with a frequency of 1000 cps and a voltage of 40 v; the bias circuit and the auxiliary heater were supplied from a 27 v dc source. The rectifier bridge consisted of four diodes of the "D9E" type.

Figure 4 shows the dependence of t_2, t_3 and $T = t_2 + t_3$ on the control circuit supply voltage for $I_{bias} = -20$ ma, ambient temperature of +20°C, and a maximum heater current of 25 ma; this corresponds to an overheating of $\theta_{ov} = 40°C$.

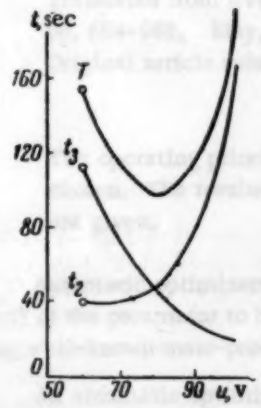

Fig. 4

For u ≈ 80 v, the curve T = f(u) has a minimum for which $t_2 = t_3$, and thus the generator instability which is caused by a variation in the control circuit supply voltage becomes minimal.

This fact should be taken into account in choosing the supply voltage for the control circuit.

As we have noted above, the duration of a period of oscillation depends on the bias current.

As a result of the experiment, we established the fact that for u = 80 v and $\theta_0 = +20°C$ a variation of I_{bias} from -20 to -25 ma led to a variation of up to 30% in the duration of a period. This verifies the necessity of stabilizing the bias current.

The effect of temperature is manifested chiefly in a variation of the volt-ampere characteristic of the thermistor. A variation in the parameters of the remaining elements of the network due to fluctuations in the temperature of the medium causes an insignificant error. Thus, when the temperature varies from -40 to +50°C the temperature instability of a period of oscillation for the generator did not exceed 1.4%.

We should keep in mind the fact that in these tests the thermistor was located inside a thermostat.

Thus, when just the HT is thermostated we insure the satisfactory temperature stability of the generator. As we have already noted above, this is achieved by means of an auxiliary heating winding which is shunted by another thermistor.

When tests were made under normal temperature conditions the generator showed good stability. Thus, for u = 80 v, $I_{bias} = -26$ ma and $\theta_0 = 20°C$ the maximum deviation from $T_{op} = 90$ sec did not exceed 2 seconds (i.e., it was approximately 2%).

4. Variants of the Pulse Generator Network

The described pulse generator network is not the only possible one. Figure 5 shows other variants of a contactless pulse generator network.

In the networks shown in Figs. 5, a and 5, b an indirectly heated thermistor is used; in the networks shown in Figs. 5, c, 5, d and 5, e a directly heated thermistor is used.

The network in Fig. 5, b differs from the network in Fig. 5, a because the thermistor shunts the control winding of the CMR and a multiplier resistor R_m is connected in the control circuit.

Whereas in the networks shown in 5, a and 5, b a stepwise variation of the heating current occurs for operation or release of the relay, in Figs. 5, c, 5, d and 5, e it is the resistance in the control circuit winding which varies stepwise under the same conditions.

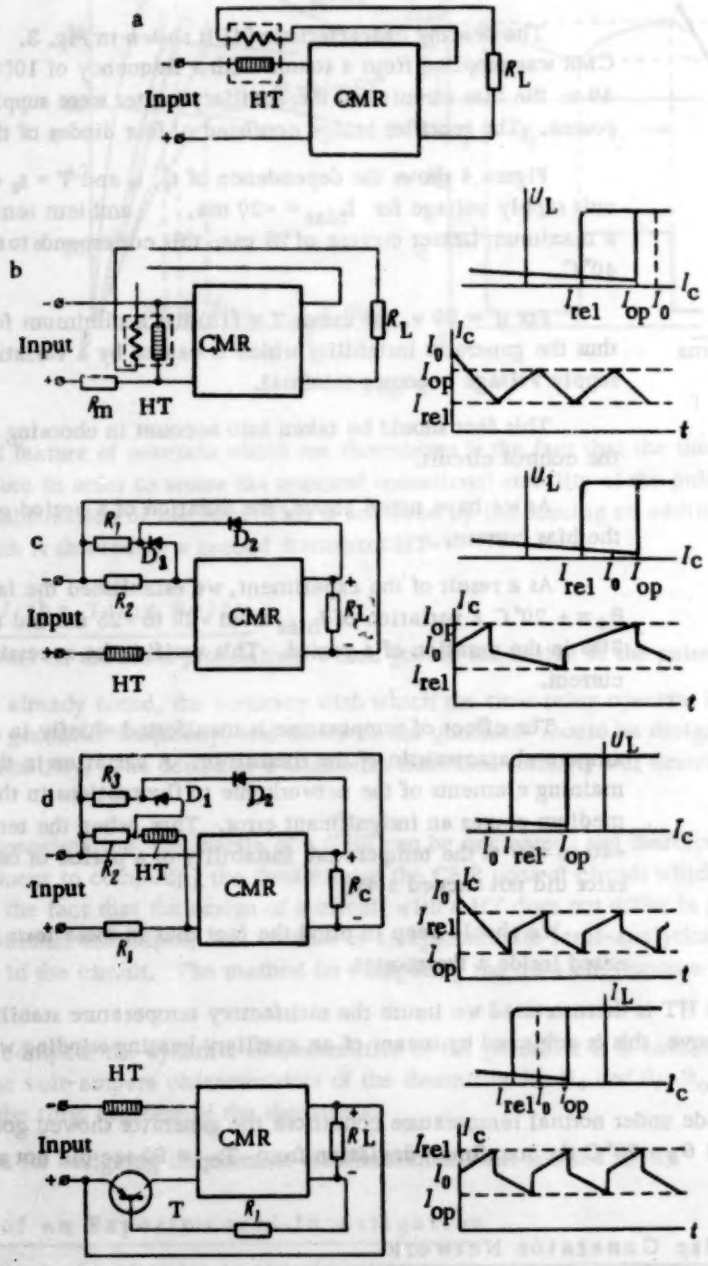

Fig. 5

However, whereas in Figs. 5, c and 5, d semiconductor diodes are used to vary the input resistances, the network in Fig. 5, c uses a transistor as a variable resistance.

The advantage of the networks shown in 5, a and 5, b resides in the fact that there is no galvanic coupling between the input and output of the CMR.

LITERATURE CITED

1. N. P. Udalov and E. V. Zaitsev, "A generator time relay based on semiconductor thermistors," Izvestiya Vysshikh Uchebnykh Zavedenii, Energetika, 8 (1959).
2. N. M. Tishchenko, Contactless Magnetic Relays, from the book: Text for the Design of Automation Elements and Systems, Third Edition [in Russian] (Defense Press, 1959).
3. N. P. Udalov, Transient Responses in the Simplest Circuit with Semiconductor Thermistors, from the book: Semiconductor Thermistors [in Russian] (State Power Engineering Press, 1959).
4. N. P. Udalov, "On computing circuits with indirectly heated semi-conductor thermistors," Avtomatika i Telemekhanika 17, 4 (1956).
5. G. K. Nechaev, Thermistors in Temperature Control [in Russian] (State Technical Press, Ukrainian SSR, 1959).

AN AUTOMATIC PNEUMATIC OPTIMIZER

N. V. Grishko

(Moscow)

Translated from Avtomatika i Telemekhanika, Vol. 22, No. 5,
pp. 654-663, May, 1961
Original article submitted July 30, 1960

The operating principle of an automatic optimizer is described and its optimum parameters are chosen. The results obtained in testing it with an electronic mock-up of the controlled device are given.

Automatic optimizers consists of devices which are specially constructed for tracking the maximum (or minimum) of the parameter to be optimized. However, a simple and reliable automatic optimizer can be constructed by using well-known mass-produced components.

An automatic optimizer, which has been developed at the hydropneumatic automation laboratory of the Institute of Automation and Remote Control, Academy of Sciences, USSR, is described below. It is to be constructed by using individual components of the pneumatic standardized unit system (SUS), which is produced by the Tizpribor plant, and of the electropneumatic command device KEP-12U, which is produced by the Kalugapribor plant. The possibility of constructing such an automatic optimizer by using mass-produced devices can greatly speed up the work on introducing extremal control in the practice of industrial automation.

The present article describes some of the results obtained in the experimental investigation of an automatic optimizer, which operated in combination with an electronic mock-up of the system to be controlled.

I. Operating Principle of the Automatic Optimizer

The block diagram of the automatic optimizer (Fig. 1) contains four basic units.

1. The integrator* 1 with two inputs. In the figure, the inputs are denoted by y_- and y_+ in dependence on the sign of the integral that is obtained when the signal is supplied only to one of the inputs.

2. The summation device 2, which adds the integrator output x_{11} and the trial oscillations x_2.

3. The floating reading system 3, which consists of an inertial element consisting of the resistor r, the capacitor c, and the power amplifier A. The output y of the system to be controlled represents the input of the floating

*Instead of the integrator, a more complex linear device with an optimum weighting function can be provided; this optimal device can also be nonlinear (see remark at the end of this article).

reading system, while its output is the signal y_{fl}, which is obtained by smoothing-out the signal y(t); if the value of the output y of the system to be controlled is constant, $y_{fl} = y$.

4. The control unit 4. Figure 1 shows the contacts $k_1, \ldots, k_5$ of the control unit as well as the device M which controls them. The generator of square trial oscillations x_2 with the period T_2 has been organized by means of contact k_5 and a certain constant signal x_0. The magnitude of the constant signal x_0 is equal to the double value of the square trial oscillation amplitude, i.e., $x_0 = 2x_{2m}$, where $x_{2m} + x_{2max}$.

The switching of contacts $k_1, \ldots, k_4$ alters the scheme of supplying the signals y and y_{fl} to the integrator outputs y_- and y_+. The $k_1, \ldots, k_4$ contacts are switched simultaneously. These switchings have the same period T_2, and consequently they are performed in step with the oscillations x_2. During a single half-period, the output y of the system to be controlled is supplied, for instance, to the integrator input y_+ (Fig. 1). At the same time, the output y_{fl} of the floating reading system is fed to the input y_-. During the next half-period, the reverse process takes place, etc. In other words, this means that the difference $y-y_{fl}$ during one half-period is integrated with the plus sign, while it is integrated with the minus sign, during the next half-period, etc.

5. The limiter 5 which limits the integrator output value. For a simpler explanation of the operating principle of the optimizer we shall assume that the limiter 5 and the floating reading system 3 are absent, i.e., $y_{fl} \equiv 0$; we shall also neglect a number of other secondary factors.

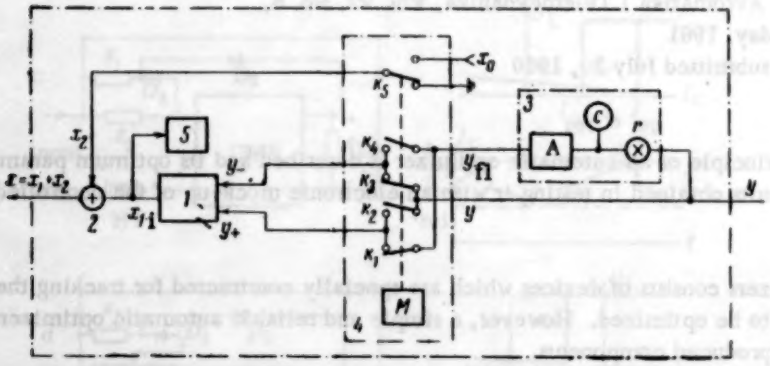

Fig. 1. Block diagram of the optimizer.

Consider the operation of an automatic optimizer in conjunction with an inertialess system whose positional response is shown in Fig. 2. For the sake of determinancy, let us assume that the system, which consists of the optimizer and the system to be controlled, is positioned to the left of the extremum (points 1 or 2).

The operation of contacts $k_1, \ldots, k_4$ consists in alternately supplying the output y of the system to be controlled to the two integrator inputs. Thus, the output y of the system to be controlled is integrated with the plus sign over one-half of the period T_2; during the next half-period, it is integrated with the minus sign, etc. At the same time, square oscillations x_2, which transfer the system from position 1 to position 2 and vice versa are supplied to the input of the system to be controlled (Fig. 2). If the system is to the left of the extremum, the output y of the system to be controlled is larger in position 1 than in position 2. Therefore, the integrals over adjacent half-periods are correspondingly not equal to each other with respect to absolute magnitude. The sum of these integrals, which have opposite signs, yields over one period a positive increment at the optimizer output, which brings the system closer to the extremum.

Similarly, the system approaches the extremum if it was initially positioned to the right instead of to the left of the extremum.

For tracking the maximum instead of the minimum, the phase relationship between the oscillations of contacts k_4 and $k_1, \ldots, k_3$ should be reversed.

Let us clarify the purpose of the floating reading system. In the absence of the floating reading system, the integrator output x_{1l} performs near-sawtooth oscillations during the scanning and tracking process, which is connected

with the fact that the quantity y is alternately integrated with the plus and minus signs. These additional (besides x_2) sawtooth oscillations lower the quality of the optimizer. The greater the output value of the system to be controlled (and also the longer the period T and the smaller the integrator's time constant), the greater the oscillation amplitude and, consequently, the lower the performance quality. In order to eliminate sawtooth oscillations, it is necessary to eliminate the large constant component of the output y of the system to be controlled. For this, it is necessary to integrate not the entire quantity y, but only a portion of it, which is measured from a certain variable level y_{fl}. Thus, the floating reading system filters out the low-frequency oscillation components of the quantity y; in this, the x_2 oscillations are transmitted after they are slightly smoothed out (see sections III and IV).

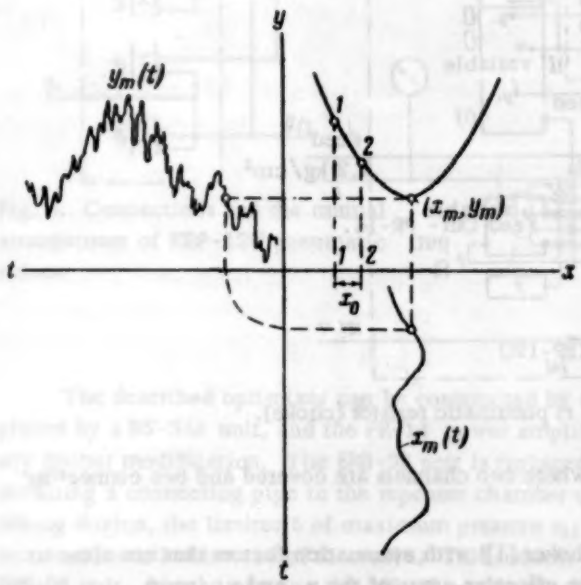

Fig. 2. Extremal response of the controlled system; x_m and y_m are the extremum coordinates.

Due to the presence of the floating reading system, sawtooth oscillations are absent if the extremum is kept stationary, since $y-y_{fl} = 0$ (Fig. 2).

In the transient process, the basic component x_1 of the movement toward the extremum (for jump-like variations of its location) is monotonic. Sawtooth oscillations can arise only for a short time immediately after a large jump in the magnitude of location of the extremum occurs.

Moreover, due to the presence of the floating reading system, the effect of unequal time constants in integrating the positive and negative values of the $y-y_{fl}$ difference is reduced; in the device described here, the above time constants differ by 10%.

Limiter 5 serves for limiting (at the top) the region in which the extremal system's output varies. Limiting is necessary either for technical reasons or for preventing the "jamming," of the system as the control unit stops when the extremal position passes beyond the stops. In the pneumatic optimizer under consideration, the limiting of the range from below takes place spontaneously: the pressure x_{11} can not be less than zero. The lower limit of the range is adjusted to the summation device 2.

The extremum tracking process is described here only in general terms. Actually, the processes in an extremal system are somewhat more complicated due to the interation of phenomena when the magnitudes of y, y_{fl}, etc. change. The particulars of these phenomena can be readily explained by considering individual idealized operating regimes of the system in greater detail. Some aspects of the tracking process will be considered in dealing with the choice of optimum parameters.

II. Description of the Optimizer's Pneumatic System

It is assumed that the system to be controlled has a pneumatic output y and a pneumatic input (for instance, pneumatic command in an ordinary-type regulator).

The layout of the pneumatic optimizer is shown in Fig. 3.

We shall describe the pneumatic equipment used in the optimizer.

1. The reset control unit 5RB-9B of the standardized unit system is used as the integrator 1. If the 5RB-9B unit is used in this way, the pressure in the repeater of the reset control unit serves as its output. In order to bring out this pressure, a connecting pipe, u, is provided, while the regular outlet is plugged. In this case, the 5RB-9B unit supplies the pressure x_{11}, which is proportional to the integral of the difference between the pressures fed to its two inputs y_- and y_+.

The pressure regulator of the 5RB-9B unit is used as the limiter 5 which limits the maximum pressure at the integrator output. For this, the following two channels are covered by means of a membrane that is located under the pressure-setting device; the channel through which the feed pressure is supplied to the setting device and the channel

through which the setting pressure produced by the setting device are brought out. With these modifications, the connecting pipe "setting" of the 5RB-9B unit serves as the input of the limiter of maximum pressure x_{1l}. (It should be noted that limiter 5 can be provided as a separate device.)

Since the "setting" connecting pipe now serves a different purpose, one of the inputs of the 5RB-9B unit is unavailable. In order to restore the integrator input, a new connecting pipe, which is marked by y_- in Fig. 3, is installed in the vertical channel for the setting pressure below the membrane that covers this channel.

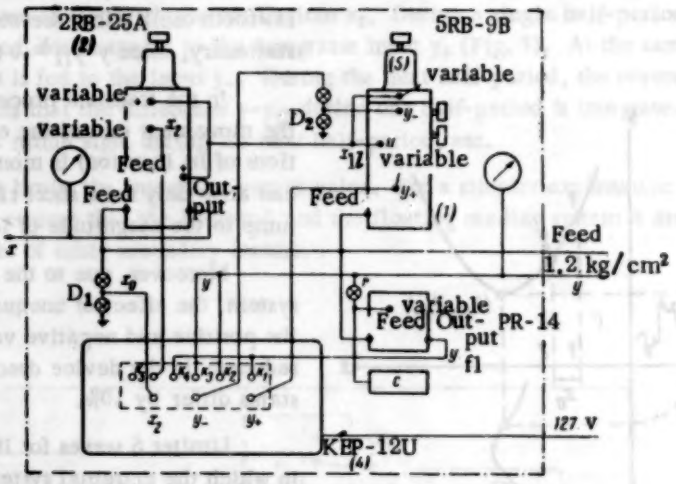

Fig. 3. c) Pneumatic capacitor; r) pneumatic resistor (choke).

It is obvious that this modification of the 5RB-9B unit, where two channels are covered and two connecting pipes are installed, will hardly affect its reliability.

The divider D_2, which is based on pneumatic resistors (chokes [1]) with attenuation factors that are close to unity, is intended for compensating the difference between the effective areas of the y_- and y_+ inputs.

2. The summation unit 2RB-25A of the SUS system for four quantities to be summed (two with the plus sign and two with the minus sign) is used as the summation device 2.

The integrator output x_{1l} is fed to the two "positive" chambers of the summation device, as a result of which the gain with respect to x_{1l} is equal to 2.4. The operating range in which the integrator output x_{1l} varies is thereby restricted; this range is of the order of 0.5 atm if x_1 varies in the 1 atm range.

The oscillations x_2 are fed to one of the "negative" chambers of the summation device. The summation device's gain with respect to x_2 is equal to -1.2.

3. The intermediate relay PR-14 of the SUS system is used as the power amplifier 3 in the floating reading system. The power amplifier is necessary because of the large leakages in the pneumatic contacts (pneumatic valves) and because the volume c is commensurable with the capacity of the integrator's chambers and piping.

4. A KEP-12U electropneumatic command device is used as the control unit. Methods for connecting this device to the extremal system are shown in Figs. 3 and 4. In this, the outlet to atmosphere in valves $k_1, \ldots, k_4$ is plugged.

The pressure x_0 is produced by means of the divider D_1 (Fig. 3), which is similar to the D_2 divider, but has an attenuation factor of the order of 0.03.

In constructing the automatic optimizer, the absolute values of the cross-sectional areas of passages in the chokes are determined by taking into account the leakages and the capacities of the chambers and piping.

The KEP-12U device can be replaced by a control unit which is based on pneumatic relays [1]. It contains a simple pneumatic oscillator. Since the ratio of half-period durations is unstable, a trigger at the output of which the oscillation half-periods are considerably closer to each other is installed beyond the generator. It should be noted

that a high oscillation period stability is not required from the generator. The square trial oscillations x_2 are obtained from the trigger output through divider D_1. The trigger output is controlled by means of four pneumatic valves, which are connected in the same way as the KEP-12U valves in Fig. 4. It should be noted that a two-nozzle relay can be used instead of each valve pair [1].

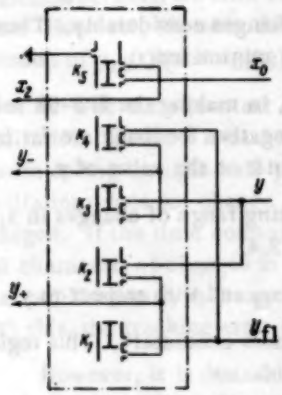

Fig. 4. Connections and the mutual arrangement of KEP-12U pneumatic valves

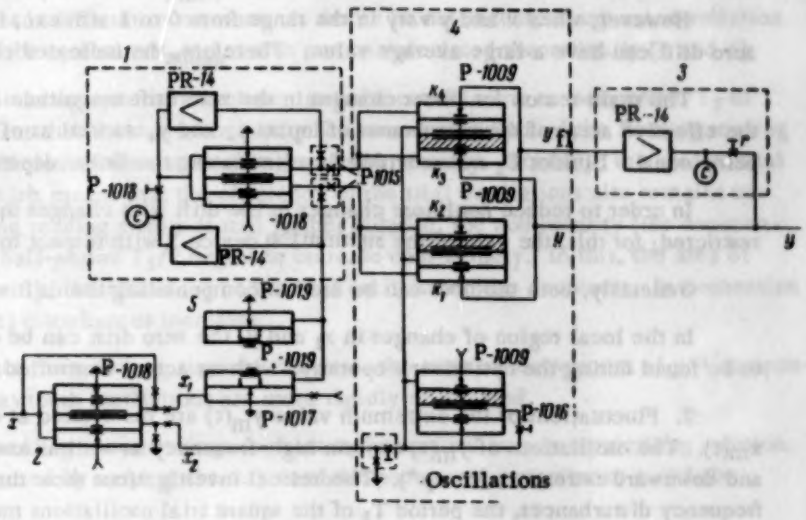

Fig. 5

The described optimizer can be constructed by using small-size SUS units. In this, the 2RB-25A unit is replaced by a BS-34A unit, and the PR-14 power amplifer is replaced by PR-14M. These units can be used without any further modification. The 5RB-9B unit is replaced by a 4RB-32A unit, where the modification consists only in installing a connecting pipe in the repeater chamber of the reset control device. Since this unit does not contain a setting device, the limiter 5 of maximum pressure x_{11} is constructed by using a P-280 pressure reducer, where a nozzle is installed instead of the valve. This reducer is connected in the same manner as the setting device of the 5RB-9B unit. Instead of using the 5RB-9B or the 4RB-32A unit, the integrator can be constructed on the basis of the layout described in [2]. One of the above control units can be used as the control unit in a small-size optimizer.

Figure 5 shows an optimizer variant which is based on elements that have been developed at the IAT AN SSSR hydropneumatic automation laboratory [1], the mass-production of which has been organized at the Tizpribor plant.

III. Adjustment of the Automatic Optimizer

In adjusting the system, the integrator zero drift is minimized in the first place. As a rule, this adjustment is performed only once, when the optimizer is constructed; later, it is necessary only to check and correct the adjustment if the characteristics of the automatic optimizer equipment have changed.

In adjusting the optimizer for another system to be controlled of if the extremum tracking conditions have changed, the following parameters must be adjusted: the period and the phase of trial oscillations, the oscillation amplitude, the floating reading system's time constant, the range in which the extremal system's output pressure x changes, and the integrator time constant.

1. Minimization of the integrator zero drift. The integrator zero drift causes the extremal system to settle in an equilibrium position which is at a certain distance from the extremum. This distance is the greater, the greater the integrator zero drift and the smaller the coefficient of the parabola that approximates the extremal characteristics of the system to be controlled. Thus, if a fixed extremum is maintained, a position error arises and, consequently, the systems performance deteriorates. In order to reduce this error, it is necessary to minimize the integrator zero drift. It should be noted that this error constitutes the main component of the error in maintaining the extremum in the absence of disturbances and displacements of the extremum position. In the case of intensive $x_m(t)$ and $y_m(t)$ oscillations, the dynamic error and the error due to disturbances can be considerably larger than the position error, which will in this case be negligible.

It is better to minimize the system's zero drift for the optimizer as a whole instead of separately minimizing it at the integrator. The minimization of the optimizer's zero drift can be performed during the short period of time when the optimizer is disconnected from the control process without taking it off the system to be controlled.

The zero drift (its constant component) is minimizedby means of a screw, which determines the nozzle position in the 5RB-9B reset control unit.

However, when x and y vary in the range from 0 to 1 atm exc, the zero drift changes considerably. Thus, the zero drift can have a large average value. Therefore, the indicated changes must be minimized.

The main reason for linear changes in the zero drift magnitude is the fact that, in making the 5RB-9B units, the effective areas of the membranes of inputs y_- and y_+ as well as of positive and negative feedback are far from being equal. Divider D_2 was provided for eliminating the linear dependence of the drift on the value of y.

In order to reduce nonlinear changes in the drift with changes in x_{1i}, the operating range of changes in x_{1i} was restricted; for this, the gain of the summation device 2 with respect to x_{1i} was set at 2.4.

Generally, both methods can be used in compensating the drift with respect to x_{1i} and with respect to y.

In the local region of changes in x_1 and y, the zero drift can be compensated more accurately. This region is to be found during the optimizer's operation with an actual controlled system.

2. Fluctuations of the extremum value $y_m(t)$ are manifested as disturbances in tracking the extremum position $x_m(t)$. The oscillations of $y_m(t)$ contain high-frequency as well as low-frequency components (the so-called upward and downward extremum "creep"). Theoretical investigations show that, in the sense of stability with respect to low-frequency disturbances, the period T_2 of the square trial oscillations must be as small as possible. The degree to which the period can be reduced is limited only by the inertness of the system to be controlled and also by changes in the inertness and lag times in the system to be controlled.

Actually, the smoothing-out of oscillations x_2 while they are passing through an inertial controlled system must not be exaggerated; otherwise, their efficiency would drop, and the error in tracking the extremum would begin to increase due to high-frequency disturbances (the high-frequency components of the $y_m(t)$ oscillations).

In the case of an inertial system to be controlled, the oscillations of the valve k_5 (Figs. 1 and 4) must lead the oscillations of valves $k_1, \ldots, k_4$ with respect to phase. The lead must be adjusted in such a manner as to compensate the lag of the trial oscillations x_2 that is caused by the inertness and lags in the system to be controlled. The phase shift between oscillations x_2 that are supplied to the input of the system to be controlled and the corresponding oscillations at the system's output must be as close to zero as possible; the phase shift can also be equal to $2\pi n$ or πn for a sufficiently small integer n. The reduction in the T_2 value (and, corresponding, the increase in n) is limited by variations in the lag and inertness of the system to be controlled. In taking into account changes in the lag, the value of T_2 must be chosen in such a manner that the oscillation amplitude of the phase shift be considerably less than $\frac{1}{2}\pi$. In the opposite case, the efficiency of trial oscillations would drop, and the extremum tracking error due to high-frequency disturbances would increase.

For a large n, it is assumed that the smoothing-out of oscillations x_2 by the inertness of the system to be controlled is still not sufficient.

The adjustment of T_2 is effected by adjusting the KEP-12U device.

3. The optimum amplitude of oscillations x_{2m} is determined in such a manner as to provide a compromising solution of the contradiction which arises in striving simultaneously to reduce the extremum tracking error caused by trial oscillations and the error caused by the integrator zero drift and the high-frequency disturbances at the output of the system to be controlled.

If the disturbances (oscillations of the extremum value $y_m(t)$) are not intensive and the position $x_m(t)$ of the extremum changes very slowly, the main cause of the error in maintaining the extremum is the integrator zero drift. Although the zero drift was minimized, we did not succed in making it equal to zero throughout the entire range of changes in y and x. Then, with a decrease in $x_0 = 2x_{2m}$, the stable equilibrium position of the extremal system, which is located to the side of the extremum, becomes increasingly further removed from the extremum.

For $x_0 = 0$, as a result of the zero drift, the system moves to the stop and the error in maintaining the extremum will be very large. The error will also be large for exceedingly large values of x_0, since the system, whose average position is at the extremum, will perform about this position oscillations with an exceedingly large amplitude.

It is necessary to find such an optimum value $x_0 = 2x_{2m}$ that the average of the y values in positions 1 and 2 (Fig.2,a) is at a minimum.

In the presence of intensive $y_m(t)$ oscillations, the error due to the zero drift can be relatively unimportant. An exact optimum adjustment of the x_0 value under disturbance conditions is more complicated than the one described above. The optimum x_0 value is chosen in such a manner as to provide a compromising solution of the contradiction between the error due to disturbances (due to the $y_m(t)$ oscillations) and the error due to the trial oscillations. However, the error due to disturbances is difficult to measure. It should be noted that, if any autocorrelation function of $y_m(t)$ [and $x_m(t)$] can be found, the optimum $x_{2m_{opt}}$ value can be calculated theoretically [3 and 4].

4. The time constant of the floating reading system is so chosen as to be equal to one or two periods T_2 of oscillations x_2. This is determined by the fact that there is no necessity for a constant output of the floating reading system during a single half-period. It is sufficient if the output changes almost linearly. Actually, the area of trial oscillations does not change in this case, which means that the efficiency of the trial oscillations also remains unchanged. If the time constant of the floating reading system is still further reduced, the nonlinearity (the exponential character) of changes in y_{fl} during the half-period $T_2/2$ begins to increase considerably. In this, the area of trial oscillations x_2 decreases, and consequently, the efficiency of the trial oscillations also decreases. In connection with this, the tracking error due to the $y_m(t)$ disturbances increases.

However, it is desirable to reduce the time constant, since in this case, the constant component of y is compensated more quickly and consequently, the sawtooth oscillations are more rapidly eliminated.

Thus, the magnitude of the floating reading system's time constant is determined by a compromising solution. The adjustment of this time constant is effected by varying the values of the pneumatic capacitance c and the pneumatic resistance r.

5. The range of changes in the output x_1 of the extremal system is adjusted by means of the spring screw of the 2RC-25A summation device and the screw in the pressure setting device of the 5RB-9B reset control unit. The adjustment should be started with regulating the lower limit of changes in pressure x, since the adjustment of the limiter determining the upper limit of changes in x would be otherwise disturbed.

6. The integrator time constant should be determined in such a manner as to provide a compromising solution of a contradiction similar to the contradiction arising in developing optimal servosystems. The system as a whole must smooth out sufficiently well the high-frequency components of oscillations of the extremum $y_m(t)$, and it must not overly smooth out changes in the position $x_m(t)$ of the extremum that is to be tracked. The low-frequency components of oscillations of the extremum value are filtered out in the process of measuring the system's remoteness from the extremum. The indicated low-frequency and high-frequency oscillations of $y_m(t)$ are manifested as disturbances in tracking the extremum position. The adjustment of the integrator time constant is brought about by adjusting the chokes DD and AP of the 5RB-9B unit. If the DDchoke is completely closed and the AP choke is open, the time constant is equal to 20 sec. An exact optimum adjustment of the time constant under the above conditions is complicated; the optimum time constant can be calculated theoretically by using the autocorrelation functions of the $y_m(t)$ and $x_m(t)$ quantities [3].

In order to improve the quality of extremal control, the gain of the converter at the output of the extremal system must be as large as possible, without, however, saturating the converter output during the extremum tracking process. In this, the error due to the integrator zero drift decreases, while the error due to oscillations of the extremum value, i.e., the error due to disturbances, remains the same as before.

IV. Experimental Investigation

The pneumatic extremal system was tested in conjunction with an electronic system, which contained a quadrator with inertial elements ahead of it and beyond it, a ball noise generator, and converters for transforming pressure into electrical voltage and vice versa (EDMU-1 and EPD-32).

The extremum tracking process under conditions where changes in the extremum positions have the character of random switchings is recorded on the oscillograms shown in Fig. 6.

For low disturbance intensities and small changes in the position of the extremum, the error in maintaining the extremum was caused only by the integrator zero drift. The accuracy in maintaining the extremum for a fixed extremum position in the absence of disturbances was equal to 1-1.5% for a 1 kg/cm^2 range of changes in pressure y.

The accuracy can be increased by a factor of 2 to 3 by more carefully adjusting the divider D_2 and the screw which determines the nozzle position in the 5RB-9B unit, especially if the minimization of the zero drift is performed for the local region of changes in the coordinates of the extremum.

At the present time, industrial tests of the optimizer are in progress in one of the synthetic alcohol plants.

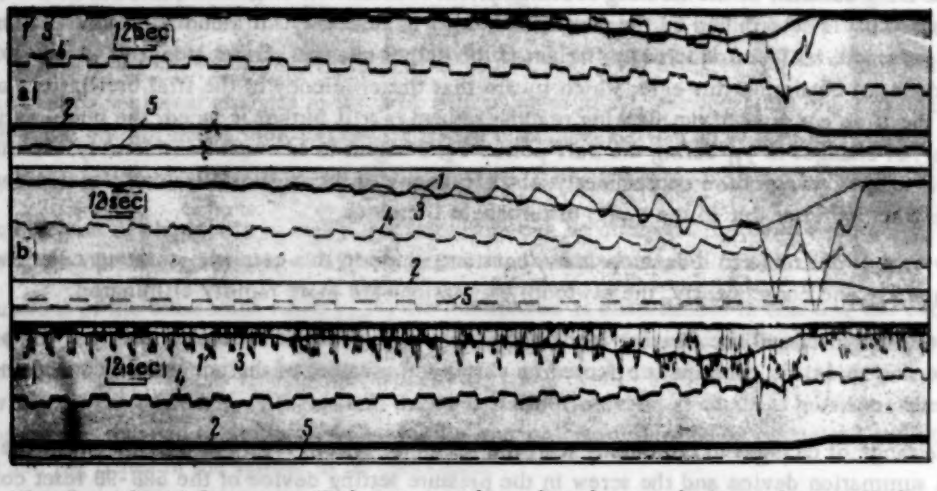

Fig. 6. a) Inertialess controlled system without disturbances; b) inertial controlled system without disturbances and with 1-sec time constants of the inertial elements; c) inertialess controlled system in the presence of disturbances. 1) output y of the controlled system; 2) extremum position $x_m(t)$; 3) output y_{fl} of the floating reading system; 4) output x of the automatic optimizer; 5) trial oscillations x_2.

Remark. We shall now determine the position of the described automatic optimizer among other optimizers.

By comparing the known automatic optimizers [3], it was established that the optimizer described in [3 and 4] is apparently more efficient in tracking the extremum in the presence of intensive steady-state random disturbances with Gaussian distributions for a controlled system which has at least a little inertia.

The optimal characteristics of the extremal system described in [3 and 4] were determined in further theoretical investigations. On the basis of the analogy with optimal linear servosystems, it can be said that, under the above conditions, the optimizer [4] provides the optimum solution of the problem of extremum tracking in a large class of linear automatic optimizers.

It appeared that the indicated optimum characteristics make it possible to simplify the block diagram of the extremal system and the construction of its equipment without impairing its performance. The described pneumatic realization of the extremal system was developed by using these results. It differs from the system [4] by the combination of several functions in a single device.

The integrator represents the continuous element in the described optimizer. In this, the weighting function of the entire system is represented by an exponential, which is an optimum function under conditions where the system to be controlled has little inertia, the variations of the extremum position have the character of random switchings, and the oscillations of the extremum value (disturbance) constitute white noise. Under different conditions, for instance, if the extremum position changes linearly over a long period of time, a different weighting function, corresponding to a system where a more complicated device is used instead of the integrator, would yield better results (see, for instance [4]).

In the foregoing, we have discussed optimal systems in the class of linear systems. It should be noted that, in the class of all possible linear systems, the optimal linear systems are absolutely optimal only in the case of a

Gaussian distribution of random steady-state changes in the magnitude and position of the extremum. Otherwise, nonlinear optimizers can be absolutely optimal [5 and 6]. Thus, if extremum tracking is to be further improved, more complex linear and nonlinear unsteady-state devices must be introduced instead of the integrator. It should be noted that the advantage of nonlinear systems is strongly pronounced only if the noise-to-useful signal ratio is small [6].

The optimum adjustment of this extremal system as well as of the system described in [4] can be performed automatically by means of another similar extremal system.

LITERATURE CITED

1. T. K. Berends and A. A. Tak', "Pneumatic relay systems," Avtomatika i Telemekhanika 20, 11 (1959).*
2. V. V. Aronovich and R. S. Patushinskaya, "Automatic control of the direct ethylene hydration process," Khimicheskaya Promyshlennost', 2 (1960).
3. N. V. Grishko, "On optimal extremal systems," Transactions of the Seventh Scientificotechnical Conference of Young Scientists from IAT AN SSSR on Automatic Control, which was held on March 14-16, 1960.
4. N. V. Grishko, "Extremal regulator with extremum tracking" Avtomatika i Telemekhanika 20, 4 (1959).
5. D. H. Laning and R. G. Battin, Random Processes in Automatic Control Problems [Russian translation] (IL, 1958).

NOISE STABILITY OF FREQUENCY REMOTE CONTROL SYSTEMS IN THE CASE OF FLUCTUATING NOISE

Yu. I. Chugin

(Moscow)

Translated from Avtomatika i Telemekhanika, Vol. 22, No. 5,
pp. 664-678, May, 1961
Original article submitted September 9, 1960

The present article is concerned with the determination of the noise stability of remote control systems with frequency modulation of the carrier and the separation of commands with respect to the subcarriers for arbitrary levels of fluctuating noise. The probability of command suppression and the probability of spurious command formation are used as the estimation criterion. The influence of the structure and the parameters of the receiving device on its noise stability is investigated.

Introduction

Frequency remote control systems which have a high degree of noise stability are used to an ever increasing extent in remote control devices.

The theoretical calculation of such systems has not yet been treated to a sufficient extent in the literature.

The present article describes an investigation of the noise stability of remote control systems with frequency modulation of the carrier by channel (subcarrier) frequencies. In the receiving device (Fig. 1), the carrier frequency is demodulated, while the channel frequencies are divided by means of frequency selectors and are then detected. A threshold device and a final device are connected to the detector output in each channel. At each instant of time, the carrier frequency is usually modulated by one of the subcarriers, since only a single command is transmitted at a time, while an additional command, which is used for protection purposes (for disconnecting the receiver if the transmitting device breaks down), is transmitted in the intervals between the operating commands.

The probability of command suppression and the probability of spurious command formation are used as the noise stability criterion in command remote control.

*See English translation.

Figure 1 shows a typical block diagram of a receiving device for frequency remote control systems. The complete circuit of the device comprises band filters Φ_1, Φ_2, and Φ_3, a frequency discriminator, FD, detectors D, and limiters, 1 and 2, at the discriminator's input and output.

In order to find the probability of command suppression in the remote control channel (the channel which transmits the signal), it is necessary to know separately the magnitudes of noise and of the sinusoidal signal at the channel filter Φ_3 output as well as the distribution of the total oscillation envelope. In order to determine the probability of spurious command formation in the channel that does not contain the signal, it is necessary to know the noise magnitude and the distribution of its envelope. In calculations, the signal and noise magnitudes at the output of filter Φ_2 are determined first, and these values are then used for determining the corresponding values at the output of filter Φ_3.

The following assumptions are made in analysis.

1. Limiters 1 and 2 are close to idealized limiters.
2. Filters Φ_1 and Φ_3 have a Gaussian characteristic.
3. Detectors D are linear and inertialess, and they have a transmission factor equal to unity.
4. The threshold devices at the outputs of the detectors are inertialess with zero time of return to the initial state.

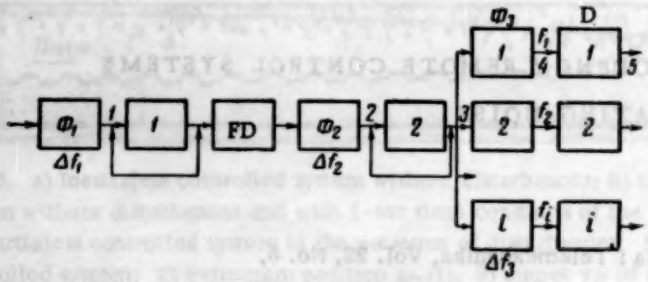

Fig. 1

5. The discriminator output voltage is determined by the expression

$$U_d = kA(\omega - \omega_z)$$

where k is a constant factor, A is the voltage amplitude at the discriminator output, and ω_z is the frequency of the discriminator's "zero" point.

The above conditions are not very strict, and they are usually fulfilled in actual devices.

1. Signal and Noise at the Filter Φ_2 Output

Let us determine the signal powers Q_{s2} and the noise power Q_{n2} at the output of filter Φ_2 in the presence and absence of limiter 1.

With Limiter 1

The signal power at the outputs of the discriminator and the filter Φ_2, whose transmission factor in its transmission band is $K(\omega) = 1$, will be equal to [1]

$$Q_{s2.0} = D^2 \frac{\omega_d^2 (1 - e^{-z})^2}{2} \qquad (1)$$

where $D = kA = 4\alpha_0 k/\pi$, α_0 is the limiting level of the symmetric limiter 1, $z = (U_s/U_n)_1^2$ is the signal power-to-noise power ratio at the receiver input (at the output of filter Φ_1), and ω_d is the frequency deviation amplitude in the given channel; $\omega_d = 2\pi f_d$.

In Eq. (1), the term $(1-e^{-z})^2$ takes into account the suppression of signals by noise. The noise power at the output of filter Φ_2, whose transmission band is $\Delta f_2 = f_2 - f_1$, is equal to

$$Q_{n\,2.0} = \int_{f_1}^{f_2} W(f)\,df \tag{2}$$

where W(f) is the energy spectrum of noise at the discriminator output. According to [5 and 6], in the presence of limiter 1, the noise spectrum for the entire range of z values ($0 \leq z < \infty$) and the initial spectrum portion, when $2f_{max}/\Delta f_1 \leq 0.2$ can be represented as

$$W(f)_0 = D^2\left[11{,}6\Delta f_1 e^{-1.085z} + \frac{9{,}9\Delta f_1 (1-e^{-z})^2}{z}\left(\frac{2f}{\Delta f_1}\right)^2\right] \tag{3}$$

where Δf_1 is the complete band of output filter Φ_1.

The first term of expression (3) defines the noise spectrum component that is independent of the frequency, and the second term defines the component that is quadratically dependent on frequency. If $z \leq 3$, the second term in expression (3) can be neglected as a small quantity.

Expression (3) is valid under the condition that the carrier frequency ω_s is equal to the center frequency of the output filter [$\Phi_1(\omega_0)$] and the frequency of the discriminator's "zero" point ($\omega_s = \omega_0 = \omega_z$), i.e., that the modulation of the discrimination of the carrier is absent. It was shown in [1] that, in the case of a low limiting level in the presence of carrier frequency modulation, the low-frequency components of noise at the discriminator output ($2f_{max}/\Delta f_1 \leq 0.2$) vary to a slight extent (the high-frequency components of the noise spectrum are subject to the greatest changes). Consequently, within the indicated limits, expression (3) can be considered as approximately valid even in the presence of modulation.

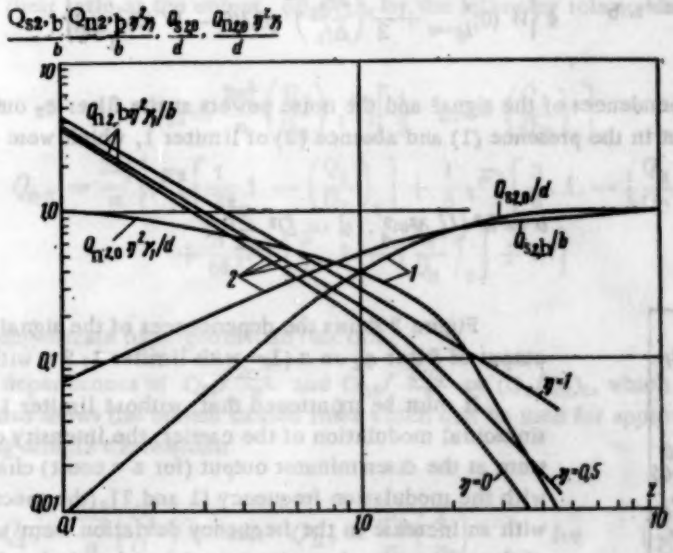

Fig. 2

On the basis of (1), (2) and (3), for $z \leq 3$, the signal power-to-noise power ratio at the output of filter Φ_2 will be equal to

$$\left(\frac{Q_s}{Q_n}\right)_{2.0} = \frac{0.85\,(1-e^{-z})^2\,\eta^2\gamma_1}{e^{-1.085z}} \tag{4}$$

where

$$\eta = \frac{2f_d}{\Delta f_1}, \qquad \gamma_1 = \frac{\Delta f_1}{2\Delta f_2}.$$

Without Limiter 1

The signal power at the outputs of the discriminator and filter Φ_2 will be in this case equal to [1]

$$Q_{s\,2.b} = \frac{\pi}{4} k^2 (U_c)_1^2 \omega_d^2 z e^{-z} \left[I_0\left(\frac{z}{2}\right) + I_1\left(\frac{z}{2}\right) \right]^2 \tag{5}$$

where $I_0(x)$ and $I_1(x)$ are modified zero and first-order Bessel functions of the first kind.

The noise power at the output of filter Φ_2 is determined by using Eq. (2), where the spectrum $W(f)_b$ for slow sinusoidal modulation ($f_{mod} \ll \Delta f_1/2$, $2f_{max}/\Delta f_1 \leq 0.2$ and $0 \leq z < \infty$ is equal to (see Appendix)

$$W(f)_b = 4\pi^2 k^2 \left(\frac{\Delta f_1}{2}\right) (U_n)_1^2 \left[W(0)^*_{f_d=0} + \frac{1}{2} \left(\frac{2f_d}{\Delta f_1}\right)^2 (0.405 - W(0)^*_{f_d=0}) \right] \tag{6}$$

where

$$W(0)^*_{f_d=0} = 0{,}405 e^{-0{,}8z} \qquad \text{for} \qquad 0 \leqslant z \leqslant 1.5$$

and

$$W(0)^*_{f_d=0} = \frac{0{,}183}{z} \qquad \text{for} \qquad 1.5 < z < \infty.$$

On the basis of (1), (2), and (3), for $z \leq 3$, the ratio of signal power to noise power at the output of filter Φ_2 will be given by

$$\left(\frac{Q_s}{Q_n}\right)_{2.b} = \frac{\pi z^2 e^{-z} \left[I_0\left(\frac{z}{2}\right) + I_1\left(\frac{z}{2}\right) \right]^2 \eta^2 \gamma_1}{4 \left\{ W(0)^*_{f_d=0} + \frac{1}{2} \left(\frac{2f_d}{\Delta f_1}\right)^2 [0{,}405 - W(0)^*_{f_d=0}] \right\}}. \tag{7}$$

Figure 2 shows the dependences of the signal and the noise powers at the filter Φ_2 output on the signal-to-noise ratio (z) at the receiver input in the presence (1) and absence (2) of limiter 1, which were calculated by using Eqs. (1), (2), and (5);

$$b = k^2 (U_s)_1^2 \omega_d^2 \,.\; d = D^2 \frac{\omega_d^2}{2}.$$

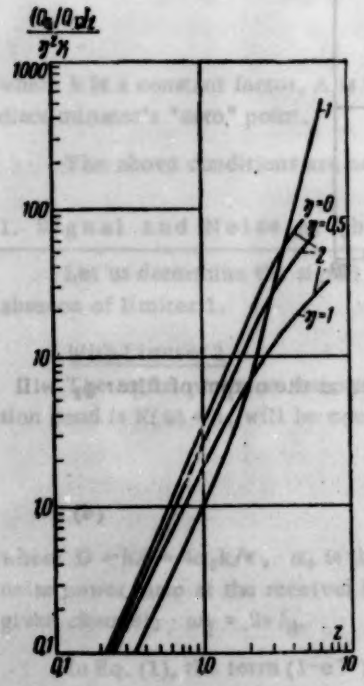

Fig. 3

Figure 3 shows the dependences of the signal-to-noise ratios at the output of filter Φ_2 on z (1 – with limiter 1; 2 – without limiter 1).

It must be mentioned that, without limiter 1 and in the presence of sinusoidal modulation of the carrier, the intensity of the noise energy spectrum at the discriminator output (for z = const) changes in correspondence with the modulation frequency [1 and 7] (the spectrum intensity increases with an increase in the frequency deviation from ω_0), i.e., in the presence of the subcarrier, the noise is correlated with the signal.

2. Signal and Noise at the Outputs of Channel Filters

In order to calculate the signal and noise powers at the outputs of channel filters Φ_3, it is generally necessary to consider the passage of noise that is correlated with the signal through limiter 2 and filter Φ_3. For such a case, exact calculations are very complicated. It can be shown that, in a wide range of z, this correlation can be neglected regardless whether limiter 1 is present or absent. As was shown in [1 and 7], the correlation of noise with the signal in the absence of limiter 1 is considerable; however, the noise action at the output of limiter 2 will mainly affect only the shift of the instant of time when the sinusoidal voltage passes through zero. In correspondence with this, the calculations can be performed for uncorrelated noise with

$\eta = 0$. In the case of powerful noise, when the noise voltage that is superimposed on the signal can attain the limiting level of limiter 2, the correlation between noise and the signal becomes so weak that the difference between noise intensities for $f_d = 0$ and $f_d = \max$ is small. In this case, the calculations can also be performed for uncorrelated noise that corresponds to $\eta = 0$.

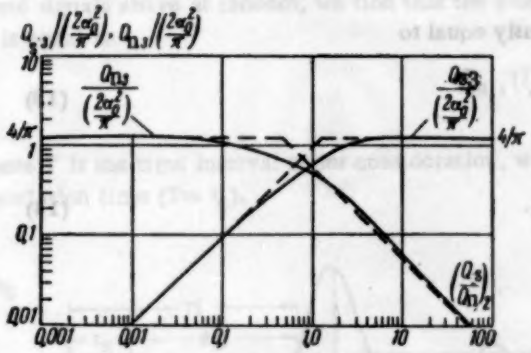

Fig. 4

Until the present time, the signal and noise passage through the limiter with a Gaussian distribution has been considered in the literature. The noise at the filter Φ_2 output differs from Gaussian-distribution noise; however, if the band relationship is given by $\Delta f_2 \ll \Delta f_1$ it can be considered as Gaussian-distribution noise. It should be noted that the above relationship between the bands is usually valid for industrial remote control systems. Under these assumptions, we shall determine the magnitudes of the signal and noise at the outputs of channel filters in the presence and absence of limiter 2.

With Limiter 2

The signal power Q_{s3} and the noise power Q_{n3} (in the frequency band near the input signal first harmonic) at the output of the idealized symmetrical limiter 2 with the characteristic

$$y = f(x) = \begin{cases} \alpha_0 & x > 0 \\ -\alpha_0 & x < 0 \end{cases}$$

are expressed in terms of their ratio at the output $(Q_s/Q_n)_2$ by the following relationships [4]:

$$Q_{s3} = \frac{2\alpha_0^2}{\pi}\left(\frac{Q_s}{Q_n}\right)_2 {}_1F_1^2\left[\frac{1}{2}\ \ 2.-\left(\frac{Q_s}{Q_n}\right)_2\right] \tag{8}$$

$$Q_{n3} = \frac{2\alpha_0^2}{\pi}\left\{{}_1F_1^2\left[\frac{1}{2}.1.-\left(\frac{Q_s}{Q_n}\right)_2\right] + \frac{1}{8}\,{}_1F_1^2\left[\frac{3}{2}.1.-\left(\frac{Q_s}{Q_n}\right)_2\right] + \right. \tag{9}$$
$$\left. + \frac{3}{64}\,{}_1F_1^2\left[\frac{5}{2}.1.-\left(\frac{Q_s}{Q_n}\right)_2\right] + \ldots\right\}$$

where ${}_1F_1(\beta, \gamma, -x)$ is a degenerate hypergeometric function.

Figure 4 shows the dependences of $Q_{s3}/\frac{2\alpha_0^2}{\pi}$ and $Q_{n3}/\frac{2\alpha_0^2}{\pi}$ on $(Q_s/Q_n)_2$, which were plotted by using Eqs. (8) and (9) [4]. The figure also shows the broken dashed lines which can be used for approximating these functions. They are given by the following simple expressions:

$$Q_{s3} = \frac{2\alpha_0^2}{\pi}\left(\frac{Q_s}{Q_n}\right)_2 \quad \text{and} \quad Q_{n3} = \frac{2\alpha_0^2}{\pi}\left(\frac{4}{\pi}\right) \quad \text{for} \quad \left(\frac{Q_s}{Q_n}\right)_2 < 1 \tag{10}$$

$$Q_{s3} = \frac{2\alpha_0^2}{\pi}\left(\frac{4}{\pi}\right) \quad \text{and} \quad Q_{n3} = \frac{2\alpha_0^2}{\pi}\,\frac{2}{\pi\left(\frac{Q_s}{Q_n}\right)_2} \quad \text{for} \quad \left(\frac{Q_s}{Q_n}\right)_2 \geq 1. \tag{11}$$

It is obvious from Fig. 4 that the approximation of functions (8) and (9) by the broken curves (10) and (11) yields a considerable error in the $(Q_s/Q_n)_2 \approx 1$ region.

The noise spectrum at the limiter output depends on the limiting level. For a low limiting level, the effective width of the output noise spectrum (in the band near the input signal first harmonic) is approximately equal to the transmission band of an idealized filter that is connected ahead of the limiter, while the spectrum intensity is uniform [2].

In this case, the noise power at the channel filter output in the i-th channel is given by

$$Q_{n4} = C_0^2 Q_{n3} \frac{\Delta f_3}{\Delta f_2}. \tag{12}$$

Here, Δf_3 is the energy transmission band of channel filter Φ_3 with the center frequency f_i, and C_0 is the filter transmission factor for the center frequency.

The signal power at the channel filter output will be obviously equal to

$$Q_{s4} = C_0^2 Q_{s3}. \tag{13}$$

and the sinusoidal signal amplitude will be

$$E_s = \sqrt{2Q_{s4}}. \tag{14}$$

Without Limiter 2

The signal power at the output of channel filter Φ_3 is

$$Q_{s4} = C_0^2 Q_{s2} \tag{15}$$

where Q_{s2} is determined from Eq. (1) or (5), while the noise power is given by

$$Q_{n4} = C_0^2 W(f_i)\,\Delta f_3 \approx C_0^2 Q_{n2} \frac{\Delta f_3}{\Delta f_2}. \tag{16}$$

$W(f_i)$ is given by Eq. (3) or (6), while the approximate equation is valid for $z \leq 3$ in the presence of filter Φ_2.

3. Probability of Command Suppression

Let us consider the process of command suppression.

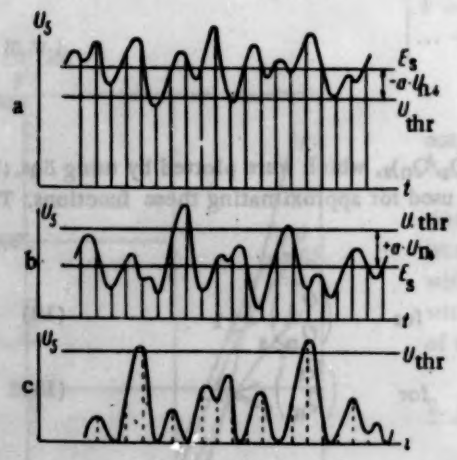

Fig. 5

As can be seen from Eqs. (1) and (5) and Fig. 4, the amplitude of the sinusoidal signal E_s (14) at the output of channel filter Φ_3 and consequently, the signal level at the output of detector D continuously decrease with an increase in the noise level at the receiver input. In this, as follows from Eq. (2), the noise power at these points simultaneously increases. The above phenomenon first leads to partial command suppression and, for a high noise level, to complete suppression of the commands. For the sake of simplicity, we shall consider that the commands transmitted through the ith channel under consideration follow each other without pause. In this, the beginnings of commands are distributed at random in time.

Figure 5, a and b, shows the shape of command signals at the detector output (the envelope of the total sinusoidal signal and noise voltage at the output of channel filter Φ_3) for the two limiting cases corresponding to the beginning of command suppression (a) and to the almost complete suppression of commands (b) (the rise and decay times of the command signal fronts are assumed to be short in comparison with the command duration, which is obviously true for $\Delta f_3 \gg 1/\tau_c$). In Fig. 5, a and b, U_{thr} designates the operating level of the threshold device and E_s denotes the signal level with respect to which the noise acts; this level is equal to the sinusoidal signal amplitude at the linear detector input. It is obvious that the signal level can occupy any of the intermediate positions with respect to U_{thr}.

If a certain constant level is taken for the signal E_s level and the level of U_{thr} is assumed to be variable, the cases given in Fig. 5, a and b can be represented in a different manner (Fig. 6).

It is obvious from Fig. 5, a and b, and Fig. 6 that the suppression of command signals will occur either due to negative overshoots of the detector output voltage that intersect the U_{thr} level (a) or due to the intervals between the positive overshoots of this voltage that exceed U_{thr} (b). Suppression will occur in the case where the command signal voltage is lower than the operating level U_{thr} over the entire period τ_c during which the command is transmitted (Fig. 6). If the duration τ_0 of overshoots at the level U_{thr} (a) is less than τ_c, suppression will not occur. If $\tau_0 \geq \tau_c$, only those commands whose beginning lies in the $\Delta_0 = \tau_0 - \tau_c$ interval will be suppressed. If we consider that the command signals arrive at random, we find that the probability of signal suppression by a single overshoot with duration τ_0 is equal to

$$P_{su,1}(U_{thr}) = \frac{\tau_0 - \tau_c}{T}$$

where T is the time interval under consideration, which is of much greater magnitude than the fluctuation process correlation time ($T \gg \tau_c$).

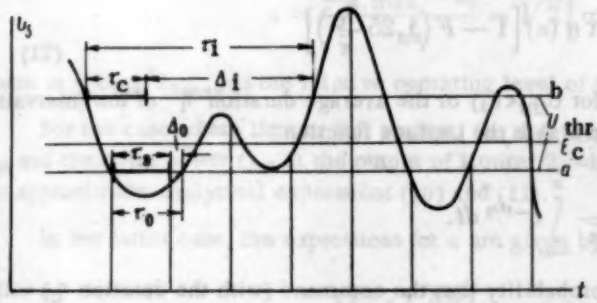

Fig. 6

By considering all overshoots $\tau_0 \geq \tau_c$ or the intervals $\tau_1 \geq \tau_c$ between them and by averaging over the time T, we find that the probability of command suppression at the U_{thr} level for the case a or b will be given by

$$P_{su}(U_{thr}) = \frac{\bar{\tau}(\tau \geq \tau_c) - \tau_c}{T} n_\tau(U_{thr}, \tau \geq \tau_c) \qquad (17)$$

where $\bar{\tau}(\tau \geq \tau_c)$ is the average duration of overshoots (for $U_{thr} < E_s$) or of the intervals between them (for $U_{thr} < E_s$) at the U_{thr} level of all $\tau \geq \tau_c$ ($\tau = \tau_0$ for the case a and $\tau = \tau_1$ for the case b), and $n_\tau(U_{thr}, \tau \geq \tau_c)$ is the average number of downward overshoots of all $\tau \geq \tau_c$ during the time T.

The values of $\bar{\tau}(\tau \geq \tau_c)$ and $n_t(U_{thr}, \tau \geq \tau_c)$ are determined by the following expression:

$$\bar{\tau}(\tau \geq \tau_c) = \frac{\int_{\tau_c}^{\infty} \tau w(\tau)\, d\tau}{\int_{\tau_c}^{\infty} w(\tau)\, d\tau}$$

$$n_\tau((U_{thr} \cdot \tau \geq \tau_c) = n(U_{thr})\, T P(\tau \geq \tau_c) = n(U_{thr})\, T \int_{\tau_c}^{\infty} w(\tau)\, d\tau \qquad (18)$$

where $w(\tau)$ is the distribution density of the durations of overshoots or intervals between them at the U_{thr} level, $n(U_{thr})$ is the average number of downward overshoots at the U_{thr} level per unit time, and $P(\tau \geq \tau_c)$ is the probability that the overshoots (or the intervals between them) will have a duration $\tau \geq \tau_c$ at the U_{thr} level.

By substituting (18) in (17), we obtain the expression for the probability of command suppression.

After normalization, we obtain the equation for the probability of suppression at the level a:

$$P_{su} = n(a)\left[\bar{\tau}(a.\ \tau \geq \tau_c) - \tau_c\right] P(a, \tau \geq \tau_c) =$$
$$= n(a)\left[\int_{\tau_c}^{\infty} \tau w(\tau)\, d\tau - \tau_c \int_{\tau_c}^{\infty} w(\tau)\, d\tau\right] \qquad (19)$$

where a is the relative limiting level

$$a = \frac{U_{thr} - E_c}{U_{n\,t}} \qquad (20)$$

n(a) is the average number of overshoots of the envelope of the total signal and noise voltage at the a level per unit time, and $w(\tau) = w(a, \tau)$ is the distribution density of the durations of overshoots (or the intervals between them) at the level a.

The distribution of the linear detector output voltage in the channel with the signal (the envelope of the sinusoidal signal and noise) is expressed by the generalized Rayleigh law. For large signal-to-noise ratios ($E_s/U_{n4} > 4$) this distribution approaches the Gaussian distribution.

For the Gaussian as well as for the Rayleigh distribution, an exact analytical expression for the distribution of durations $w(\tau)$ has not yet been found. The experimental data provided in a number of papers [8 and 9] indicate that the distribution of the durations of overshoots and intervals between them for a Gaussian and a Rayleigh process can be coarsely approximated by the Rayleigh distribution for all limiting levels.

If we use such approximation, i.e., if we assume that

$$w(\tau) = \frac{dP(\tau)}{d\tau} = \frac{d}{d\tau}\left[1 - e^{-\frac{\pi}{4}\left(\frac{\tau}{\bar{\tau}}\right)^2}\right]$$

expression (19) will be given by

$$P_{su} = n(a)\int_{\tau_c}^{\infty} e^{-\frac{\pi}{4}\left(\frac{\tau}{\bar{\tau}}\right)^2} d\tau = 2\bar{\tau}\, n(a)\left[1 - F\left(1{,}25\,\frac{\tau_c}{\bar{\tau}}\right)\right] \tag{21}$$

where $\bar{\tau} = \bar{\tau}(a)$ is the average duration $\bar{\tau}_0$ of overshoots (for $U_{thr} < E_s$) or the average duration $\bar{\tau}_1$ of the intervals between them (for $U_{thr} > E_s$) of all $\tau \geq 0$ at the level a and F(x) is the Laplace function

$$F(x) = \frac{1}{\sqrt{2\pi}}\int_{-\infty}^{x} e^{-t^2/2}\, dt.$$

It is obvious from Eq. (21) that, for determining the probability that the command (with the duration τ_c) will be suppressed, it is necessary to know the relative limiting level a (20), the average duration $\bar{\tau}$ of overshoots (or intervals between them) at this level, and their average number n(a) per unit time. As follows from (1), (5), (8), and (13), the limiting level a depends on the signal-to-noise ratio (z) at the input of the receiving device and on its structure and parameters.

Assuming that the detector output voltage in the control channel has a Gaussian distribution ($E_s/U_{n4} > 4$), we have [3]:

$$n(a) = \delta f_s e^{-a^2/2}, \tag{22}$$

$$\bar{\tau} = \frac{P(-\infty < \xi < a)}{n(a)} = \frac{F(a)}{\delta f_s e^{-a^2/2}} \tag{23}$$

where δf_s is the average width of the fluctuation spectrum; for a Gaussian frequency response of the channel filters Φ_s with the energy transmission band Δf_s, it is equal to $\delta f_s \approx 0.4\,\Delta f_s$.

By substituting (22) and (23) in (21), we obtain an expression for the probability of command suppression for an arbitrary level a.

In the general case, this expression will have a complex form. Simpler expressions for P_{su} are obtained for particular a values.

Beginning of Suppression (Fig 5, a).

In this case, the value of z is negative, and the average overshoot duration is $\tau_0 \ll \tau_c$. If $|a| > 2$, we have:

$$F(-a) = 1 - F(a) \approx \frac{e^{-a^2/2}}{\sqrt{2\pi}\,a}.$$

$$F(x) \approx 1 - \frac{e^{-x^2/2}}{\sqrt{2\pi}\,x} \quad \left(x = 1{,}25\,\frac{\tau_c}{\bar{\tau}_0}\right) \text{ и } \bar{\tau}_n \approx \frac{1}{\sqrt{2\pi}\,\delta f_s\, a}$$

Then

$$P_{su} = \frac{\exp[1/2\,a^2(1+\pi^2\tau_c^2\delta f_s^2)]}{\pi^2 \delta f_s \tau_c\, a^2}. \tag{24}$$

Nearly Complete Suppression (Fig. 5, b).

In this case, the value of a is positive, and the average duration of the intervals between overshoots is $\bar{\tau}_i \gg \tau_c$. If $a > 2$, we have:

$$F(a) \approx 1 - \frac{e^{-a^2/2}}{\sqrt{2\pi}\,a}. \qquad F(x) \approx \frac{1}{2} + \frac{x}{\sqrt{2\pi}}. \qquad \bar{\tau}_i \approx \frac{e^{a^2/2}}{\delta f_3}.$$

Then

$$P_{su} = 1 - \delta f_3 \tau_c\, e^{-a^2/2}. \tag{25}$$

By expressing the values of E_s^* (14) and U_{n4} in terms of the signal power Q_{s4} and the noise power Q_{n4} at the outputs of channel filters, we obtain the equation for the magnitude of a:

$$a = \frac{\alpha E_{s.\max} - E_s}{U_{n4}} = \sqrt{2}\left[\alpha \sqrt{\frac{Q_{s4.\max}}{Q_{n4}}} - \sqrt{\frac{Q_{s4}}{Q_{n4}}}\right] \tag{26}$$

where $\alpha = U_{thr}/E_{s\max}$ is the relative operating level of the threshold device, while $E_{s\max} = E_s$ for $z \to \infty$.

For the case where limiter 2 is present, Q_{s4} and Q_{n4} are found from Eqs. (12) and (13) by using the signal power Q_{s3} and the noise power Q_{n3} at the output of limiter 2, which are determined from the curve given in Fig. 4 or from the approximate analytical expressions (10) and (11).

In the latter case, the expressions for a are given by

$$a = \sqrt{2}\sqrt{\frac{\Delta f_2}{\Delta f_3}}\left[\alpha - 0.88\sqrt{\left(\frac{Q_s}{Q_n}\right)_2}\right] \quad \text{for} \quad \left(\frac{Q_s}{Q_n}\right)_2 < 1$$

$$a = 2\sqrt{\frac{\Delta f_2}{\Delta f_3}}(\alpha - 1)\sqrt{\left(\frac{Q_s}{Q_n}\right)_2} \quad \text{for} \quad \left(\frac{Q_s}{Q_n}\right)_2 \geqslant 1. \tag{27}$$

In the absence of limiter 2, the values of Q_{s4} and Q_{n4} are determined by using Eqs. (15) and (16). The signal power Q_{s2} at the output of filter Φ_2 and the noise energy spectrum $W(f_i)$ at the discriminator output can be found by using Eqs. (1) and (3) if the limiter 1 is present or by using Eqs. (5) and (6) in the case where the limiter is absent.

4. Probability of Spurious Operation

The formation of spurious commands in the frequency system under consideration can take place due to the noise voltage that acts at the outputs of the channel filters in the absence of the signal corresponding to the given filter (the case of channels without the signal). The noise voltage level depends on the signal-to-noise ratio at the receiver input and is determined by Eq (12) or (16). Let us determine the probability that a command will appear in the kth channel during the period of time τ_c in which a command is transmitted through the ith channel. It can be shown that this probability can be calculated on the basis of the equations derived for the suppression probability. The curve given in Fig. 5, c shows the detector output voltage in a channel without the signal. We shall assume that the moments of arrival of command signals in the ith channel are distributed at random. Spurious operation will occur if the fluctuating voltage exceeds the U_{thr} level at least at a single point during the time interval τ_c that is equal to the command duration. There will be no spurious operation if the time interval τ_c falls within the interval between overshoots, i.e., if the fluctuating voltage does not exceed U_{thr} at any point during the time τ_c. It can be readily seen that the pattern of the absence of spurious operation is similar to the above considered pattern of the presence of suppression, where the probability of the fluctuating voltage being everywhere lower than U_{thr} during the time interval τ_c was determined.

The probability of spurious operation at the level $a_0 = U_{thr}/U_{n4}$ can be determined by taking into account expressions (19) and (21), since

$$P_{sp} = 1 - P_{su} = 1 - n(a_0)\left[\bar{\tau}_i(a_0,\ \tau_i \geqslant \tau_c) - \tau_c\right] P(a_0,\ \tau_i \geqslant \tau_c) =$$

$$= 1 - 2\bar{\tau}_i\, n(a_0)\left[1 - F\left(1.25\,\frac{\tau_c}{\bar{\tau}_i}\right)\right] \tag{28}$$

where τ_1 is the duration of the interval between positive (with respect to the zero level) fluctuating voltage overshoots at the a_0 level, $n(a_0)$ is the average number of voltage overshoots at the a_0 level per unit time, $\bar{\tau}_i(a_0, \tau_i \geq \tau_c)$ is the average interval duration at the a_0 level of all $\tau_i \geq \tau_c$, $\bar{\tau}_i$ is the average interval duration at the a_0 level of all $\tau_i \geq 0$, and $P(a_0, \tau_i \geq \tau_c)$ is the probability that the intervals at the a_0 level have the duration $\tau_i \geq \tau_c$.

The detector output voltage in the channel without the signal (the noise envelope) has a Rayleigh distribution. In this case, the values of $n(a_0)$ and $\bar{\tau}_i$, which determine P_{sp} are equal to [3]

$$n(a_0) = \sqrt{2\pi}\delta f_3 a_0 e^{-a_0^2/2}. \qquad \bar{\tau}_i = \frac{P(\xi < a_0)}{n(a_0)} = \frac{1 - e^{-a_0^2/2}}{\sqrt{2\pi}\,\delta f_3 a_0 e^{-a_0^2/2}}.$$

We shall determine the expression for P_{sp} at the beginning of spurious operations. In this case $\bar{\tau}_i \gg \tau_c$, and

$$F(x) \approx \frac{1}{2} + \frac{x}{\sqrt{2\pi}} \qquad \left(x = 1{,}25\,\frac{\tau_c}{\bar{\tau}_i}\right).$$

Then

$$P_{sp} = 1 - n(a_0)(\bar{\tau}_i - \tau_c).$$

If we take into account that the average duration $\bar{\tau}_0$ of overshoots and the average duration $\bar{\tau}_i$ of the intervals between them are related by the expression

$$\bar{\tau}_0 + \bar{\tau}_i = \frac{1}{n(a_0)}$$

we obtain the following equation for the beginning of spurious operations:

$$P_{sp} = n(a_0)(\bar{\tau}_0 + \tau_c). \tag{29}$$

If $a_0 \to 0$, then $\bar{\tau}_i \ll \tau_c$ and as follows from (28), $P_{sp} \to 1$.

It should be noted that the equations obtained here for the probability P_{su} of command suppression and the probability P_{sp} of spurious operation can also be used in the case of signals whose shape at the detector output differs from a rectangular shape. In this case, the signal should be approximated by a trapezium, and the command duration τ_c should be understood as the duration of the upper flat portion of the trapezium. The proposed method for analyzing the noise stability of frequency remote control systems can obviously be used for determining the noise stability of other systems where the effect of fluctuating noise on the pulse signal reception is investigated.

5. Effect of the Receiving Device's Structure and Parameters on its Noise Stability

Let us consider the effect of limiters at the discriminator input (1) and output (2) on the frequency receiver noise stability. We shall make a comparison between three receiving device structures: I) limiter 1 is connected and limiter 2 is absent; II) limiter 2 is connected and limiter 1 is absent; III) both limiters 1 and 2 are connected. Figure 7 shows the dependence of the signal power and the noise power at the outputs of channel filters Φ_3 on the signal-to-noise ratio (z) at the receiver input in the case of equality of the output signal power for $z \to \infty$. The calculations were performed by using the formulas derived above and the curves for

$$\gamma_1 = \frac{\Delta f_1}{2\Delta f_3} = 5 \text{ and } 20 \quad \eta = \frac{2f_d}{\Delta f_1} = 1 \left(g = \frac{8\alpha_0^2}{\pi^2}\right).$$

It is obvious from Fig. 7 that, for $z < 3$ and for the receiving device structure II, the signal power has a larger, and the noise power a smaller, value than is the case for structure III, i.e., structure II secures a greater noise stability than structure III does. In comparison with structure II, structure I provides a lesser probability of spurious operation, but a considerably greater probability of command suppression, as is shown by calculations.

From the equations for P_{su} and P_{sp}, it is obvious that, by varying the relative operating level α of the threshold device, these probabilities can be redistributed. Since it is difficult to compare systems with different P_{su} and P_{sp}, it

is necessary first to compare the magnitudes of one of the probabilities, for instance P_{sp}. It can be shown that, in this case, the noise stability of the systems is determined by the signal-to-noise ratio at the output of the channel filter Φ_3. Figure 8 shows the dependence of the signal-to-noise ratio $E_s/U_{n4}\sqrt{\gamma}$ on the z value for the three receiving device structures. It is obvious from Fig. 8 that, for $z < 3$, structure II yields the best signal-to-noise ratio at the output, and consequently, the greatest noise stability of all the three structures. Thus, for weak signals ($z < 3$), which case is of the greatest practical interest for remote control systems, it is advisable to use a receiving device with limiter 2 at the discriminator output and without limiter 1 ahead of the discriminator. It should be noted that the conclusion that a receiver having only the limiter 2 has the greatest noise stability is valid only for those remote control systems whose operation is highly reliable for a signal-to-noise ratio $z < 3$ at the input. As a rule, telemetering systems require large signal-to-noise ratios for reliable transformation of information, and therefore, the above conclusion may not be valid for them.

Besides selecting the device's structure, the correct choice of its parameters is also an important task.

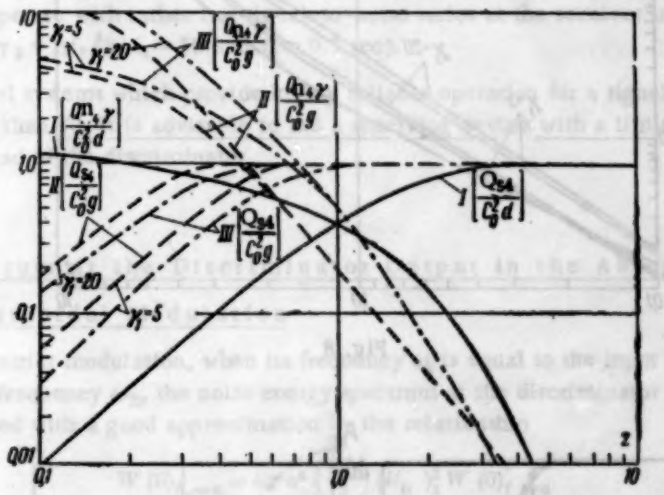

Fig. 7

The receiver under consideration has three filters with the transmission bands Δf_1, Δf_2, Δf_3. Let us consider the influence which the band magnitudes of these filters exert on noise stability. It can be readily shown that the noise stability can always be improved by narrowing the band of output filter Φ_3; however, this narrowing is limited by the system's speed. As can be seen from the complete equation for $(Q_s/Q_n)_2$ (which is valid for $0 \leq z < \infty$), the system's noise stability can be improved by restricting the input filter Φ_1 band to the optimum value Δf_{1opt}. The value of Δf_{1opt} that corresponds to the maximum of $(Q_s/Q_n)_2$ can be determined by using the complete equation for $(Q_s/Q_n)_2$. For $\gamma_1 < 5$ the value obtained for Δf_{1opt} will be approximate, since the equation for the spectrum W(f) yields an accurate value only for $\gamma_1 \geq 5$.

Let us consider the influence of the Δf_2 band in the presence of limiter 2 (structure II).

It is obvious from Fig. 7 that the narrowing of the Δf_2 band (the increase in γ_1) leads, for the assigned relative operating level α of the threshold device, to an increase in the noise power Q_{n4} and consequently to a greater probability of spurious operation. However, in this, the signal power Q_{s4} increases and, as calculations, the probability P_{su} of suppression decreases. Thus, for α = const and in the presence of limiter 2, the P_{su} and P_{sp} values can be redistributed by varying the band Δf_2. By increasing the transmission band Δf_2, the magnitude of P_{sp} can be reduced to very small values regardless of the presence or absence of the carrier. Calculations show that, for instance, for $U_{thr} = 0.5 E_{s\,max}$, $\Delta f_3 = 20$ cps, and $\tau_c = 0.1$ sec, it is necessary that the condition $\Delta f_2 > 50\Delta f_3$ be satisfied in order to secure $P_{sp} < 0.001\%$.

As was mentioned above, the other method of redistributing P_{su} and P_{sp} consists of changing the operating level α of the threshold device. By taking into account both of the above-described possibilities of redistributing P_{su} and P_{sp}, it can be shown that a reduction of the band Δf_2 would result in greater noise stability. This is confirmed by Fig. 8, from which it is clear that an increase in γ_1 leads to an increase in the signal-to-noise ratio at the output of filter Φ_3.

It should also be mentioned that, moreover, the introduction of limiter 2, leads to the equalization of the noise stabilities of all channels in the device. In the absence of limiter 2, the channel with the highest subcarrier has the worst noise stability (for $z > 1$).

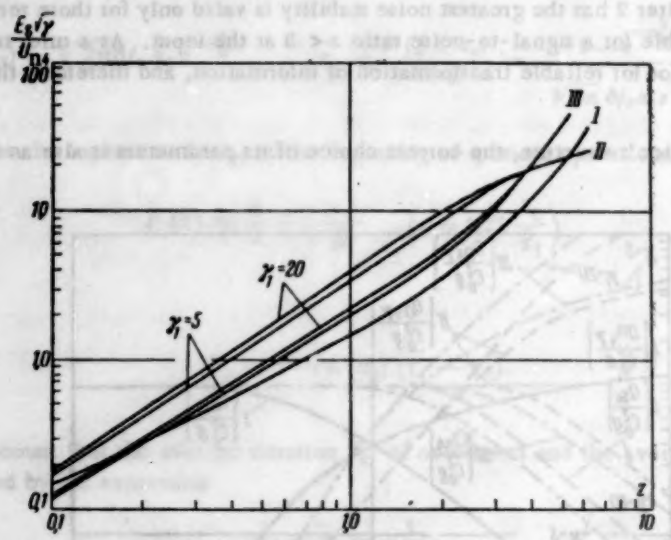

Fig. 8

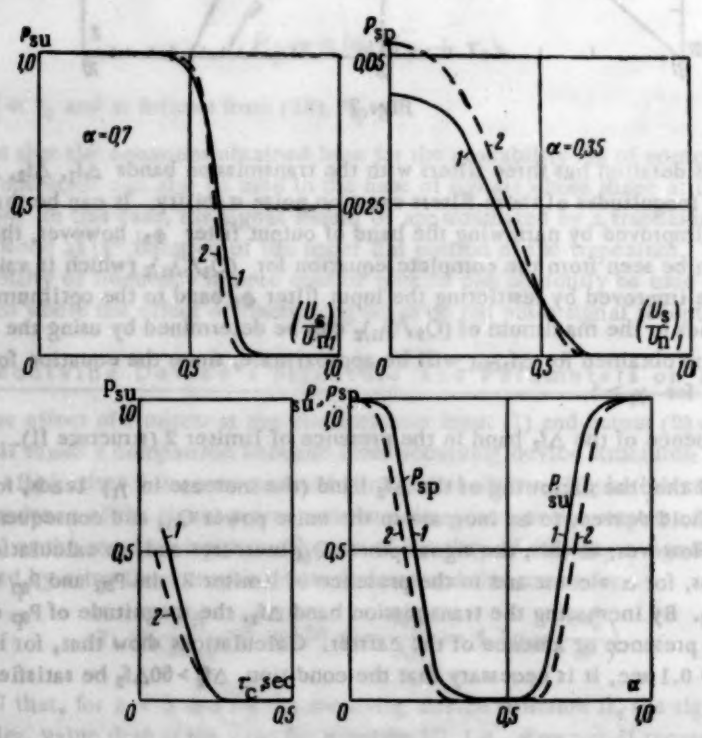

Fig. 9

6. Experimental results

The experimental investigations of the noise stability of the frequency system (Fig. 1) were performed on a radio remote control system with a portable transmitting device, which has been developed at IAT AN SSSR.

Figure 9 shows the dependences of P_{su} and P_{sp} on $(U_s/U_n)_1 = \sqrt{z}$ (for $\tau_c = 0.1$ sec), of P_{su} on τ_c (for $(U_s/U_n)_1 = 0.6$ and $\alpha = 0.7$), and of P_{su} and P_{sp} on α (for $U_s/U_n = 0.6$ and $\tau_c = 0.1$ sec), which were obtained by experiment (1) and by calculations (2) for the case where limiter 1 is absent and limiter 2 is present (the transmission bands of the input filter, the second filter, and the channel filter were $\Delta f_1 = 20$ kc, $\Delta f_2 = 1$ kc, and $\Delta f_3 = 20$ cps, respectively). The P_{sp} vs $(U_s/U_n)_1$ curve was plotted for $\alpha = 0.35$, since, for $\alpha = 0.7$, the value of P_{sp} is almost equal to zero for any noise level at the input.

Figure 9 shows that the experimental and theoretical data are in fairly good agreement.

SUMMARY

1. Spectral methods which were formerly used for frequency telemetering systems [5 and 6], make it possible to derive theoretical equations for estimating the noise stability of remote control systems in the presence of arbitrary-level fluctuating noise.

2. The theoretical and experimental results indicate that frequency remote control systems have high noise stability and that they can operate with rather low signal-to-noise ratios at the receiver input (up to $(U_s/U_n)_1 = 0.6 - 0.7$, for $\gamma_1 = \Delta f_1/2\Delta f_2 = 10$, $\gamma_2 = \Delta f_2/2\Delta f_3 = 50$ and $\tau_c = 0.1$ sec).

3. In remote control systems which provide highly reliable operation for a signal-to-noise ratio $(U_s/U_n)_1$ at the receiver input that is less than $\sqrt{3}$, it is advisable to use a receiving device with a limiter at the discriminator output and without a limiter ahead of the discriminator.

APPENDIX

Noise Energy Spectrum at the Discriminator Output in the Absence of Limiter 1 in the Case of Carrier Sinusoidal Modulation

In the absence of carrier modulation, when its frequency ω_s is equal to the input filter center frequency ω_0 and the discriminator "zero" frequency ω_z, the noise energy spectrum at the discriminator output at the zero frequency $f = 0$ [1] can be represented with a good approximation by the relationship

$$W(0)_{f_d=0} = 4\pi^2 k^2 \left(\frac{\Delta f_1}{2}\right)(U_n)_1^2 W(0)^*_{f_d=0}$$

where

$$W(0)^*_{f_d=0} \begin{cases} 0.405\, e^{-0.8z} & \text{for} \quad 0 \leqslant z \leqslant 1.5 \\ \dfrac{0.183}{z} & \text{for} \quad 1.5 < z < \infty. \end{cases}$$

If the signal frequency deviates from ω_0, the spectral intensity increases approximately following a quadratic dependence and attaining, for $f_d = \Delta f_1/2$ an intensity that corresponds to the action of noise alone without the signal: $W(0)^*_n (W(0)^*_n = W(0)^*_{f_d=0}$ for $z = 0$ [1 and 7].

For an arbitrary value of f_d, the maximum energy spectrum value $W(0)^*_{f_{dmax}}$ will be equal to

$$W(0)^*_{f_d\,max} = W(0)^*_{f_d=0} + \left(\frac{2f_d}{\Delta f_1}\right)^2 [W(0)^*_n - W(0)^*_{f_d=0}].$$

In the case of slow sinusoidal modulation ($f_{mod} \ll \Delta f_1/2$), the noise energy spectrum for $f = 0$ can be determined by using the equation

$$\overline{W(0)} = 4\pi^2 k^2 \left(\frac{\Delta f_1}{2}\right)(U_n)_1^2 \left\{W(0)^*_{fd=0} + \frac{1}{2}\left(\frac{2f_d}{\Delta f_1}\right)^2 [0{,}405 - W(0)^*_{fd=0}]\right\}.$$

For sinusoidal modulation of the carrier frequency and if limiter 1 is not provided ahead of the discriminator, the noise spectrum intensity W(f) is approximately uniform for all low-frequency noise components ($2f_{max}/\Delta f_1 \leq 0.2$) [1], on account of which one can consider that $W(f) \approx W(0)$ within the indicated limits.

LITERATURE CITED

1. D. Middleton, The Spectrum of Frequency-Modulated Waves After Reception in Random Noise, I. Q. Appl. Math., vol. 7, No. 2 (1949).
2. B. R. Levin, Theory of Random Processes and its Application in Radio Engineering [in Russian] (Soviet Radio Press, 1957).
3. V. I. Bunimovich, Fluctuating Processes in Radio Receivers [in Russian] (Soviet Radio Press, 1951).
4. W. B. Davenport, Signal-to-Noise Ratios in Band-Pass Limiters, J. Appl. Phys., vol. 24, No. 6 (1953).
5. Yu. I. Chugin, "Optimum frequency deviation in single-channel telemetering systems," Avtomatika i Telemekhanika, 19, 4 (1958).*
6. Yu. I. Chugin, "Noise stability of single channel frequency telemetering systems in the presence of intensive fluctuating noise," Collection: Automatic Control [in Russian] (AN SSSR Press, 1960).
7. N. M. Blachman, The Demodulation of a Frequency-Modulated Carrier and Random Noise by a Discriminator. J. Appl. Phys., vol. 20, No. 10 (1949).
8. V. I. Tikhonov, "Experimental investigation of the distribution of fluctuation overshoots with respect to duration," Radiotekhnika, 11, 8 (1956).
9. S. O. Rice., Mathematical Analysis of Random Noise. Bell System Tech. J., vol. 23, No. 3 (1944); vol. 24, No. 1 (1945).

*See English translation.